Modelling root exudation and plant-microbe interactions under CO_2 fertilization in a mature forest

Kristian Schufft[1,2,3], Katrin Fleischer[4], Anja Rammig[3], Lin Yu[5], Mingkai Jiang[6], Belinda E. Medlyn[7], Sönke Zaehle[1,8]

[1] Department Biogeochemical Signals, Max Planck Institute for Biogeochemistry, Jena, Germany
[2] International Max Planck Research School for Global Biogeochemical Cycles, Max Planck Institute for Biogeochemistry, Jena, Germany
[3] Technical University of Munich, School of Life Sciences, Freising, Germany
[4] Systems Ecology, Amsterdam Institute for Life and Environment, Vrije Universiteit Amsterdam, Amsterdam, The Netherlands
[5] Department of Earth System Sciences, Hamburg University, Hamburg, Germany
[6] State Key Laboratory for Vegetation Structure, Function and Construction (VegLab), College of Life Sciences, Zhejiang University, Hangzhou, Zhejiang, China, 310030
[7] Hawkesbury Institute for the Environment, Western Sydney University, Penrith NSW Australia
[8] Michael Stifel Center Jena for Data-driven and Simulation Science, Friedrich Schiller University Jena, Jena, Germany
Correspondence to: Kristian Schufft (kschufft@bgc-jena.mpg.de)

Abstract. Root exudation, defined as plant labile carbon (C) allocation ~~into soils through~~ from fine roots into soils, is a substantial yet often overlooked pathway of the terrestrial ~~carbon~~C cycle. Root exudation is ~~likely~~expected to increase under rising ~~levels of~~ atmospheric CO_2, ~~but the implications of the increase in this flux are~~yet its consequences for soil C and nutrient cycling remain poorly ~~understood. Increased~~constrained. Additional labile C ~~availability in soils~~input may stimulate microbial growth and increase soil ~~carbon~~C storage but ~~at the same time~~ microbial nutrient acquisition could offset this ~~accumulation by~~ through enhanced decomposition of soil organic matter~~.~~.

Here, we implement a dynamic representation of root exudation ~~based on~~, driven by plant surplus ~~carbon~~C and nutrient limitation, in the microbial ~~–~~ explicit terrestrial biosphere model QUINCY-JSM ~~(QUantifying Interactions between terrestrial Nutrient CYcles and the climate system).~~. We evaluate the ~~effect~~effects of elevated CO_2 (eCO_2) on root exudation and ~~its consequences for~~on microbial C, nitrogen (N) and phosphorus (P) cycling using observations from the Eucalyptus Free Air CO_2 Enrichment (EucFACE) experiment in a soil ~~phosphorus~~P impoverished forest. In ~~the~~this experiment, ~~more than half of additional~~ eCO_2 increased gross primary productivity (GPP) and soil respiration, but more than half of additional GPP under ~~elevated CO_2 (~~eCO_2~~)~~ could not be assigned to ~~a~~ measured ~~vegetation flux.~~ biomass production or autotrophic respiration, and was likely allocated belowground.

With the explicit implementation of root exudation, ~~our~~the model predicted that ~~elevated CO_2 caused an increase in~~eCO_2 increases belowground ~~carbon flux~~C allocation and ~~an increase in~~ microbial growth, but has a limited effect on soil ~~carbon~~C storage. Root exudation ~~was~~ increased ~~to~~by 30 %, but more than half of this additional input was directly respired by microbes. ~~As a result~~Thus, root exudation gives a possible explanation for the ~~not measured vegetation flux and the~~unmeasured fraction of plant C allocation, effectively closing the gap between enhanced GPP and increased heterotrophic respiration under eCO_2 ~~observed~~ in the experiment. ~~Increased~~Although increased C input through root exudation ~~also enhanced~~stimulated microbial growth, ~~but in order to support this growth,~~ microbes ~~mostly gained nutrients from~~partially met their higher nutrient demand through decomposition and mineralization of organic matter~~. As a consequence, increased decomposition~~, which negated the build-up of microbial necromass. Our study ~~emphasizes~~highlights the ~~role~~importance of root exudation as a key pathway in vegetation C allocation under eCO_2 and identifies microbial ~~activity for~~responses to this flux as a key modulator of soil ~~carbon~~C sequestration ~~under elevated CO_2 and guides~~in nutrient limited forests, thereby guiding further research regarding plant-microbe interactions.

Short summary. Root exudation describes a process in which plants allocate labile carbon (C) through roots into soils, thereby influencing microbial ~~carbon~~C and nutrient cycling. We implemented root exudation in a computer model that simulates ecosystem processes. Increased atmospheric CO_2 ~~led to~~ increased root exudation, but the additional input was partially offset by enhanced microbial respiration. Our research brings new perspectives in modelling soil ~~carbon~~C and nutrient cycling in forests under increasing CO_2.

~~1~~1. Introduction

Increasing atmospheric CO_2 concentrations have the potential to drive increased ecosystem carbon sequestration, but there is considerable uncertainty about how much additional C can be stored, particularly where soil nutrient availability is low. CO_2 fertilization leads to higher leaf-level photosynthesis and biomass production (BP) (Norby et al., 2005; Walker et al., 2019, 2021), potentially increasing C sequestration in biomass, and in soils when biomass turn over. However, increased growth must be supported by nutrients and if soil nutrient availability cannot meet increased plant nutrient demands, the CO_2 fertilization effect on plant growth is typically reduced (Fleischer et al., 2019; Norby et al., 2010; Zaehle et al., 2014).). Soil nutrient availability is thus a major determinant of whether CO_2 fertilization leads to a positive effect on carbon sequestration in biomass. Nonetheless, additional carbon sequestration can occur in soils under nutrient limitation: allocation of C towards mycorrhizae (Drake et al., 2011) and root exudation has been observed to increase in some studies (Norby et al., 2024; Phillips et al., 2011) to support additional nutrient acquisition, and this belowground carbon allocation may induce additional soil carbon storage. Therefore, plant nutrient availability for growth may affect if CO_2 fertilization has a positive effect on carbon sequestration via allocation towards biomass production or induce soil carbon sequestration, via increased belowground allocation.

A critical question for C sequestration under elevated CO_2 (eCO_2) and nutrient-limited conditions is how much of the extra C allocated belowground remains as organic carbon in the soil system, or is quickly re-emitted to the atmosphere via respiration. The ultimate fate of the C allocated belowground is shaped by an interplay of microbial growth, decomposition, and nitrogen (N) and phosphorus (P) availability. On the one hand, soil microbial organisms are a key driver in soil organic matter cycling as they decompose and take up organic material to gain C, N and P, thereby respiring CO_2 and mineralizing N and P, making them plant-available again. At the same time, their necromass contributes substantially to soil organic C, N and P stocks through organo-mineral associations (Liang et al., 2019). Under additional labile C input four competing mechanisms regulate soil C sequestration:

(i) Inputs of low molecular weight compounds, such as root exudates, may increase microbial growth. However, the amount of C that can be incorporated in microbial biomass depends on microbial nutrient availability. Under microbial nutrient stress a higher fraction of plant-derived C will be directly respired, while under sufficient nutrient availability, microbial biomass C will increase (Manzoni et al., 2012; Spohn, 2015).

(ii) Increased microbial growth can promote microbial necromass formation (Cotrufo et al., 2013). Although microbial necromass is a readily available source of C, energy and nutrients, microbial biomolecules also are often stabilized through formation of aggregates or sorption to mineral soil matrix, making them inaccessible for enzymatic degradation and contributing to long-term C storage (Kästner et al., 2021; Liang et al., 2017; Sokol et al., 2019). Hence, increased microbial growth induced by additional C inputs has the potential to increase soil organic carbon, and enhance long-term ecosystem C storage.

(iii) On the other hand, increased microbial growth can lead to higher microbial demands for N and P. Microbial necromass represents a source for growth that is rich in N and P. Therefore, increased microbial growth induced by additional C inputs may also induce high microbial demand for nutrients and a shift towards an increased depolymerization and respiration of old organic material (van Groenigen et al., 2014; Vestergård et al., 2016; Yin et al., 2013). This mechanism, often described as priming, has the potential to offset the accumulation of C in soil organic matter (SOM) and thereby increase soil carbon turnover. During this process the enhanced decomposition will increase biological gross mineralization of N and P.

(iv) Additional feedback comes into play under P limitation. Microbes and plants may use biochemical mineralization to acquire P (Margalef et al., 2017; Turner et al., 2014; Walker and Syers, 1976). In this process, P is mobilized via phosphatase enzymes that cleave terminal P from organic compounds (McGill and Cole, 1981; Nannipieri et al., 2011). In contrast to regular biological mineralization, this pathway does not require a complete decomposition of organic material and has therefore no direct influence on soil C cycling. Whether increased root exudation under eCO_2 will lead to an increase in soil C storage therefore depends on the interaction, quantity and nature of microbial growth and nutrient acquisition.

Free Air CO_2 enrichment (FACE) experiments allow to study the effect of elevated CO2 on plant C allocation and SOM cycling on ecosystem scale, including the advantages of inclusion of mature trees, natural climate conditions and low disturbances (McLeod and Long, 1999). In previous FACE experiments, namely Duke FACE and ORNL FACE, which were located in temperate N limited forests, eCO_2 has led to an initial increase in NPP. However, the effect persisted only in Duke FACE and diminished in ORNL after 10 years (Norby et al., 2010; Walker et al., 2019). At Duke FACE a stronger increase in N uptake and change in plant nitrogen use efficiency allowed for a sustained response in NPP to eCO_2, while in ORNL FACE where progressive N limitation decreased the response of NPP under eCO_2 (Finzi et al., 2007; Zaehle et al., 2014). One explanation points to increased belowground C allocation in Duke FACE, causing an increase in SOM cycling and therefore enhanced plant nitrogen availability via priming (Drake et al., 2011).

To clarify and quantify the interactions between C and nutrients under rising atmospheric CO_2, model data synthesis can be used, bringing together measurements from FACE experiments and terrestrial biosphere models (TBM). Model data synthesis for FACE experiments identified C allocation, nitrogen uptake and soil nitrogen cycling as key processes for CO_2 responses under N limitation (De Kauwe et al., 2014; Zaehle et al., 2014). However, most models were unable to fully reproduce the dissimilar responses to eCO_2 under nitrogen limitation. While the initial increase in NPP could be reproduced, models generally tend to show decreased response in NPP due to progressing N limitation (Zaehle et al., 2014). One possible explanation is the missing representation of root exudation and priming effects, that would allow plants to acquire nutrients via increased belowground C allocation. Further model development showed that including priming effects based on increased litter and root exudation or representation of mycorrhiza fungi, improved simulated N availability and NPP response for Duke FACE for first order decomposition soil models (Grant, 2013; Thurner et al., 2024). Although the results highlight the role of soil organic matter cycling for plant growth, they paid little attention to the microbial mechanisms and P cycle interactions that affect soil C sequestration under elevated CO_2.

To further investigate the competing dynamics of microbial growth and nutrient acquisition on soil C storage under eCO_2 we use the terrestrial biosphere model QUINCY JSM, which accounts for C, N, and P dynamics and explicitly represents the effect of microbial processes that shape soil C cycling (Thum et al., 2019; Yu et al., 2020). We parameterize and apply our model to the Eucalyptus Free Air CO_2 Enrichment (EucFACE) facility (Crous et al., 2015; Ellsworth et al., 2017). EucFACE is of particular relevance because it is the first large scale FACE experiment investigating the impact of eCO_2 on forest ecosystems under P limitation. Despite the fact that P limitation is widespread P globally previous forest FACE experiments have been principally conducted in N limited temperate forests (Du et al., 2020). Similar to N limited systems, root exudation is an important mechanism for plant P acquisition (Lambers, 2022; Pantigoso et al., 2023; Reichert et al., 2022) and is likely to increase under enhanced P limitation (De Andrade et al., 2022; Wang and Lambers, 2020) or eCO_2.

Field measurements and model data synthesis for EucFACE highlight the importance of root exudation for plant C allocation and P cycling under eCO_2. At the site eCO_2 led to a 12 % increase of gross primary productivity (GPP), but the effect on biomass production and autotrophic respiration was comparatively small. Notably, more than 50 % of surplus GPP under eCO_2 could not be attributed to a measured vegetation flux in this experiment (Jiang et al., 2020). Instead, this C was traced to an 17 % increase in heterotrophic soil respiration, without a statistically significant increase in soil C. Jiang et al. (2020) hypothesized that increase in heterotrophic respiration to be related to additional C input via root exudation, potentially for nutrient acquisition. However, eCO_2 did only invoke weak effects on plant P availability, suggesting that despite increased belowground C allocation, microbial competition for nutrients constrain additional plant P uptake (Jiang et al., 2024b) Model data synthesis was done before and during the experiment: (Medlyn et al., 2016) found that response of NPP to eCO_2 was related to model nutrient cycling assumptions: In models with integrated P cycle, under eCO_2 plant uptake remained unchanged, preventing a strong response in NPP to eCO_2, whereas in other models eCO_2 increased NPP up to 20 %. However, uncertainties arise from P acquisition strategies plants might use under increased C supply (Reichert et al., 2022). Jiang et al. (2024a) compared 8 TBMs, including QUINCY JSM, to the experimental results of EucFACE, and further pointed to the lack of representation of trade mechanisms between plant C allocation and nutrient availability. As most other models, QUINCY JSM, allocated additional plant C in either autotrophic respiration, growth or storage but not in heterotrophic respiration. This disagrees with observations and indicates a missing representation of nutrient acquisition strategies and plant microbe interactions in these models. A substantial part of the ecosystem response of EucFACE to eCO_2 lies in plant microbe interactions and how their alteration affects soil carbon cycling, which cannot be captured by models yet.

Here we aim to address a key missing link between belowground C allocation and nutrient cycling by implementing dynamic root exudation. We modelled root exudation based on plant fine root respiration and nutrient status. We define root exudation as the combined flux of labile carbon and nitrogen through free exudation, rhizodeposition and loss via mycorrhiza. The explicit representation of microbial processes in QUINCY JSM allows to decompose the CO_2 effect on soil C sequestration in distinct mechanisms. Therefore, we can assess how increased root exudation under eCO_2 influences soil C storage as a result of competing effects of microbial growth and nutrient acquisition:

~~1) We first analyze how much of the additional C input is used for microbial growth and how much is matched by increased heterotrophic respiration.~~

~~2) Additional microbial growth will increase microbial nutrient demand. We therefore investigate the sources of additional, N and P and quantify the amounts released by decomposition of microbial necromass and by biochemical mineralization.~~

~~3) In order to assess the net effect of eCO_2 on soil storage we investigate the simultaneous build-up and decomposition of microbial necromass and evaluate whether increased root exudation leads to accelerated turnover of soil pools.~~

~~Simulation results are compared with data from the EucFACE experiment.~~ Increasing atmospheric CO_2 concentrations have the potential to drive increased ecosystem carbon (C) sequestration, but there is considerable uncertainty about how much additional C can be stored in ecosystems, particularly where soil nutrient availability is low. Observation and modeling studies suggest, that CO_2 fertilization leads to higher leaf-level photosynthesis and biomass production (BP) (Norby, 2025; Walker et al., 2019, 2021), potentially increasing C sequestration in vegetation biomass, and in soils when vegetation biomass turn over. However, increased growth must be supported by nutrients and if soil nutrient availability cannot meet increased plant nutrient demands, the CO_2 fertilization effect on plant growth is typically reduced (Fleischer et al., 2019; Norby et al., 2010; Wieder et al., 2015; Zaehle et al., 2014). Under elevated CO_2 (eCO_2), plants may allocate additional C derived from increased photosynthesis to root exudation and mycorrhizae to compensate for nutrient limitations, by increasing microbial decomposition and mineralization of organic matter (Drake et al., 2011; Phillips et al., 2011; Reay et al., 2025). Observations and models suggest that root exudation is a key mechanism for plant responses under eCO_2, but there are major uncertainties about microbial responses and the consequences on soil C sequestration, especially for different natures of nutrient limitations.

Free Air Carbon Enrichment (FACE) experiments in nitrogen (N) limited forests suggest increased root exudation and cycling of soil organic matter helped in maintaining BP response to eCO_2. In Duke FACE and ORNL FACE, which were located in temperate N-limited forests, eCO_2 has led to an initial increase in BP. However, only at Duke FACE eCO_2 increased N uptake and change in plant nitrogen-use-efficiency allowed for a sustained response in BP to eCO_2, while in ORNL FACE progressive N limitation decreased the response of BP under eCO_2 after 10 years (Norby et al., 2010; Walker et al., 2019; Zaehle et al., 2014). One explanation is that plants maintained N availability under eCO_2 at Duke FACE, by promoting enhanced decomposition of soil organic matter (SOM) via increased root exudation, thereby increasing N mineralization but offsetting accumulation of C in soil pools (Drake et al., 2011; Terrer et al., 2021).

Synthesis of observations from FACE experiments and terrestrial biosphere models (TBMs) highlighted the role of plant-soil interactions but also revealed model limitations. Model-data synthesis identified C allocation, N uptake and soil N cycling as key processes for CO_2 responses under N limitation (De Kauwe et al., 2014; Zaehle et al., 2014). However, most models were unable to fully reproduce the dissimilar responses to eCO_2 under N limitation. While models reproduced the initial increase in BP, they generally tended to show decreased response in BP due to progressing N limitation. This suggests a missing link between plant C allocation and nutrient acquisition, and highlights importance for root exudation in plant responses to eCO_2

in N limited forests. However, it is not clear how additional root exudation under eCO_2 controls microbial growth and soil C sequestration, and if results for N limited forests can be transferred to phosphorus (P) limited systems.

Despite the fact that P limitation is widespread globally (Du et al., 2020), previous forest FACE experiments have been principally conducted in N-limited temperate forests. The Eucalyptus Free Air CO_2 Enrichment (EucFACE) facility (Crous et al., 2015; Ellsworth et al., 2017) is the first large scale FACE experiment investigating the impact of eCO_2 on forest ecosystems under P limitation. At the site eCO_2 increased gross primary productivity (GPP) by 12 %, but the effect on biomass production and autotrophic respiration was comparatively small (Jiang et al., 2020). Notably, Jiang et al. (2020) found that more than 50 % of additional GPP under eCO_2 could not be attributed to biomass production or autotrophic respiration, in this experiment. Instead, this C was traced to an 17 % increase in heterotrophic soil respiration, without a statistically significant increase in soil C sequestration. The results suggest that increased root exudation and induced cycling of SOM are also relevant for P limited systems under eCO_2. (De Andrade et al., 2022; Lambers, 2022; Reichert et al., 2022; Wang and Lambers, 2020) However the plant-microbial mechanisms which link increased GPP with soil respiration, and its implication for soil C sequestration in this system, remain poorly understood.

Similar to model-data synthesis for N limited forest, model-data synthesis for EucFACE identified nutrient limitation and C allocation as key mechanisms for understanding BP and soil activity response to eCO_2. Medlyn et al. (2016) found that in models with integrated P cycle, under eCO_2 plant uptake remained unchanged, preventing a strong response in BP to eCO_2, whereas in other models eCO_2 increased BP up to 20 %. Jiang et al. (2024a) compared 8 TBMs, to the experimental results of EucFACE, and further pointed to the lack of adequate representation of plant C allocation. Most models allocated additional plant C in either autotrophic respiration, growth or storage but not in heterotrophic respiration. This disagrees with C budget results from (Jiang et al., 2020) and indicates a missing representation of root exudation and plant-microbe interactions in these models, therefore neglecting possible implication for soil C storage under eCO_2.

Here we aim to address the key missing link between GPP increase, plant C allocation and cycling of C, N and P in soils by implementing root exudation in the microbial-explicit, terrestrial biosphere model, QUINCY-JSM (Thum et al., 2019; Yu et al., 2020) to simulate CO_2 fertilization at EucFACE. Like in other models, previous simulations with QUINCY-JSM, showed a mismatch between simulated and observed C allocation and response of soil heterotrophic respiration to eCO_2 for EucFACE (Jiang et al., 2020). We therefore implemented root exudation in QUINCY-JSM. We assume root exudation as dynamic flux, based on plant fine root respiration and nutrient status. We use our model to investigate how root exudation affects underlying mechanisms of microbial soil C sequestration under eCO_2.

Microbes fulfill a central role in soil C sequestration, by decomposing and respiring organic material, controlling nutrient release and contributing to organic matter formation and long-term C sequestration, via production of necromass and its

formation of organo-mineral associations (Kästner et al., 2021; Liang et al., 2017, 2019; Sokol et al., 2019). Observational data alone may not be sufficient to disentangle contributions of individual processes. Therefore, we use our model to investigate three competing mechanisms that may regulate soil C sequestration response in microbial necromass to altered microbial growth and nutrient acquisition as a result of increased root exudation (Figure 1).

(1) Exudates regulate gross growth of microbial biomass, which in turn influences gross necromass production (Figure 1 (1)) (Cotrufo et al., 2013). The capability of microbes to transform additional C input into biomass depends on their carbon-use efficiency (CUE). Carbon-use efficiency of microbial growth has been shown to be constrained under nutrient limitations (Manzoni et al., 2012; Spohn, 2015). If microbes are not able to fulfill their stoichiometric nutrient requirement for growth, excess C will be respired as waste respiration, leading to a decline in CUE (Schimel and Weintraub, 2003). How much of the additional C input is ultimately transferred into biomass and necromass therefore depends on microbial nutrient limitation.

(2) Under N or P limitation, microbes can stimulate the depolymerisation of nutrient rich microbial necromass to potentially acquire more N and P (Figure 1 (2)) (van Groenigen et al., 2014; Vestergård et al., 2016; Yin et al., 2013). While this may happen proportional to growth, microbes may also change their relative investment into nutrient acquisition strategies. Either way, the additional depolymerization of microbial necromass under increased root exudation, often referred to as priming, will result in an increased respiration of old organic C and has the potential to offset the gross growth of necromass.

(3) Under strong P limitation, P can be gained through biochemical mineralization without the need to decompose necromass (Figure 1 (3)) (Margalef et al., 2017; Turner et al., 2014; Walker and Syers, 1976). In this process, microbes use phosphatase to hydrolyze terminal phosphate groups from organic matter as inorganic PO_4 that is available for plants and microbes (McGill and Cole, 1981; Nannipieri et al., 2011). As this mechanism does not require the full depolymerization of microbial necromass it decouples microbial nutrient acquisition from C cycling and does not directly decrease C storage.

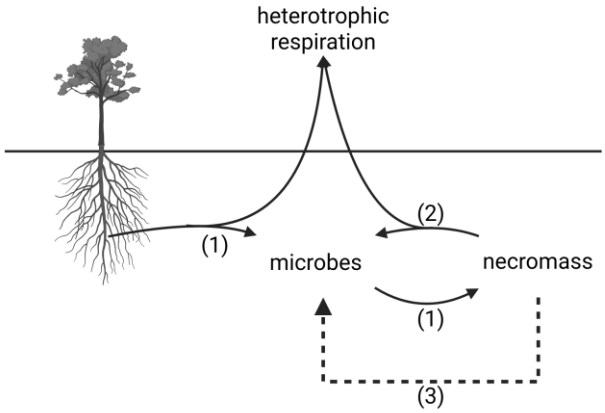

Figure 1: Conceptual diagram of microbial contributions of soil organic formation. (1) plant litter and exudates support microbial growth and necromass production, mediated by microbial CUE. (2) Microbes decompose microbial necromass for nutrient acquisition. (3) Biochemical mineralization allows for P acquisition from microbial necromass without decomposition. Created with BioRender.com

With this study we aim for a first quantification of root exudation fluxes for the EucFACE experiment. We test our implementation against observations regarding allocation of additional GPP under eCO_2 in the ecosystem. We further aim to answer the following objectives:

(1) To which extent did increased root exudation under eCO_2 contribute to gross microbial growth, gross necromass production and increased heterotrophic respiration?

(2) Was priming, as a mechanism for microbial N acquisition, increased by higher root exudation under eCO_2?

(3) Was biochemical mineralization, as a mechanism for microbial P acquisition, increased by higher root exudation under eCO_2?

(4) Was net necromass production, defined as the difference between gross necromass production and decomposition, increased by higher root exudation under eCO_2?

We conclude our study by presenting key aspects in which linking models with field measurements can be used to further improve understanding of plant-~~soil~~microbe interactions under increasing levels of CO_2.

2. Material and Methods

2.1 Model application

~~2.1~~ **We apply our model, QUINCY-JSM, to the Eucalyptus Free Air CO_2 Enrichment (EucFACE) experiment. Our goal is to quantify competing soil mechanisms on C storage for increased root exudation under eCO_2 in a P-limited forest.** ~~**Overview of modelled processes in QUINCY**~~

~~QUINCY-JSM has two components, a terrestrial biosphere model (QUINCY, (Thum et al., 2019)) coupled to the integrated Jena Soil model (JSM, (Yu et al., 2020)) and simulates coupled ecosystem N, P, C and water dynamics (Fig. 1 for an overview). In the following sections we first summarize key processes represented in QUINCY and JSM, before introducing the new root exudation module.~~

~~QUINCY simulates the function of vegetation, which is described by five structural pools (leaves, fine roots, coarse roots, sapwood and heartwood) and three non-structural pools (labile, storage and fruits) that all contain C, N, and P. Photosynthesis is calculated after Friend and Kiang (2005) along a vertical canopy gradient (Kull and Kruijt, 1998), with photosynthetic activity assumed proportional to leaf nitrogen content, but attenuated in the presence of sink limitation on growth (Thum et al., 2019). Acquired C is added to the labile pool, from which it is used to cover the cost for respiration. Maintenance respiration is calculated for each tissue based on tissue N content and temperature (Lloyd and Taylor, 1994). In addition QUINCY accounts for growth respiration (Atkin et al., 2014) and nutrient uptake respiration (Zerihun et al., 1998). The remaining C in the labile pool is then used for, root exudation, growth, storage (Fig. 1 upper panel). N and P taken up by plant roots, or recycled from senescing tissues are added to the labile pool. Excess labile C, N and P are stored in a reserve pool, from where these elements can be retrieved to buffer low levels of the labile pool, e.g., to ensure the regrowth of foliage and roots, root exudation (Sect. 2.3) and structural components at the start of the growing season. Upon senescence of structural pools, a fixed fraction of nutrients is recycled and returned into the labile pool. The remaining biomass (C, N, P) enters the soil via litterfall in form of three litter pools (soluble, polymeric, wood). Vegetation and soil processes are calculated at 30 min time step. All physical and biogeochemical soil processes are modelled for 15 discrete soil layers, with exponentially increasing depth and a minimum layer depth of 6.5 cm. The model accounts for differences in vegetation by twelve plant functional types (PFTs), of which for this study we use only the dry broadleaved evergreen type to represent vegetation at the site.~~

Therefore, we implemented root exudation, based on plant labile pool dynamics, in our model. We parameterize and apply our model to the EucFACE experiment (Crous et al., 2015; Ellsworth et al., 2017) . We first evaluate our model against field measurements for ambient (aCO_2) conditions, then evaluate our results against measured CO_2 responses of plant C allocation to see if our model can simulate the suggested increase in root exudation under eCO_2. We further quantify the simulated increase in belowground C allocation and its effect on gross microbial growth. To assess feedback via microbial nutrient acquisition strategies we identify sources for gross microbial growth in C, N and P and potential shifts in sources with eCO_2. We conclude by comparing simulated influx and outflux of microbial necromass C, N and P pools and their turnover rates, for aCO_2 and eCO_2 conditions. QUINCY-JSM has two components, a terrestrial biosphere model (QUINCY (QUantifying

Interactions between terrestrial Nutrient CYcles and the climate system, (Thum et al., 2019)) coupled to the integrated JSM (Jena Soil Model, (Yu et al., 2020)) and simulates coupled ecosystem N, P, C and water dynamics (Figure 2 for an overview). In the following sections we first summarize key processes represented in QUINCY and JSM, before introducing the new root exudation module.

2. 2 Overview of modelled processes in QUINCY

QUINCY simulates the function of vegetation, which is described by five structural pools (leaves, fine roots, coarse roots, sapwood and heartwood) and three non-structural pools (labile, storage and fruits) that all contain C, N, and P. Photosynthesis is calculated after Friend and Kiang (2005) along a vertical canopy gradient (Kull and Kruijt, 1998), with photosynthetic activity assumed proportional to leaf N content, but attenuated in the presence of sink limitation on growth (Thum et al., 2019). Acquired C is added to the labile pool, from which it is used to cover the cost for respiration. Maintenance respiration is calculated for each tissue based on tissue N content and temperature (Lloyd and Taylor, 1994). In addition, QUINCY accounts for growth respiration (Atkin et al., 2014) and nutrient uptake respiration (Zerihun et al., 1998). The remaining C in the labile pool is then used for root exudation, growth, storage (Figure 2 upper panel). Nitrogen and P taken up by plant roots, or recycled from senescing tissues are added to the labile pool. Excess labile C, N and P are stored in a reserve pool, from where these elements can be retrieved to buffer low levels of the labile pool, e.g., to ensure the regrowth of foliage and roots, root exudation (Sect. 2.4) and structural components at the start of the growing season. Upon senescence of structural pools, a fixed fraction of nutrients is recycled and returned into the labile pool. The remaining biomass (C, N, P) enters the soil via litterfall in the form of three litter pools (soluble, polymeric, wood). Vegetation and soil processes are calculated at 30 min time-step. All physical and biogeochemical soil processes are modelled for 15 discrete soil layers, with exponentially increasing depth and a minimum layer depth of 6.5 cm. The model accounts for differences in vegetation by twelve plant functional types (PFTs), of which for this study we use only the dry broadleaved evergreen type to represent vegetation at the site.

2. 3 Overview of modelled processes in JSM

~~Soil biogeochemistry is modelled by a microbially explicit and vertically resolved SOM model (JSM ,(Yu et al., 2020), Fig. 1 lower panel). All biogeochemical soil pools and processes are modelled for 15 discrete soil layers, along a vertical soil gradient. Soil layer thickness increases exponentially with depth. JSM considers five different SOM pools: dissolved organic matter (DOM), microbial biomass, microbial residues, and organo-mineral associated DOM and microbial residues (Table 1). Depolymerization, DOM uptake and associated biological nutrient mineralization, and inorganic nutrients uptake are affected by the abundance of microbial biomass, either modelled by using forward Michaelis Menten or reverse Michaelis Menten kinetics (Schimel and Weintraub, 2003). Microbes take up carbon from DOM (Fig. 1, process 1). Nutrients are acquired from DOM or by immobilization of soluble nutrients (Fig. 1, process 2). DOM taken by microbes either enters microbial biomass or becomes mineralized, based on element specific use efficiencies. Carbon use efficiency of the microbial biomass varies as a function of nutrient availability between 30 % and 50 %, mimicking a change in microbial decomposer community.~~

~~Mineralized C is emitted from soil as heterotrophic respiration. Soil organic matter and inorganic forms of nutrients are transported between soil layers via water transport (for nutrients and dissolved organic matter) and bioturbation. Microbial decay is modelled as first order decay with a constant turnover time of ~150 days. Dead microbial biomass is partitioned into DOM and microbial residue, corresponding to microbial necromass (Fig. 1, process 3). The fraction of N and P entering DOM is higher than for C, to represent the lower C-to-nutrient ratio in cytoplasma (Schimel and Weintraub, 2003). Additionally, a constant fraction of N is transferred into inorganic soluble pools to mimic grazing on living microbial biomass (Wutzler et al., 2022) (Eq. A1 to A5, Table A2). Decomposition of soluble and woody litter follows first order decay, whereas the depolymerization of polymeric litter (Fig. 1, process 4a) and microbial residue (Fig. 1, process 4b) into DOM is a function of microbial biomass pool and in addition varying enzyme allocation based on microbial nutrient status (Wutzler et al., 2017; Yu et al., 2020). Organo-mineral associated DOM and residue pool are protected from depolymerisation, but are exchanged with the 'free' DOM/ residue pool via first order sorption kinetics (Fig. 1, process 5). Soil solution NH_4 and PO_4 are in adsorption/desorption interaction with soil surfaces, simulated by Langmuir equilibrium (Yu et al., 2023). Adsorption, plant uptake and microbial uptake of soluble nutrients are in direct competition with each other (Tang and Riley, 2013). In addition to biological nutrient mineralization that results from microbial DOM uptake, PO_4 further mobilized through biochemical mineralization via acid phosphatase (Fig. 1, process 6). Biochemical mineralization is regulated by the production of phosphatase, which is assumed to be affected by root and microbial biomass, as well as the C allocation for productions of other enzymes. This process allows for an additional pathway of access to P from microbial residue and both organo-mineral associated pools that cannot be directly depolymerised. As biochemical mineralization does not need complete decomposition of organic substance, it can affect the stoichiometry of target pools. Biochemical mineralization is assumed to be controlled by temperature/moisture and the C: P stoichiometry of the target pools.~~

~~New N enters the system via deposition and asymbiotic N fixation (Fig. 1~~Soil biogeochemistry is modelled by a microbially explicit and vertically resolved SOM model (JSM, (Yu et al., 2020), Figure 2 lower panel, Tab. 1). All biogeochemical soil pools and processes are modelled for 15 discrete soil layers, along a vertical soil gradient. Soil layer thickness increases exponentially with depth. JSM considers five different SOM pools: dissolved organic matter (DOM), microbial biomass, microbial necromass, and organo-mineral associated DOM and microbial necromass (Table 1). Depolymerization, DOM uptake and associated biological nutrient mineralization, and inorganic nutrients uptake are affected by the abundance of microbial biomass, either modelled by using forward Michaelis-Menten or reverse Michaelis-Menten kinetics (Schimel and Weintraub, 2003). Microbes take up C from DOM (Fig. 2, process 1). Nutrients are acquired from DOM or by immobilization of soluble nutrients (Fig. 2, process 2). DOM taken by microbes either enters microbial biomass or becomes mineralized, based on element-specific use-efficiencies. Carbon-use efficiency of the microbial biomass varies as a function of nutrient availability between 30 % and 50 %, mimicking a change in microbial decomposer community. Mineralized C is emitted from soil as heterotrophic respiration. Soil organic matter and inorganic forms of nutrients are transported between soil layers via water transport (for nutrients and dissolved organic matter) and bioturbation. Microbial decay is modelled as first order decay with a constant turnover time of ~150 days. Dead microbial biomass is partitioned into DOM and microbial necromass,

corresponding to microbial necromass (Fig. 2, process 3). The fraction of N and P entering DOM is higher than for C, to represent the lower C-to-nutrient ratio in cytoplasm (Schimel and Weintraub, 2003). Additionally, a constant fraction of N is transferred into inorganic soluble pools to mimic grazing on living microbial biomass (Wutzler et al., 2022) (Eq. A1 to A5, Table A2). Decomposition of soluble and woody litter follows first order decay, whereas the depolymerization of polymeric litter (Fig. 2, process 4a) and microbial necromass (Fig. 2, process 4b) into DOM is a function of microbial biomass pool and in addition varying enzyme allocation based on microbial nutrient status (Wutzler et al., 2017; Yu et al., 2020). Organo-mineral associated DOM and necromass pool are protected from depolymerisation, but are exchanged with the 'free' DOM/ necromass pool via first-order sorption kinetics (Fig. 2, process 5). Soil solution NH_4 and PO_4 are in adsorption/desorption interaction with soil surfaces, simulated by Langmuir equilibrium (Yu et al., 2023). Adsorption, plant uptake and microbial uptake of soluble nutrients are in direct competition with each other (Tang and Riley, 2013). In addition to biological nutrient mineralization that results from microbial DOM uptake, PO_4 is further mobilized through biochemical mineralization via acid phosphatase (Fig. 2, process 6). Biochemical mineralization is regulated by the production of phosphatase, which is assumed to be affected by root and microbial biomass, as well as the C allocation for productions of other enzymes. This process allows for an additional pathway of access to P from microbial necromass and both organo-mineral associated pools that cannot be directly depolymerised. As biochemical mineralization does not need complete decomposition of organic substances, it can affect the stoichiometry of target pools. Biochemical mineralization is assumed to be controlled by temperature/moisture and the C: P stoichiometry of the target pools.

New N enters the system via deposition and asymbiotic N fixation (Fig. 2, process 7) and is lost by gaseous emission and lateral loss. New P enters the systems via atmospheric deposition and weathering from parent material, which is controlled by abiotic and biotic factors. On the other hand, P is made irreversibly unavailable by occlusion or leaves the system by lateral loss.

Table ~~1.~~1: Summary of soil pools in QUINCY-JSM, their turnover times and soil pools they represent.

Pool in Quincy-JSM	Turnover time	Associated soil pools	Microbial availability
Soil organic matter (SOM)			
'free' DOM	emergent	DOM/POM	Direct available
Mineral associated dissolved organic matter ~~(asDOM)~~	emergent	MAOM	Only available for biochemical mineralization (P only)
microbes	150 d	Microbial biomass	/
~~Microbial necromass~~			
Microbial ~~residue~~necromass	emergent	DOM/POM	Available for enzymatic decomposition
Mineral associated microbial ~~residue (asRes)~~necromass	emergent	MAOM	Only available for biochemical mineralization (P only)

Litter pools			
soluble	30 d	litter	Not directly available, turnover into DOM
polymeric	emergent	litter	Available via enzymatic decomposition
woody	2.5 yr	litter	Not directly available, turnover into polymeric litter

385

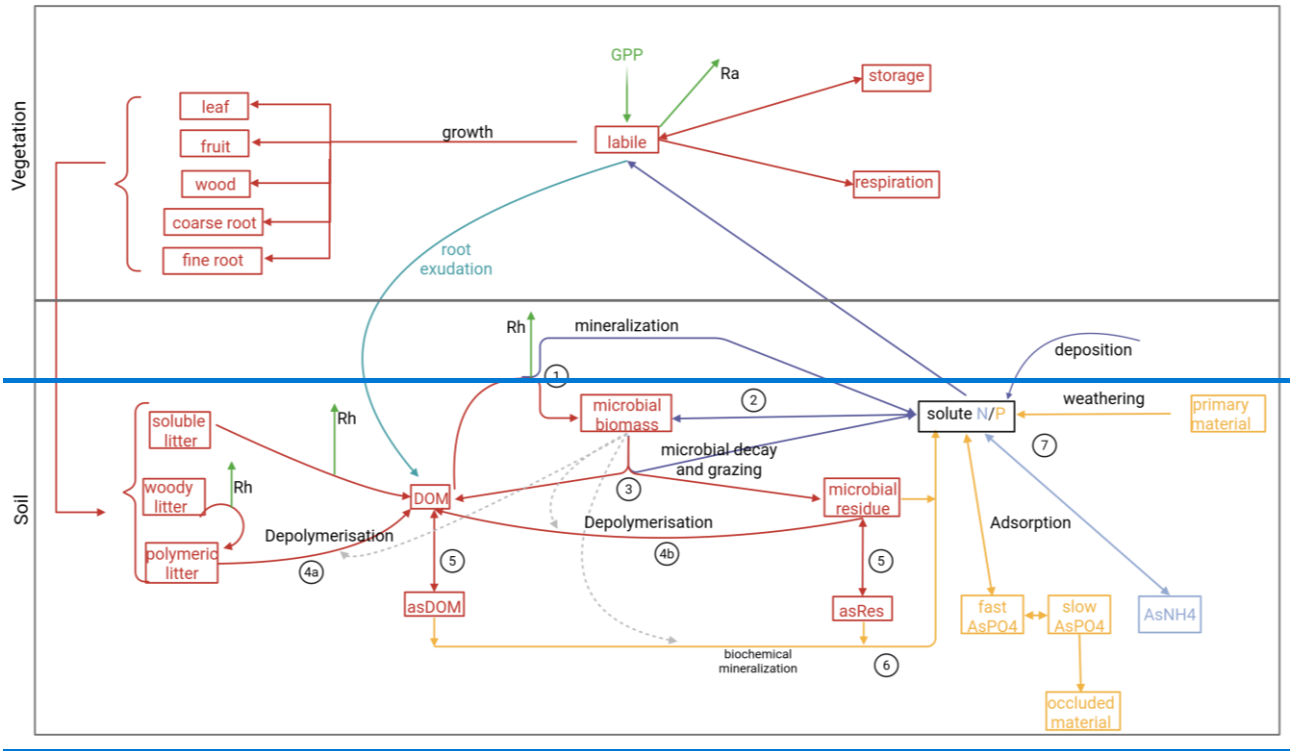

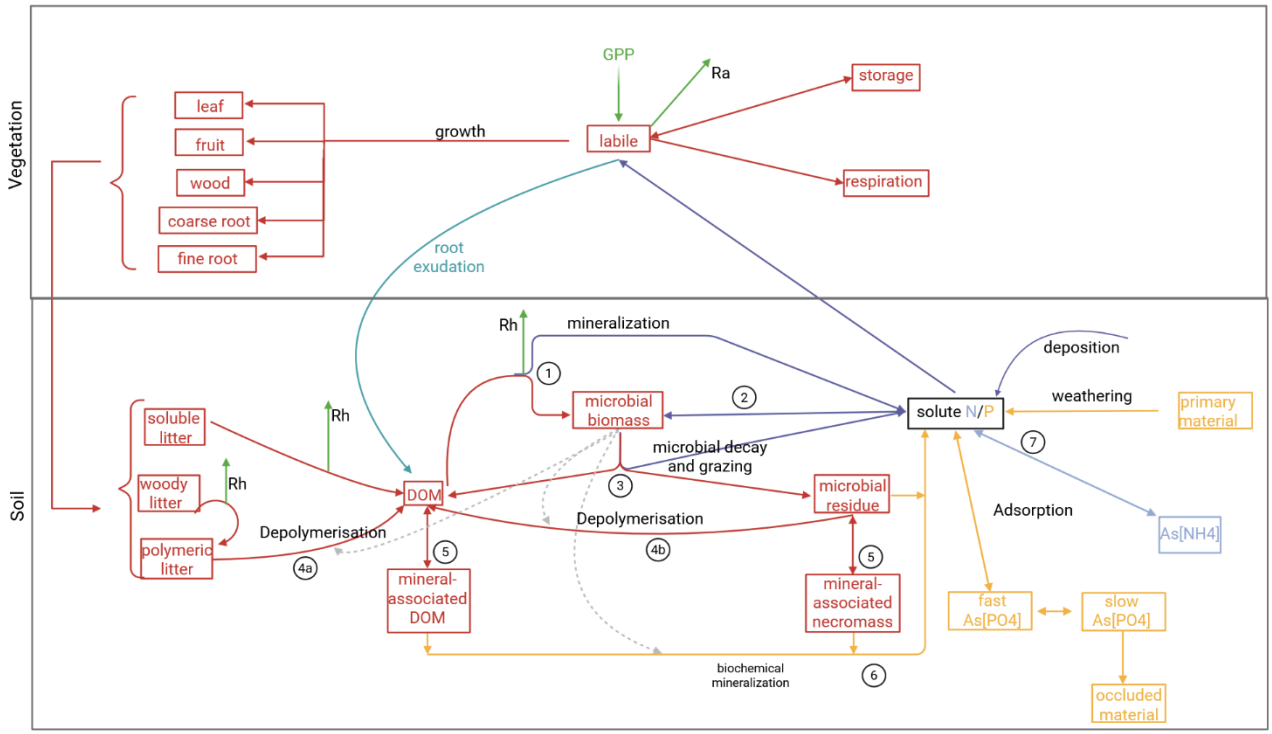

Figure ~~1~~2: Conceptual scheme of plant-soil interactions and soil processes in Quincy-JSM. Gross primary productivity determines carbon uptake by plants. Organic C, N and P can enter the soil via litterfall and root exudation (C and N). Root litterfall and root exudation can enter deeper soil layers, while other litterfall is added to the topsoil layer. Boxes represent pools (clarified in Tab. 1) and solid arrows fluxes. All soil pools and fluxes are simulated for each soil layer. Soil pools of inorganic nutrients with AS[ ] represent mineral-associated pools (sorped to the soil mineral or organic surface). Dashed arrows represent indirect influence of processes by microbes via enzyme allocation. Red arrows represent fluxes of C, N and P. Green arrows represent C only fluxes (heterotrophic respiration, C uptake). Violet arrows represent N and P fluxes. Yellow: only P fluxes; blue: only N fluxes. Modified from Yu et al. (2020). Created with BioRender.com

2.4 New implementation of dynamic root exudation in QUINCY-JSM

To improve the representation of soil-microbe interactions in QUINCY-JSM, we implemented a root exudation module (Fig. ~~2~~3). Root exudation is modelled as direct, respiration-free flux from the plant labile pool to the soil DOM pool, with a C: N stoichiometry corresponding to the current C: N ratio of the ~~labile pool (Fig. 1). We assume that there is no exudation of P.~~plant labile pool (Fig. 2). As we assume that root exudation mainly consists of carbohydrates, amino acids and carboxylates (Jones et al., 2004) we do not model exudation of P. Implementation of root exudation thus reduces the C and N available for tissue growth and storage and thereby respiration despite no change in the respiration calculations. From the DOM pool, the possible pathways for root exudates are: direct consumption by microbes, adsorption towards the mineral surface or leaching.

The rate of root exudation [gC m^{-2} s^{-1}] is modelled as a function of fine root respiration [gC m^{-2} s^{-1}] and plant nutrient status (Eq. 1). We assume that physiologically active roots have increased exudation rate, and chose root respiration as proxy for tissue activity. ~~Root respiration is simulated as function of root N mass and root temperature. Observations support the positive~~

~~relationship between root exudation and root respiration or root N content (Akatsuki and Makita, 2020; Li et al., 2021; Sun et al., 2017, 2021). Distribution of root respiration and exudation across the vertical soil profile follows the simulated root distribution. In addition, the slope of the linear relationship between root exudation and root respiration is assumed to be a function of nutrient status of the plant (Ataka et al., 2020; Prescott et al., 2020): C-to-nutrient ratios in the labile pool that are higher than average C-to-nutrient ratios required for tissue production will result in higher exudation (Eq.~~ Root respiration is simulated as a function of root N mass and root temperature. Observations support the positive relationship between root exudation and root respiration or root N content (Akatsuki and Makita, 2020; Li et al., 2021; Sun et al., 2017, 2021). Distribution of root respiration and exudation across the vertical soil profile follows the simulated root distribution. In addition, the slope of the linear relationship between root exudation and root respiration is assumed to be a function of nutrient status of the plant (Ataka et al., 2020; Prescott et al., 2020): C-to-nutrient ratios in the plant labile pool that are higher than average C-to-nutrient ratios required for tissue production will result in higher exudation (Eq. 2).

$$CEX = s * \beta_{mavg} * R_{fr} \quad (1)$$

~~Where CEX is C root exudation in [gC m^{-2} s^{-1}], R_{fr} is fine root respiration in [gC m^{-2} s^{-1}], s[unitless] is a unitless parameter that determines maximum slope and β_{mavg} [unitless] is the 7-days moving average of a scalar β reflecting nutrient shortage and surplus C in the labile pool (range 0 -1) (Thum et al., 2019), calculated by:~~

Where CEX is C root exudation in [gC m^{-2} s^{-1}], R_{fr} is fine root respiration in [gC m^{-2} s^{-1}], s[unitless] is a unitless parameter that determines maximum slope and β_{mavg} [unitless] is the 7-days moving average of a scalar β reflecting nutrient shortage and surplus C in the labile pool (range 0 -1) (Thum et al., 2019), calculated by:

$$\beta = 1 - e^{-(\lambda * \Phi)^{kex}} \quad (2)$$

Where λ [unitless] and k_{ex} [unitless] are parameters (Table 2 for values used in this study) and the modifier ~~$\Phi_C \Phi_N \Phi_P$~~ $\Phi\Phi$ represents C excess, or N and P deficiency, respectively:

$$\Phi = \Phi_C * Max(\Phi_N, \Phi_P, 1) \quad (3)$$

Where ~~$\Phi_C \Phi_C$~~ is calculated as the ratio of the actual C labile pool size (C_{lab}) [molC m-2]), compared to the target pool size (C^*_{lab} in [gC m-2]). ~~$\Phi_N \Phi_N$~~ and ~~$\Phi_P \Phi_P$~~ are calculated as the ratio of labile pool stoichiometry ($\left({}^{C}/_{N}\right)_{lab}, \left({}^{C}/_{P}\right)_{lab}$[unitless]) and labile pool target stoichiometry ($\left({}^{C}/_{N}\right)^{*}_{lab}, \left({}^{C}/_{P}\right)^{*}_{lab}$[unitless]). The target labile C pool size (C^*_{lab}) is calculated as the maximum of either the weekly sum of GPP or maintenance respiration. The N and P target labile pool sizes are calculated based on the stoichiometric last 7-day growth requirements in N and P to convert C^*_{lab} into plant biomass. The modifiers are given by:

~~$$\Phi_C = MAX\left(1, \frac{C_{lab}}{C^*_{lab}}\right) \quad (4)$$~~

$$\Phi_N = \frac{\left(C/N\right)_{lab}}{\left(C/N\right)^{*}_{lab}} \quad (5)$$

$$\Phi_P = \frac{\left(C/P\right)_{lab}}{\left(C/P\right)^{*}_{lab}} \quad (6)$$

$$\Phi_N = \frac{\left(C/N\right)_{lab}}{\left(C/N\right)^{*}_{lab}} \quad (6)$$

As a result, Φ increases under conditions in which labile C accumulates in the labile pool, and if the stoichiometry of the labile pool is wider than the target stoichiometry. The smallest value Φ can take is 1, leading to values of β close to zero. We constrained β to values larger than 0.0125 (β_{min}) reflecting a minimal root exudation flux even at nutrient saturated conditions.

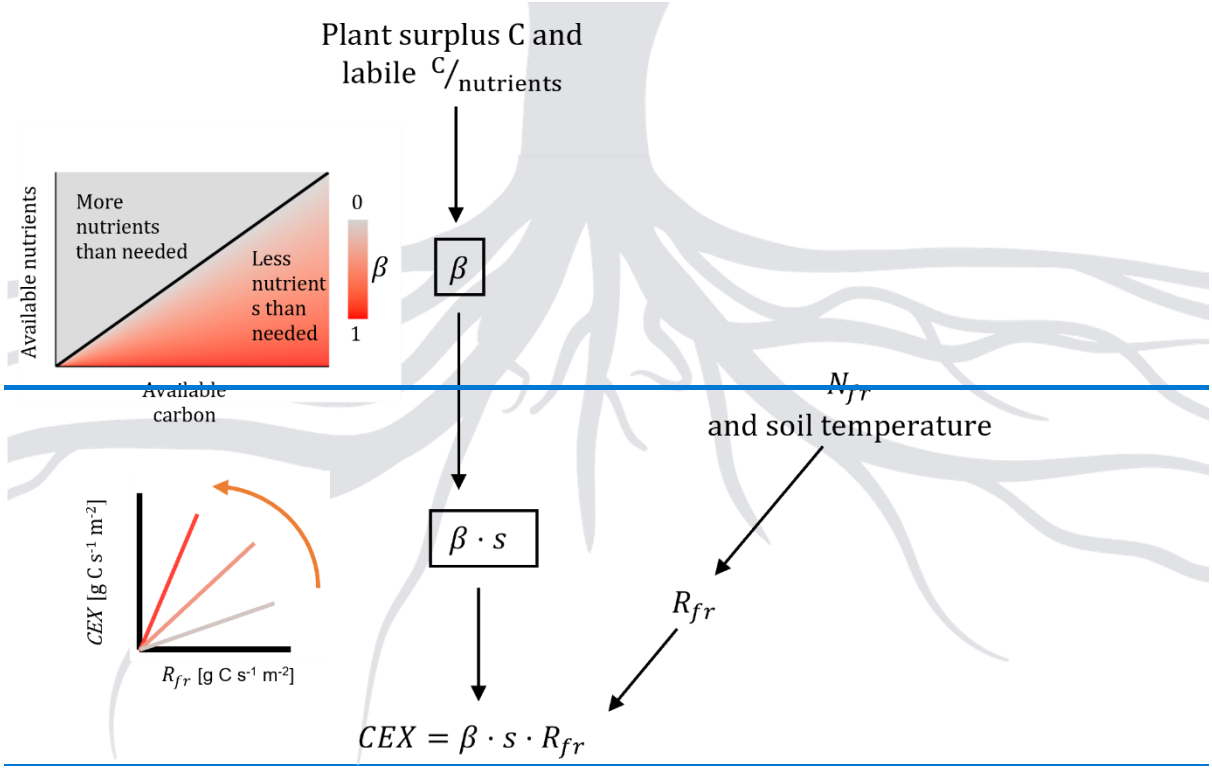

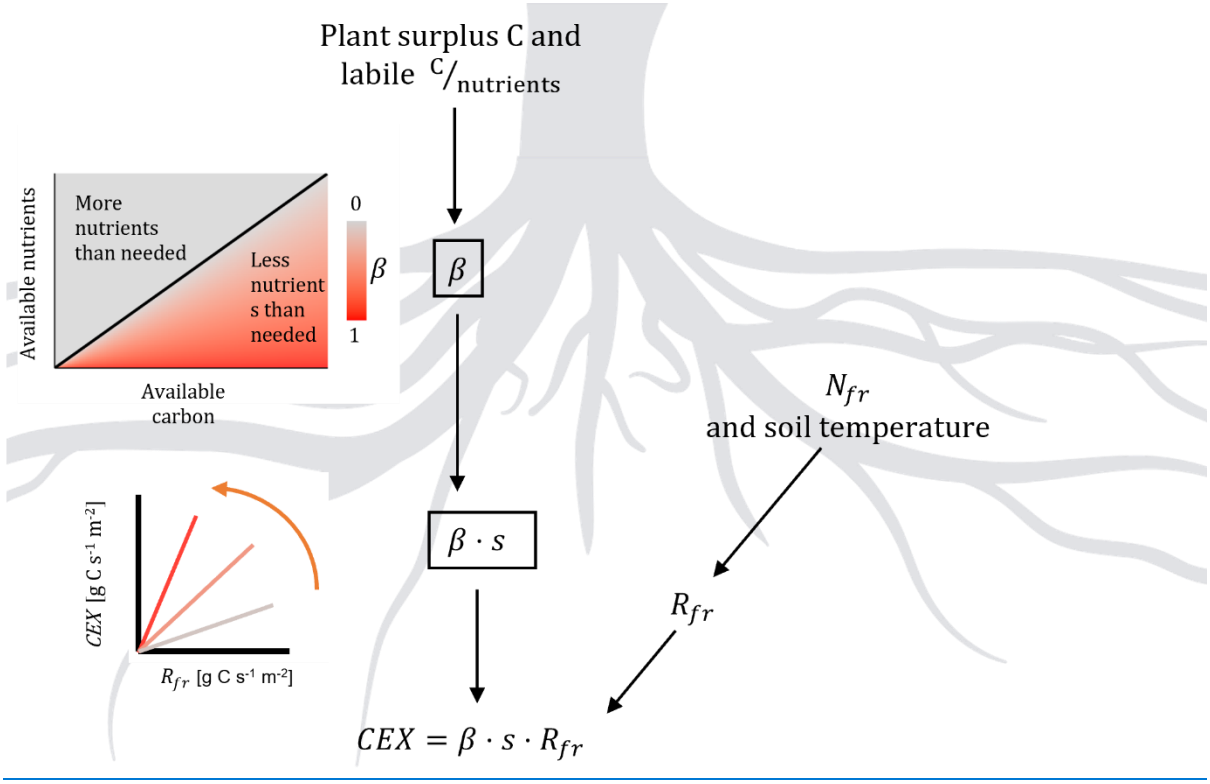

Figure ~~2~~3: Conceptual model of the nutrient modifier for carbon root exudation (CEX). Detailed description in Eq. 1-6. CEX is calculated proportional to fine root respiration (R_{fr}). Higher C surplus or higher C-to-nutrient ratio than needed for growth leads to increase in the modifiers. This is translated into a steeper slope for the relationship between root exudation rate and fine root respiration. Fine root respiration is calculated by fine root N content (N_{fr}), accounting for the influence of temperature on maintenance respiration. Created with BioRender.com

Table ~~2~~2: dynamic root exudation parameters

Parameter	Description	Value used for this simulation	reference
s	Slope conversion factor/ maximum slope	4	This study
β_{min}	Minimal value for β	0.0125	This study
k_{ex}	Weibull parameter for beta	2	Thum et al., 2019; following sink limitation
λ	Weibull parameter for beta	0.05	This study; following sink limitation

2.4 Model application

We apply our model to the EucFACE experiment. 2.5 Our goal is to quantify competing soil mechanisms on C storage for increased root exudation under eCO_2 in a P-limited forest. We first evaluate our model against field measurements for ambient conditions, then evaluate our results against measured CO_2 effects on plant C allocation to see if our model can simulate the suggested increase in root exudation under eCO_2. We further quantify the simulated increase in belowground C allocation and its effect on microbial growth. To assess feedback via microbial nutrient acquisition strategies we identify sources for microbial growth in C, N and P and potential shifts in sources with elevated CO_2. We conclude by comparing simulated influx and outflux of microbial necromass C, N and P pools and their turnover rates, for ambient and elevated conditions.

2.5 EucFACE experimental site and measurement data

The EucFACE site is located in Western Sydney, Australia (33° 37′ S, 150° 44′ E, 30 m in elevation) in a mature eucalypt woodland. For a detailed description of the site see (Drake et al., 2016; Ellsworth et al., 2017). The site has a subtropical transitional climate with an annual average temperature of 17 °C and mean precipitation of 800 mm yr^{-1}. Overstorey vegetation is dominated by *Eucalyptus tereticornis*, while understorey vegetation consists of a diverse mixture of shrubs, graminoids and forbs dominated by *Microlaena stipoides* (Piñeiro et al., 2020).

The soil is characterized as aeric podosol with a loamy sand texture up to 50 cm and a sandy clay loam texture in deeper horizons. The soil has a slightly acidic pH and low fertility (Crous et al., 2015; Ross et al., 2020). Previous experiments showed that plant growth is P limited (Crous et al., 2015). Available soil P, and plant P to soil P ratio are similar to tropical and subtropical ecosystems (Jiang et al., 2024b).

The EucFACE experiment consists of 6 FACE rings, with 25 m diameter. Three rings received ambient CO_2 levels and three rings were exposed to elevated CO_2 levels (ambient +150 ppm). In 2012 CO_2 was stepwise increased over a period of six months with an increase of 30 ppm every 5 weeks. In February 2013 the CO_2 concentration in the experiment rings reached their target of +150 ppm (Drake et al., 2016). Since then, the ecosystem has been continuously exposed to eCO_2. Measurements used in this study were taken between 2013 – 2019. Major C pools, NPP and NEP under ambient conditions were measured between 2013 – 2016. A detailed description on measurement methods is provided in (Jiang et al., 2020) and (Jiang et al., 2024b). Soil respiration is taken from (Drake et al., 2018) and supplemented by additional information from (Jiang et al., 2020).

2.6 Model parameterization

We parameterized the model following in situ based observations for *E. tereticornis*, taken under ambient conditions from 2013 – 2019, provided by Jiang et al., 2024 (Table A1). As no direct measurements of root exudation exit for this site, we

~~calibrated s and β_{min} based on the site C-budget and soil respiration data for ambient conditions from 2013-2016 (Jiang et al., 2020).~~

EucFACE experimental site and measurement data

The EucFACE site is located in Western Sydney, Australia (33° 37′ S, 150° 44′ E, 30 m in elevation) in a mature eucalypt woodland. For a detailed description of the site see (Drake et al., 2016; Ellsworth et al., 2017). The site has a subtropical transitional climate with an annual average temperature of 17 °C and mean precipitation of 800 mm yr^{-1}. Overstorey vegetation is dominated by *Eucalyptus tereticornis*, while understorey vegetation consists of a diverse mixture of shrubs, graminoids and forbs dominated by *Microlaena stipoides* (Piñeiro et al., 2020).

The soil is characterized as aeric podosol with a loamy sand texture up to 50 cm and a sandy clay loam texture in deeper horizons. The soil has a slightly acidic pH and low fertility (Crous et al., 2015; Ross et al., 2020). Previous experiments showed that plant growth is P-limited (Crous et al., 2015). Available soil P, and plant P to soil P ratio are similar to tropical and subtropical ecosystems (Jiang et al., 2024b).

The EucFACE experiment consists of 6 FACE rings, with 25 m diameter. Three rings received aCO_2 levels and three rings were exposed to eCO_2 levels (ambient +150 ppm). In 2012 CO_2 was stepwise increased over a period of six months with an increase of 30 ppm every 5 weeks. In February 2013 the CO_2 concentration in the experiment rings reached their target of +150 ppm (Drake et al., 2016). Since then, the ecosystem has been continuously exposed to eCO_2. Measurements used in this study were taken between 2013 - 2019. Major C pools, net primary production (NPP) and net ecosystem production (NEP) under ambient conditions were measured between 2013 - 2016. A detailed description on measurement methods is provided in (Jiang et al., 2020) and (Jiang et al., 2024b). Soil respiration is taken from (Drake et al., 2018) and supplemented by additional information from (Jiang et al., 2020).

2.6 Model parameterization

We parameterized the model following in situ-based observations for *E. tereticornis*, taken under ambient conditions from 2013 - 2019, provided by (Jiang et al., 2024a) (Table A1). As no direct measurements of root exudation exist for this site, we calibrated s and β_{min} to reproduce GPP, biomass and soil respiration for ambient conditions from 2013-2016 (Jiang et al., 2020) (Table B1). By this we limit the size of the root exudation flux. We ensured that the modelled exudation flux still responded to variations in the size and stoichiometry of the labile plant pool, i.e., that the flux was not controlled by empirical bounds of maximum exudation, implying that it is sensitive to changes in plant carbon and nutrient status induced by eCO_2.

2.7 Model set-up and analysis

Simulations were done for 500 years of spin-up to reach quasi-equilibrium, with a subsequent simulation length of 325 years afterward from 1700-2024, following the modelling protocol from~~: (Jiang et al., 2024a)~~ (Jiang et al., 2024a): Meteorological forcing for 1700-2012 and 2019-2024 was gained from repeated and randomized observations from 2013-2018, while CO_2, N

and P deposition followed historic values. Forcing for spin-up repeated the first 30 years of the forcing data under 280 ppm CO_2. As a result of forcing from randomized observations and ~~meterological~~meteorological extremes in observation years, and contrary to observations, our model showed a downward trend in total vegetation C from 5900 gC m^{-2} to 5700 gC m^{-2} between the ~~year 2012 and 2019 (Fig. B1)~~years 2012 and 2019 (Fig. B1). The trend did not cause major pulses in nutrient input and therefore unlikely reflects in CO_2 effects on nutrient-dependent root exudation and microbial C cycling.

~~The mean yearly change in pools and mean yearly fluxes for simulations were calculated for 2013-2019. We calculated the effect of eCO_2 by subtracting results under ambient CO_2 conditions from result under elevated CO_2. We compared the results to observed effects of eCO_2 on the C budget described in (Jiang et al., 2020).~~

The mean yearly change in pools and mean yearly fluxes for simulations were calculated for 2013-2019. We calculated the effect of eCO_2 by subtracting results under aCO_2 conditions from results under eCO_2. We compared the results to observed effects of eCO_2 on the C budget described in (Jiang et al., 2020).

We trace the fate of the ~~additional~~additionally assimilated ~~carbon~~C under eCO_2, through the ecosystem~~, standardizing~~. We standardize fluxes as the percentage of additional overstorey GPP for both simulations and observations. ~~For aboveground fluxes~~The model currently only simulates forests without understorey vegetation. To maintain comparability, we use ~~the~~observations from overstorey aboveground biomass production, overstorey autotrophic respiration and overstorey changes in vegetation C pools. However, for belowground fluxes, i.e., heterotrophic respiration, root respiration, root biomass production and changes in soil C pools we cannot differentiate between overstorey and understorey origin. ~~Therefore, we~~We still standardize them as the percentage of additional overstorey GPP but are therefore likely to overestimate the observed change per additional overstorey GPP under eCO_2 in ~~respiration~~soil fluxes.

For model analysis, microbial growth was calculated by the flux from the DOM to the microbes ($F^X_{DOM\rightarrow MIC}$ [gX m^{-2} s^{-1}]), adjusted by the current carbon- or nutrient--use efficiency (XUE [unitless]) for each soil layer separately. Most measurements for soil processes at EucFACE were taken in topsoil layers, which are also typically more active. We therefore separate model outputs between topsoil (upper 50 cm) and deep soil (below 50 cm). We estimate the contribution of fluxes from root exudation, microbial recycling upon death, and decomposition of soluble litter, polymeric litter, and microbial ~~residue~~necromass to microbial growth $F^X_{i\rightarrow growth}$ [gX m^{-2} s^{-1}] for topsoil by their relative production of DOM:

$$F^X_{i\rightarrow growth} = F^X_{DOM\rightarrow MIC} * XUE * \frac{F^X_{i\rightarrow DOM}}{\sum_{i\ in\ I} F^X_{i\rightarrow DOM}} \quad (6)$$

With I being the set of all contributing pools and $F^X_{i\rightarrow DOM}$ [gX m^{-2} s^{-1}] being the according fluxes from these pools towards DOM. Similarly, we calculated heterotrophic respiration derived from the depolymerization of ~~residue carbon~~necromass C, $Rh_{\text{~~priming~~}priming}$ [gC m^{-2} s^{-1}] as:

$$Rh_{\text{priming}} = F^C_{DOM\rightarrow MIC} * (1 - CUE) * \frac{F^X_{\text{~~residue}\rightarrow DOM}}{\sum_{i\ in\ I} F^C_{i\rightarrow DOM}} \frac{F^X_{necromass\rightarrow DOM}}{\sum_{i\ in\ I} F^C_{i\rightarrow DOM}} \quad (7)$$

2.7.1 Turnover times

To account for ~~adaption~~adaptation to sudden CO_2 increase, turnover times were calculated for 2015-2019. ~~Ecosystem carbon turnover time τ_{ES} [yr] was calculated as~~

~~$$\tau_{ES} = \frac{C_{total}}{R_{Eco}} \quad (9)$$~~

~~Where C_{total} [gX m^{-2}]. is the combined plant and topsoil carbon and R_{Eco} [gX m^{-2} yr^{-1}] the ecosystem respiration.~~ Soil turnover times τ_{soil}^{X} [yr] were calculated by dividing pool sizes with their respective outgoing fluxes as

$$\tau_{soil}^{C} = \frac{C_{litter} + C_{soil}}{R_h} \quad (8)$$

$$\tau_{soil}^{N} = \frac{N_{litter} + N_{soil} + N_{inorg}}{leaching_N + U_N^{plant} + emission_N} \quad (9)$$

$$\tau_{soil}^{P} = \frac{P_{litter} + P_{soil} + P_{inorg}}{leaching_P + U_P^{plant} + occlusion} \quad (10)$$

Where X_{litter} are the combined litter pools; X_{soil} are the combined organic topsoil pools and X_{inorg} as combined inorganic topsoil pools [gX m^{-2}]. In the denominator are processes removing N or P from topsoils, e.g., heterotrophic respiration R_h, leaching, occlusion, emission and plant uptake U_X^{plant} [gX m^{-2} yr^{-1}].

~~Necromass~~necromass turnover $\tau_{necromass}^{X}$ [yr] time was calculated as

$$\tau_{necromass}^{C} = \frac{C_{necromass}}{F_{residue \rightarrow DOM}^{C}} \quad (11)$$

$$\tau_{necromass}^{N} = \frac{N_{necromass}}{F_{residue \rightarrow DOM}^{N}} \quad (12)$$

$$\tau_{necromass}^{P} = \frac{P_{necromass}}{F_{residue \rightarrow DOM}^{P} + Biochem_{min_{necro}}} \quad (13)$$

Where $X_{necromass}$ [gX m^{-2}] is the combined pool of microbial ~~residues~~necromass and mineral-associated microbial ~~residues~~necromass and $Biochem_{min_{necro}}$ [gP m^{-2} yr^{-1}] is the biochemical mineralization from these pools.

3 Results

3.1 Model evaluation

3.1.1 Model performance under ambient conditions

~~Simulated vegetation and soil pools size and stoichiometry and vegetation fluxes under ambient conditions compared well, overall, with observations from the three control plots for the period of 2013 - 2016 (Table B1, B2). Simulated GPP had a 9 % bias, but was still within standard deviation of the observation based estimate. There are no direct observations of root exudation at EucFACE but the model estimated mean carbon root exudation (CEX) to be 366 gC m^{-2} yr^{-1} for ambient conditions, equivalent to 22 % of GPP. Exudation rate per gC fine root biomass amounted to 2 gC (gC fr)$^{-1}$ yr^{-1} and ranged from 0.1 mgC (gC fr)$^{-1}$ d^{-1} to 16 mgC (gC fr)$^{-1}$ d^{-1} on daily level, with an average C to N ratio of 176 gC gN^{-1}. Modelled soil respiration under ambient conditions is around 1207 gC m^{-2} yr^{-1}, and thus slightly larger than the observed range of 1097 (+-86) gC m^{-2} yr^{-1}. The model estimated that soil respiration was 61% heterotrophic and 39 % autotrophic root respiration, which agree well with observations that estimated 56 % and 44 %, respectively (Jiang et al., 2020).~~

Simulated vegetation and soil pools size and stoichiometry, and ecosystem fluxes under ambient conditions are in the range of observations from the three control plots for the period of 2013 - 2016 (Table B1, B2). Simulated GPP had a 9 % bias, but was still within standard deviation of the observation-based estimate. However, the model underestimated BP by 25 %. Modelled soil respiration under ambient conditions was around 1207 gC m^{-2} yr^{-1}, and thus slightly larger than the observed range of 1097 (+-86) gC m^{-2} yr^{-1}. The model estimated that soil respiration was 61% heterotrophic and 39 % autotrophic root respiration, which agree well with observations that estimated 56 % and 44 %, respectively (Jiang et al., 2020). There are no direct observations of root exudation at EucFACE but the model estimated mean C root exudation (CEX) to be 366 gC m^{-2} yr^{-1} for ambient conditions, equivalent to 22 % of GPP. Exudation rate per gC fine root biomass amounted to 2 gC (gC fr)$^{-1}$ yr^{-1} and ranged from 0.1 mgC (gC fr)$^{-1}$ d^{-1} to 16 mgC (gC fr)$^{-1}$ d^{-1} on daily level, with an average C to N ratio of 176 gC gN^{-1}.

3.1.2 Allocation ~~patterspatterns~~ of additionally acquired GPP

Our model simulated an increase in GPP and root exudation under eCO_2 (Table B3). Elevated CO_2 increased simulated annual GPP (2013-2019) by 22 %. Simulated annual root exudation and BP increased 30 % and 33% respectively and therefore increased stronger than GPP (Fig B2). While our simulations indicate, as suggested by observations, an increase in belowground allocation through root exudation, the model overestimated the observed effect in GPP (12%) and biomass production (3%). Soil respiration increased by 13%, agreeing with the observed 12% increase, although remaining lower than the 22% GPP increase. Overall, eCO_2 caused only minor shifts in plant C allocation (Fig. B2).

We further traced the fate of additional GPP and compared it with the findings from Jiang et al (2020) to see if our implementation improves plant C allocation under eCO_2 (Fig. 4, detailed numbers in supplement, Fig. B3). Our model estimated that vegetation allocated 30 % of additional GPP under eCO_2 to root exudates, providing a possible explanation for the unidentified flux in observations (Fig. 4, *Ra+BP+CEX*). Since in our model eCO_2 increased BP, the model allocated,

contrary to observations, 33 % of additional GPP to BP, and increased vegetation pools under eCO_2 (Fig. 4, *Ra+BP+CEX, change in C pools*). Our model simulated that 28 % (Fig. 4b, *Ra+Rh*), lower than the observed 56 %, of additional GPP was respired as soil heterotrophic respiration (*Rh*). This difference may result from underestimation of the effect of eCO_2 in root exudation and overestimation of allocation to BP, but may also be caused by normalizing the observed soil respiration response with GPP response derived solely from the overstory. Observations indicated a decrease of topsoil organic C equal to -12 % of the change in GPP under eCO_2 during the experimental phase, but the result was not significant. In our simulation, eCO_2 led to an increase of topsoil C equal to 3 % of the change in GPP. However, the model also simulates an accumulation of C in deeper soil layers equal to 7 % of the additional C uptake, likely caused by increased root exudation in deeper soil layers. Considering the strong variation in measurements regarding soil organic C (SOC) pools we assume that our simulations are in agreement with observations regarding topsoil C pools. Overall, our model supports the previous hypothesis from observations that a large portion of additional GPP was allocated to root exudation but caused only minor increases in SOC in topsoils (Jiang et al., 2020, 2024a).

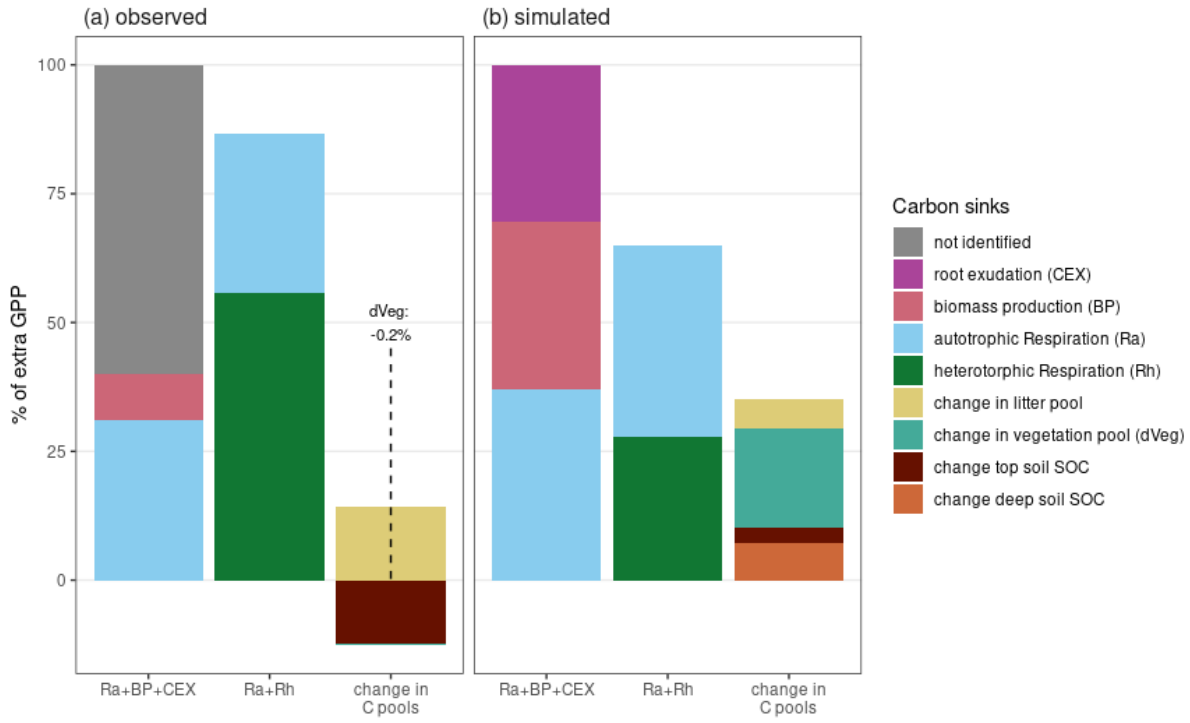

Figure 4 Comparison of the fate of additional sequestered C under CO_2 as percentage of increased overstorey gross primary productivity (GPP) for a) observations (2013-2016) (Jiang et al., 2020) and b) simulations (2013-2019). For simulations additional GPP is transferred into autotrophic respiration (Ra), biomass production (BP) and root exudation (CEX). For

observations CEX was not measured. ~~Observations indicated a major increase in belowground at the expense of aboveground biomass production. The model showed only slight changes in plant carbon allocation under eCO_2 (Fig. B2) but captured the increase in belowground C allocation with a 30 % increase in CEX, compared to a 22 % increase in GPP. Additionally, the model simulates a stronger plant CUE under eCO_2, as BP increased stronger than GPP. The responses of fluxes to CO_2 were considerably larger in the model than in the observations, starting with a higher GPP response (Table B3). QUINCY JSM simulations predicted an average 22 % increase of annual GPP under elevated CO_2 during 2013-2019, which represents an overestimation in comparison to the 12 % GPP stimulation shown in the observations (Jiang et al., 2020). Consequently, simulated CO_2 effects on other ecosystem fluxes were higher than observations. Modelled root exudation increased 30 % (Fig. B3), and modelled biomass production increased 33 % although observations only measured a 3 % increase in BP. Both BP and CEX increase more than GPP, therefore allocation to these fluxes has increased as a result of smaller requirement for autotrophic respiration. Soil respiration increased by 13%, agreeing with the observed 12% increase, although remaining lower than the 22% increase in GPP.~~

~~**Implementation of root exudation in QUINCY JSM improved allocation of additional GPP under e CO_2 but still overestimates increase in vegetation pools due to overestimation of the CO_2 effect on BP (Fig. 3). Of the additional GPP under elevated CO_2, 60 % could not be measured but were assigned as root exudation (Fig. 3a, *Ra+BP+CEX*). Our model estimates that vegetation allocates 30 % of additional GPP to root exudates, providing a possible explanation for the unidentified flux (Fig. 3b, *Ra+BP+CEX*). Implementation of root exudation improved allocation of C towards biomass production (BP) and autotrophic respiration (Ra) compared to simulations without root exudation, as it reduced the contribution of these fluxes from 49 % to 33 % and from 51 % to 37 %, respecively (Fig. B4, Fig.~~ Ecosystem respiration is composed of autotrophic respiration Ra and heterotrophic respiration Rh. Change in ecosystem Cpools is composed of change in topsoil organic C (10 cm for observation, top 50 cm for simulation), change in deep soil SOC (no observations), change in litter pool and change in vegetation (dVeg).

3.2 ~~B5).~~

~~In observations the increase in heterotrophic respiration corresponded to 56 % of the additional overstorey GPP (Fig. 3a, *R*). Implementation of root exudation improved the simulated contribution of heterotrophic respiration (Fig. B4, Fig. B5), but still underestimates the eeffect as only 28 % of additional GPP is emitted through increased heterotrophic respiration (Fig. 3b, *R*), possibly as a result of the underestimation of the effect in allocation towards root exudation.~~

~~Observations indicated a decrease of topsoil organic carbon equal to -12 % of the change in GPP under eCO_2 during the experimental phase, but the result was not significant. In our simulation eCO_2 led to an increase of topsoil equal to 3 % of the change in GPP. However, the model also simulates an accumulation of C in deeper soil layers equal to 7 % of the additional C uptake. Considering the strong variation in measurements regarding soil organic C (SOC) pools we assume that our simulations are in agreement with observations regarding topsoil C pools.~~

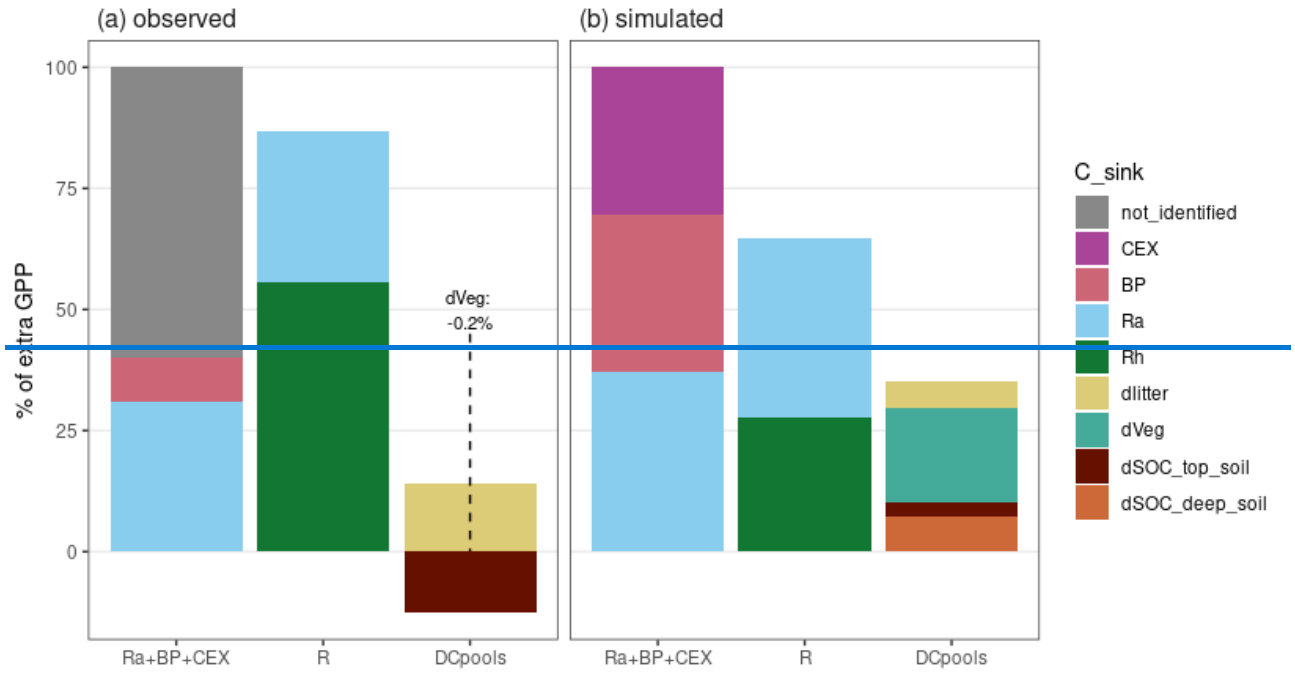

~~**Figure 3: Comparison of the fate of additional sequestered C under CO_2 as percentage of increased overstorey gross primary productivity (GPP) for a) observations (2013-2016) (Jiang et al., 2020) and b) simulations (2013-2019). For simulations additional GPP is transferred into autotrophic respiration (Ra), biomass production (BP) and root exudation (CEX). For observations CEX was not measured. Ecosystem respiration (R) is composed of heterotrophic respiration Rh and autotrophic respiration Ra. Change in ecosystem carbon pools is composed of change in topsoil organic C (dSOC_top_soil top 10 cm for observation, top 50 cm for simulation), change in deep soil SOC (dSOC_deep_soil, no observations) change in litter (dlitter) and change in vegetation (dVeg).**~~

Simulated effects of eCO_2 on ~~soil biogeochemistry~~microbial processes

3.2.1 Microbial growth ~~dynamics~~and respiration

In the model, eCO_2 increased belowground input disproportionally through high root exudation, increasing heterotrophic respiration and microbial growth (Fig. 5, detailed numbers in supplement). Our model suggests that under ambient conditions 45 % of C flux into soils originated from root exudation. ~~However more than half of these got directly respired, increasing the fraction~~Heterotrophic respiration under aCO_2 matched input to 92 %. The majority of heterotrophic respiration ~~originating from root exudation.~~(54 %) originated from decomposition of litter and microbial recycling on turnover. Microbial growth ~~increased by 14 % in topsoil layers but increased accumulation of C in soil pools is~~occurred mostly ~~caused by sequestration~~ in ~~deeper~~top soil layers~~, with less microbial activity (Fig. 4).~~. In the simulation, eCO_2 ~~led to an increase in~~ increased both biomass production and root exudation, resulting in an 20 % increase ~~in soil C input of (~~158 gC m^{-2} yr^{-1}~~. This equals an increase of 20 %)~~ in soil C input compared to ambient conditions. ~~While input under ambient treatment was composed of 45 % root exudation, the~~This additional C input under eCO_2 was composed of 70 % root exudation and ~~to 30 % litter (Fig. 4, *soil C input*). At the same time, eCO_2 increased heterotrophic respiration by 101 gC m^{-2} yr^{-1}. Under ambient conditions 92 % of C~~

~~input was respired. Due to change of input composition and input into deeper soil layers through root exudation, only 64 % of the additional C input into the soil system was emitted as additional heterotrophic respiration. We partitioned the additional heterotrophic respiration under eCO_2 into three components. More than 50 % of the additional heterotrophic respiration originated from respiration of root exudates (Rh_CEX), 15 % from depolymerisation of microbial necromass (Rh_res), i.e., microbial residues (+ 9 % increase compared to ambient conditions), and the rest from respiration of recycled microbial biomass, soluble and polymeric litter and degradation of woody biomass (Rh_other). The direct loss of more than 50 % of additional root exudation suggests that in the model~~30 % litter (Fig. 5, *soil C input*). The additional heterotrophic respiration (Fig. 5, *Heterotrophic respiration*) was to 50 % driven by respiration of fresh root exudation, suggesting that root exudates in topsoil layers are directly consumed by microbes, and then respired according to the assumptions for CUE. In our model, CUE for microbial ~~carbon use efficiency, that~~growth is dependent on the stoichiometric imbalance ~~of~~ between the source material and microbial biomass, and constrained within a range of 30% to 50%. Further 15 % of additional heterotrophic respiration under eCO_2 were caused by decomposition of necromass, i.e., priming.

~~Increased input of C increased microbial growth by 53 gC m^{-2} yr^{-1}, which is equivalent to 34 % of the additional C input, and represents a 14 % increase over ambient conditions (Fig. 4, *microbial growth*). Although the increase in microbial growth was most prevalent in topsoil, it was not accompanied by an increase in soil organic C. Instead, eCO_2 led only to an increase in 10 gC m^{-2} yr^{-1} in topsoil C, equivalent to 6 % of the additional C input, indicating that microbial increased decomposition for nutrient acquisition offset necromass build up. As root exudation followed root distribution, increased root exudation resulted in increased C input into deeper soil layer. Therefore additional 26 gC m^{-2} yr^{-1} accumulated in deeper soil layers. However, small microbial growth suggests that the underlying mechanism is the sorption of additional DOC input to mineral surfaces. As microbes did not decompose most of additional litter input over the experimental phase, eCO_2 resulted in an increase of 20 gC m^{-2} yr^{-1} in litter pools (Fig. 4, *change in C pools*). The results indicate that root exudates and depolymerization of necromass are valuable sources for microbial growth under eCO_2.~~

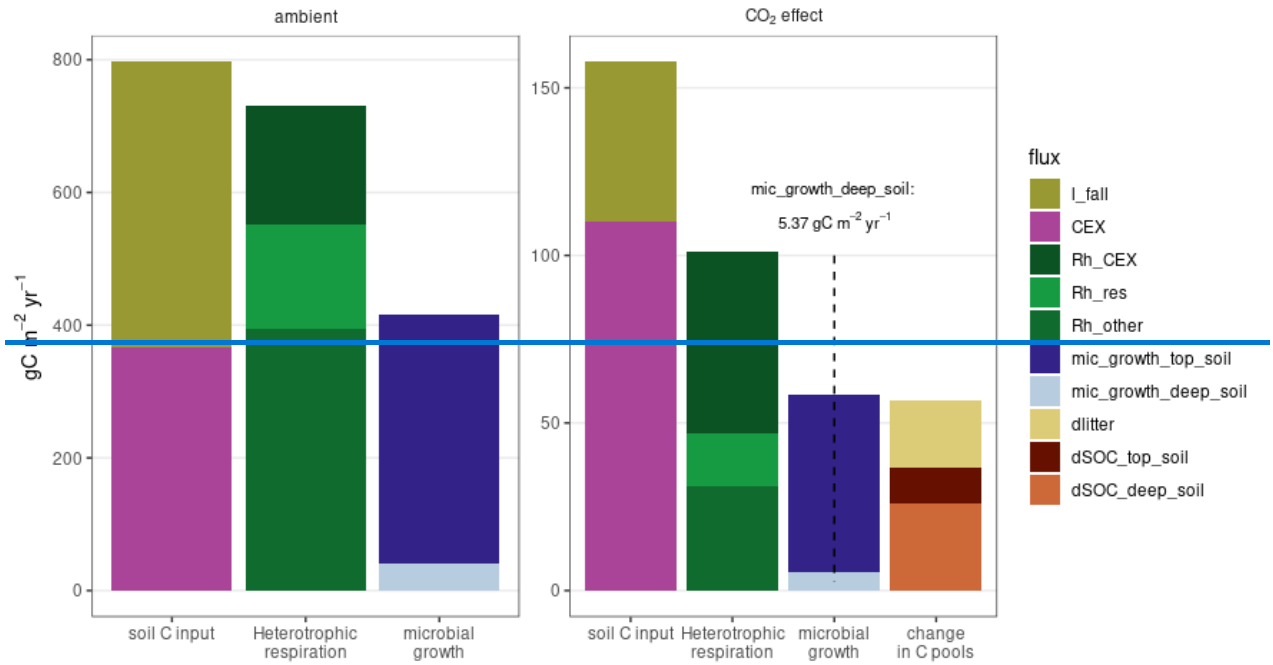

In our model, gross microbial growth and necromass production increased by 14 % and 13 %, respectively, compared to ambient conditions (Fig. 5, *microbial and necromass growth*). This means that only 34 % of the additional C input resulted in gross microbial growth in topsoils and only 22 % of the additional C input resulted in gross necromass production in topsoils. Simulated net topsoil SOC increase was small compared to overall additional C input (10 gC m^{-2} yr^{-1}, 6 % of the additional C input) (Fig. 5, change in C pools). Increased respiration of necromass, i.e.priming, suggests that additional gross necromass production was offset by microbial nutrient acquisition.

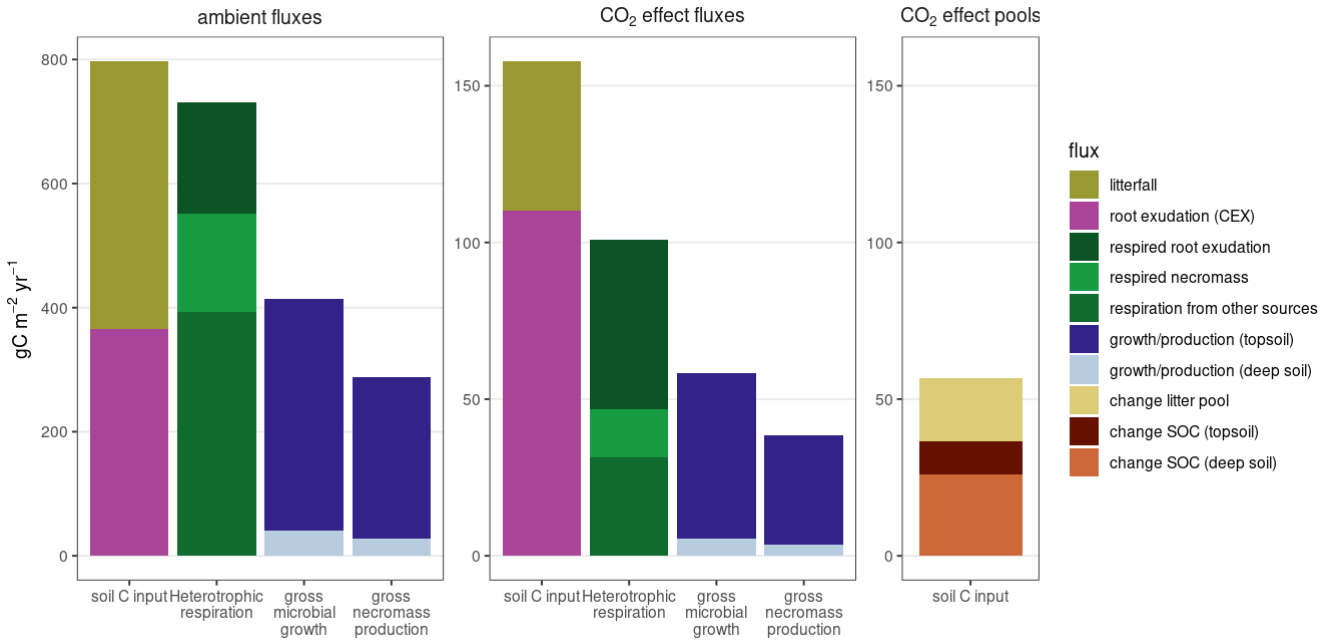

Figure 45: simulated sources and sinks for C in soil at EucFACE under ambient conditions and as CO_2 effect, ~~diplayed~~displayed as yearly average for 2013-2019. Additional C input is composed of litterfall ~~(l_fall)~~ and exudation (CEX). Elevated CO_2 induced increased heterotrophic respiration (Rh), which originated from respiration of exudation ~~(Rh_CEX),~~ respiration of microbial ~~residues (Rh_res)~~necromass and respiration of other sources, like degradation of woody biomass and respiration of directly recycled microbial biomass, soluble and polymeric litter ~~(Rh_other).~~ Additionally, eCO_2 affects growth microbial C growth in ~~top (mic_growth_top_soil)~~ topsoil and deep soil ~~(mic_growth_deep_soil),~~ change in litterpools ~~(dlitter),~~ topsoil (50 cm) soil organic ~~C (dSOC_top_soil~~carbon (SOC) and deep soil ~~organic C (dSOC_deep_soil).~~SOC.

3.2.2 Microbial resource acquisition

~~In the model, increased root exudation induced by eCO_2 increased microbial growth and biomass. Nutrients required for microbial growth were mostly gained from organic sources. Increased root exudation supplied the majority of the additional microbial growth in C, namely 60 %. To the contrary root exudation only contributed 2 % of N to additional microbial growth (Fig. 5 a, b), caused by low C: N ratio of root exudation. Instead, microbes obtained additional N for growth via uptake of soluble inorganic nitrogen (24 % of additional growth) and asymbiotic N fixation (2 % of additional growth), recycling upon microbial death (32 % of additional growth) and microbial residue depolymerization (36 % of additional growth). As a consequence, organic sources, rather than inorganic sources, supplied additional growth in N, showing that increased C input under eCO_2 also increased necromass decomposition. The increased microbial uptake of inorganic N led to a net N mineralization decrease by 14 % (Fig. B6). For P, inorganic soluble P uptake supplied most of the P for additional microbial growth under eCO_2, namely 58 %. This also included PO4 that was mobilized by biomineralization. Only 42 % of P for additional microbial growth originate from uptake of DOP, mostly from microbial recycling which contributes 36 % (Fig. 5 c).~~

~~We further investigated the effect of eCO_2 on percentage contribution of sources for microbial growth in C, N and P, respectively.~~In the model, increased gross microbial growth led to higher absolute microbial nutrient uptake from organic sources (Fig. 6). Absolute decomposition of microbial necromass increased by 9 % compared to ambient conditions, and mean annual biochemical mineralization increased by 22 % (Fig. 6, detailed numbers in supplement). As a consequence, eCO_2 resulted in a 40 % increase in annual net PO_4 mineralization (Fig. B4).

Despite causing higher nutrient demands, eCO_2 did not cause a substantial shift in the relative contribution of nutrient sources to gross microbial growth for N and P (Fig. 7, detailed numbers in supplement). For C, the contribution of root exudation increased from 30% to 34 ~~%, while for~~% (Fig. 7 a). However, root exudates contributed only minimally to microbial N uptake and not at all to microbial P ~~contribution of nutrient sources remains relatively constant~~uptake, as the model assumes a high C: N ratio and ~~depended on organic sources~~no P in root exudates (Fig. ~~5 d–f). nitrogen~~7 b, c). Microbial N was derived to 77 % (~~elevated:~~eCO_2; 75 %) ~~derived~~ from organic sources~~,~~ such as microbial recycling and depolymerized microbial necromass (Fig. ~~5 e~~7 b). For P, 45 % (~~elevated~~eCO: 46 %) of microbial ~~growth~~ P acquisition came from uptake of soluble phosphate (Fig. ~~5f). Contribution~~7 c), most of which was solubilized via biochemical mineralization (Fig. B5).

Changes in nutrient ~~sources remain nearly constant, because of~~source contributions were limited by model assumptions and the simulated nutrient conditions. Recycling of microbial biomass on turnover is ~~based on~~ controlled by a ~~fixed parameter~~constant; therefore, we expect little change regarding this flux. For N, NH_4 availability and flexibility in asymbiotic N fixation were sufficient to ~~supply~~meet inorganic ~~sources~~N demand, preventing an ~~increase in contribution from~~ increased reliance on decomposition. ~~Similar to N, recycling of microbial P follows a fixed parameter. Uptake~~ Microbial P uptake through decomposition of microbial ~~residue is mostly determined~~necromass was controlled by microbial ~~N~~C and ~~C~~N limitation ~~and P input through litter under eCO_2 is negligible. However inorganic P uptake includes phosphate from available sources and phosphate released through biomineralization. We therefore investigated P dynamics in greater detail.~~.

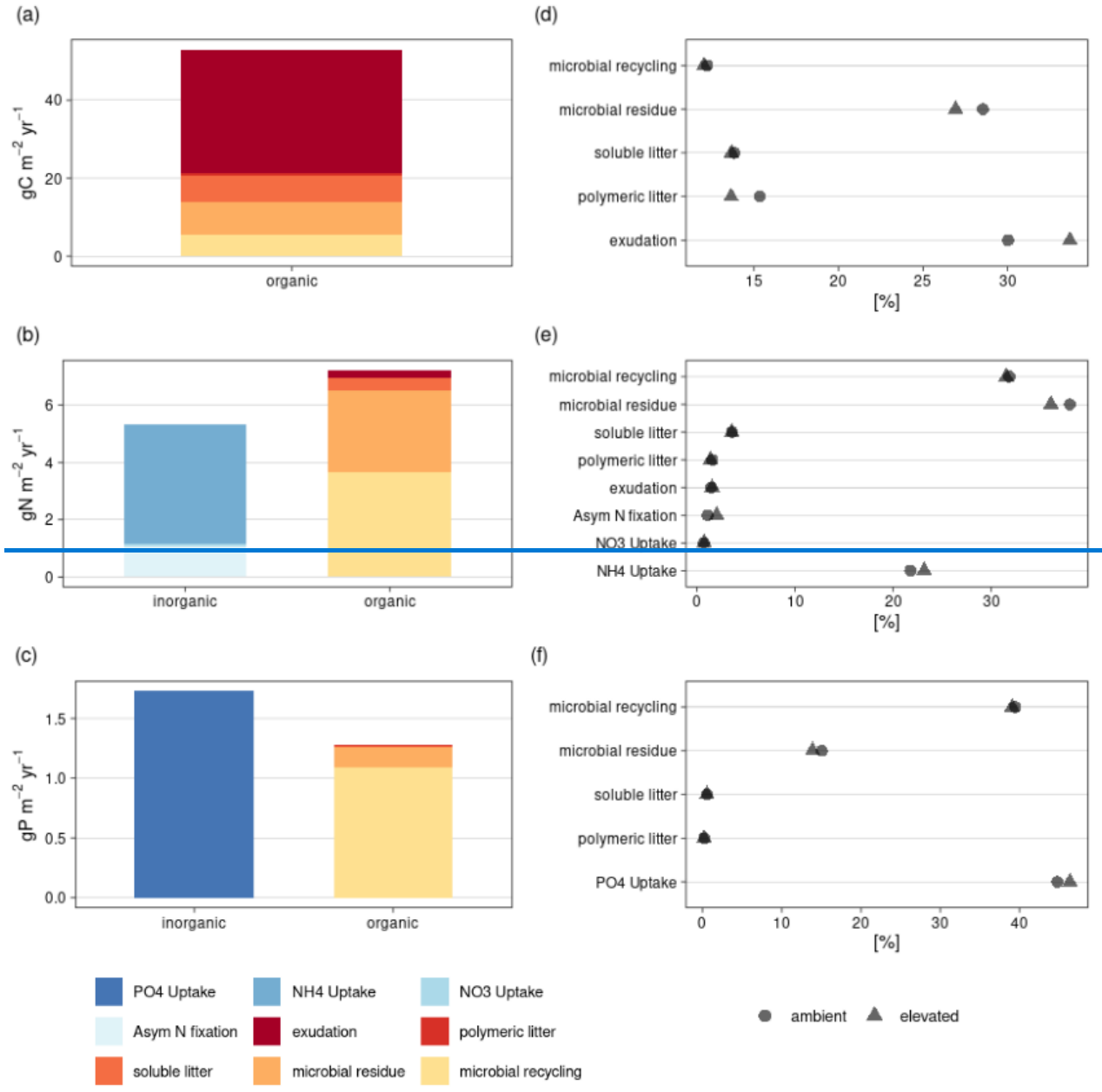
(a)
gC m^{-2} yr^{-1}
0
20
40
organic
(d)
microbial recycling
microbial residue
soluble litter
polymeric litter
exudation
15
20
25
30
[%]
(b)
gN m^{-2} yr^{-1}
0
2
4
6
inorganic
organic
(e)
microbial recycling
microbial residue
soluble litter
polymeric litter
exudation
Asym N fixation
NO3 Uptake
NH4 Uptake
0
10
20
30
[%]
(c)
gP m^{-2} yr^{-1}
0.0
0.5
1.0
1.5
inorganic
organic
(f)
microbial recycling
microbial residue
soluble litter
polymeric litter
PO4 Uptake
0
10
20
30
40
[%]
PO4 Uptake
NH4 Uptake
NO3 Uptake
Asym N fixation
exudation
polymeric litter
soluble litter
microbial residue
microbial recycling
ambient
elevated

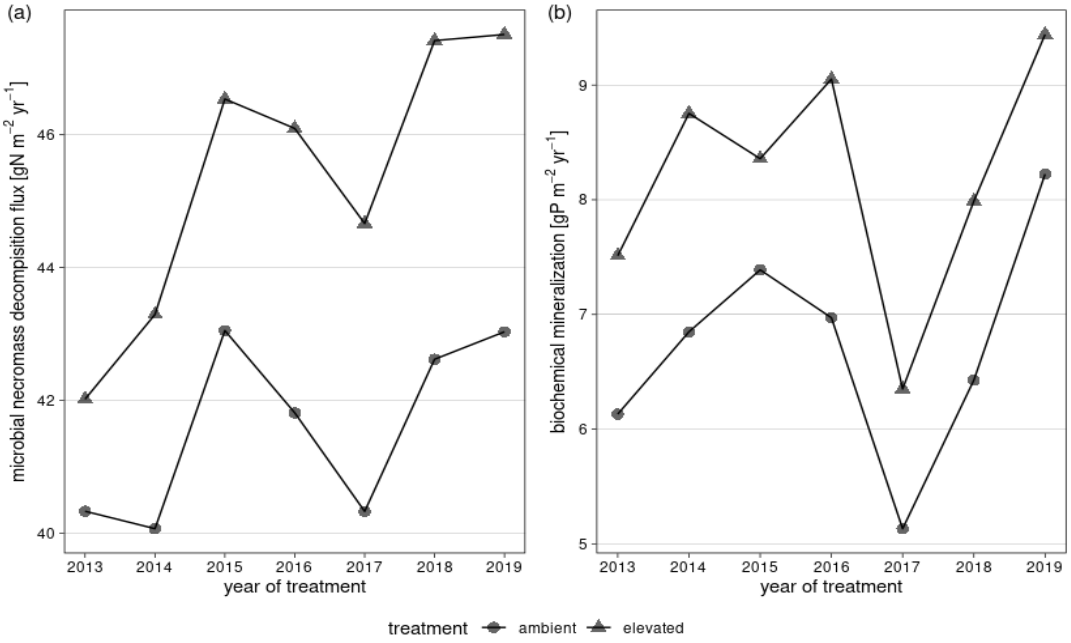

Figure ~~5~~6: Simulated ~~uptake sources (C, N, P)~~annual main fluxes for microbial, enzyme-mediated nutrient acquisition from organic matter for topsoil in treatment years for 2013-2019 a) Annual microbial necromass decomposition for N acquisition. b) Biochemical mineralization from necromass, mineral-associated microbial necromass, and mineral-associated DOM.

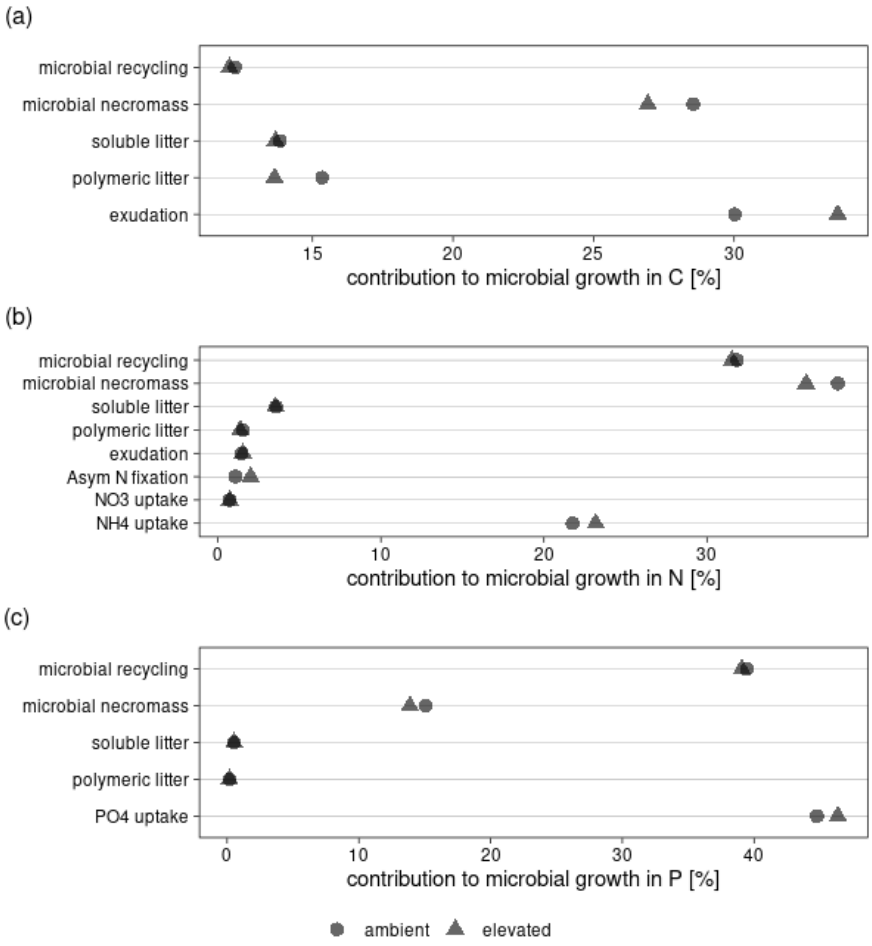

Figure 7: Simulated distribution of nutrient sources for gross microbial growth under ambient and elevated conditions for gross microbial growth at EucFACE in topsoil (50 cm) averaged for 2013-2019, calculated based on contribution of sources to DOM and microbial CUE. ~~(a-c) CO_2 effect on sources of uptake of C, N and P, respectively; (d-f) distribution of nutrient sources for microbial growth under ambient and elevated conditions. In (e-f) sources~~ Sources of gross growth are ~~divided into organic and inorganic (N and P only). Organic sources are exudation, uptake from depolymerised microbial residue, uptake from directly recycled microbial biomass and litter. Sources for inorganic N uptake are soluble NH_4 and NO_3 and asymbiotic N fixation of N_2. Inorganic P uptake is uptake of PO_4. However,~~ given for a) carbon, b) nitrogen, c) phosphorus. For P, a significant amount of ~~this~~ PO_4 is gained by biochemical mineralization of organic material (Fig. ~~6~~ B rev. 2).

~~Increased microbial uptake of PO_4 under eCO_2 was primarily driven by solubilization of PO_4 through biochemical mineralization (Fig. 6). Biochemical mineralization of organic matter increased by 22 % (1.5 gP m^{-2} yr^{-1}) in comparison with ambient conditions (Fig. B6). Elevated CO_2 affected biochemical mineralization more than gross biological mineralization or weathering, which increased by 11 % (0.3 gP m^{-2} yr^{-1}) and 7 % (<0.01 gP m^{-2} yr^{-1}) respectively. Increased microbial uptake matched increased gross biological and biochemical mineralization, thereby confirming that microbes derived additional P from organic sources (Fig. 6a). Although eCO_2 resulted in an overall 40 % increase in net PO_4 mineralization, the effect was~~

~~variable over the experimental period (Fig. 6 b). Nonetheless the simulation resulted in an increase in available inorganic PO_4 (Fig. B7).~~

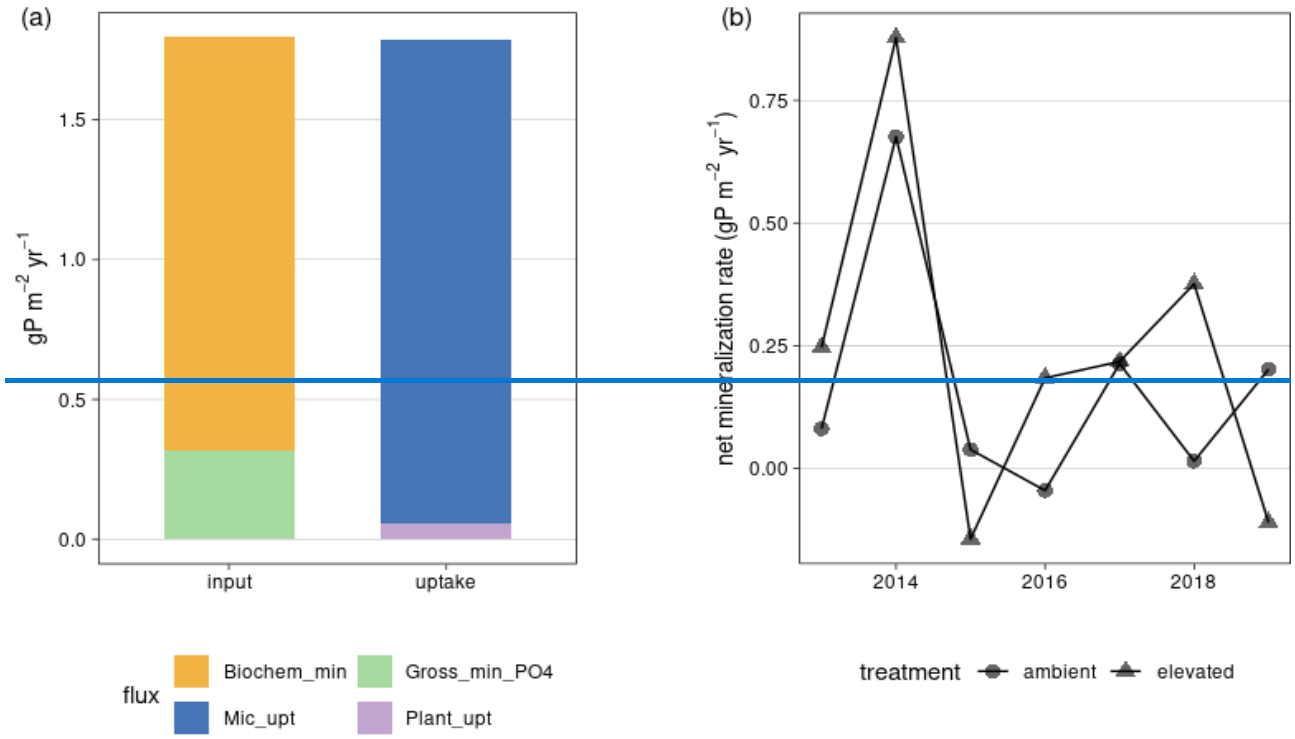

~~**Figure 6: simulated CO_2 effect on mineral P fluxes in topsoil layers (50cm). (a) Yearly average from 2013-2019 fluxes which provide (input) plant and microbes available mineral P are gross biological mineralization and biochemical mineralization. Available P get immobilized via uptake by microbes or plants. Adsorption and weathering are not displayed as the CO_2 effect on these fluxes is below 0.01 gP m^{-2} yr^{-1} (b) net PO_4 mineralization simulated for 2013-2019 for ambient and elevated CO_2**~~

~~**3.2.3 Cycling of microbial necromass**~~

~~**Microbial growth and nutrient acquisition under CO2 increased tops soil microbial necromass build up and decomposition, therefore accelerating the cycling of SOM. We separated top soil microbial necromass growth into input and output fluxes for topsoil (Fig. 7). The CO_2 induced increase in microbial growth led to a 13 % increased input flux towards microbial necromass (microbial residue and the organo-mineral associated microbial residues) for C, N and P compared to ambient conditions (Fig. 7). However, increased depolymerization under eCO_2, as result of increased priming activity and biochemical mineralization also led to increased outgoing fluxes (C: 8 %, N: 8 %, P: 30 %). Under ambient CO_2, the net balance in microbial C, N necromass cycling was close to zero. The net effect of CO_2 on the**~~ **3.2.3 Net necromass production**

We summarized simulated gross production, decomposition and biochemical mineralization of microbial necromass ~~(including organo-associated) cycling was~~("free" necromass and mineral-associated necromass) in the topsoil (Fig. 8, detailed numbers in supplement). Increased in- and outgoing fluxes to microbial necromass accelerated turnover of SOM (Tab. B 4). Elevated

CO_2, increased gross necromass production for C, N and P by 13 % (Fig. 8). However, increased depolymerization and biochemical mineralization under eCO_2 also increased outgoing fluxes (C: 9 %, N: 9 %, P: 30 %). Regardless of treatment, net effects in cycling of microbial C necromass were small for all elements relative to the size of in- and outgoing fluxes and ~~to the pools themselves. For C and N, the effect of eCO_2~~pool sizes. Under aCO_2, net necromass production in C and N was close to zero, whereas under eCO_2, net production was positive ~~leading to~~causing a ~~11~~12 gC m^{-2} yr^{-1} and 2 gN m^{-2} yr^{-1} ~~increased net input through microbial~~ necromass increase compared to ambient conditions. ~~For microbial~~Net necromass ~~P, increased biochemical mineralization led to a negative net effect in P necromass cycling~~production of P was - 1 gP m^{-2} yr^{-1} under aCO_2 and - 3 gP m^{-2} yr^{-1}~~. Both, increased depolymerization and increase biochemical mineralization were driven by increased microbial biomass and changes in enzyme allocation (Fig.~~[1]under eCO_2. However, eCO2 decreased~~ B8, Fig. B9) Despite this net effect,~~ the overall necromass P pool ~~changed by~~ only 2 ~~%. We also found that, P~~% (-2 gP m^{-2} yr^{-1}). Phosphorus remained in the ecosystem and was transferred to faster cycling pools, namely microbial biomass or dissolved organic matter (Fig. ~~B10, Fig.~~B6, Fig. B7). ~~B11). Consequently, increased root exudation left the quantity of topsoil SOM nearly unchanged, but increased its turnover rate~~

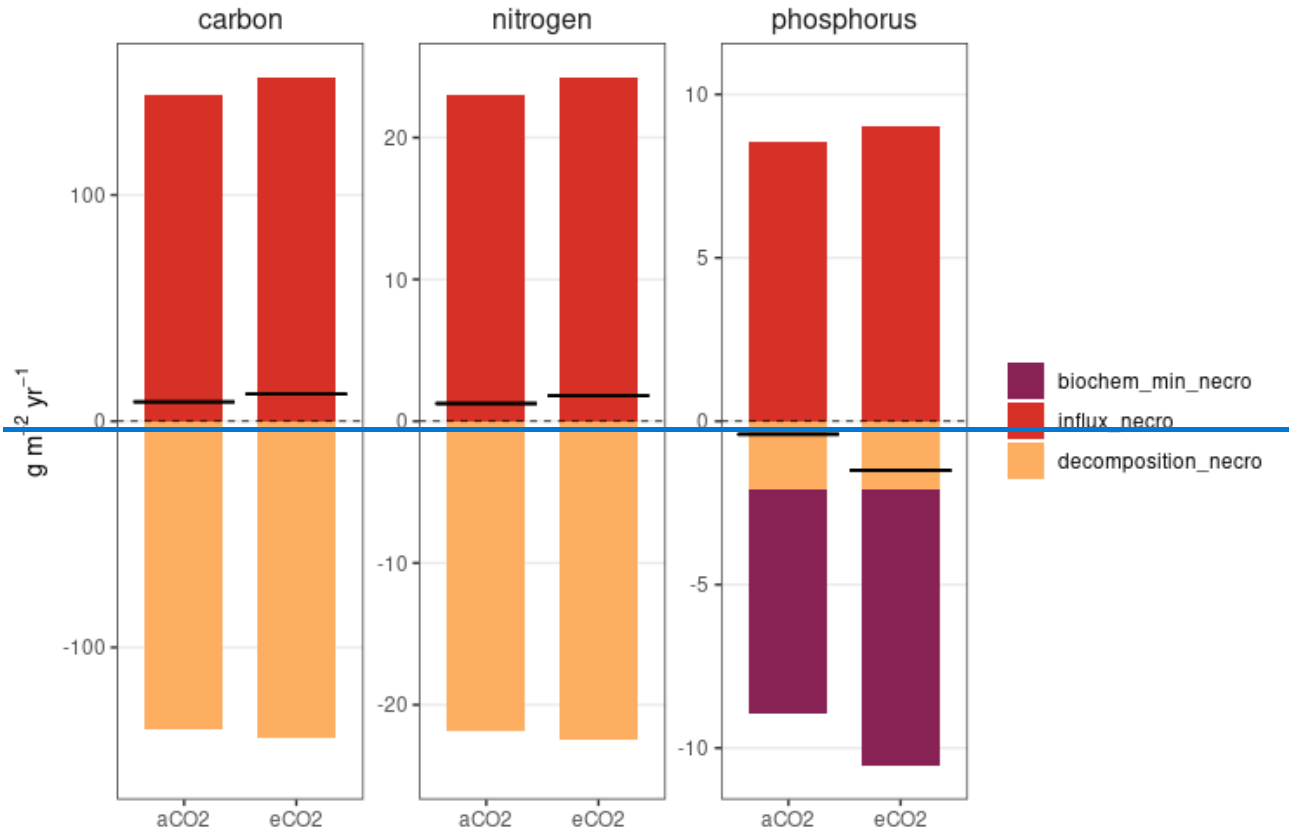

~~Figure 7: Simulated balance of C, N and P for microbial necromass (combined pool of microbial residues and mineral associated microbial residues) in topsoil (50 cm) under ambient and elevated CO_2. Influxes (red, above the dashed line) are compared with~~

~~outfluxes (yellow, below the dashed line) and, for P, biochemical mineralization (purple, below the dashed line). Black lines represent the net effect.~~

~~Elevated CO_2 led to an acceleration of biogeochemical cycling in the ecosystem (Table 3). Ecosystem carbon turnover time decreased by 10 %, caused by faster respiration of soil inputs. In soils elevated CO_2 had a more p pronounced effect on P (20 % decrease) and N (20 % decrease), then on carbon cycling (12 % decrease), possibly caused by increased plant nutrient uptake to sustain BP.~~ As, in the model, C and N cycling of microbial necromass are closely interlinked, turnover times of microbial necromass decreased by 9 % for C and N~~:~~ (Table B4). For P~~,~~ enhanced biochemical mineralization ~~caused a~~ further ~~decrease in~~decreased necromass turnover time by 21 %. Combining all soil pools, elevated CO_2 had a more pronounced effect on P (20 % decrease) and N (20 % decrease), then on C cycling (12 % decrease), possibly caused by increased inorganic nutrient cycling.

~~Table 3: **Modelled turnover times under ambient and elevated CO_2 for the ecosystem (C), soil (C, N, P) and microbial necromass (C, N, P). Calculated for 2015-2019.**~~

		$\tau_{ES}(yr)$	$\tau_{soil}(yr)$	$\tau_{necromass}(yr)$
carbon	aCO_2	10.2	17.1	30.4
	eCO_2	9.2	15.1	27.7
nitrogen	aCO_2	-	242.1	30.5
	eCO_2	-	193.2	27.7
phosphorus	aCO_2	-	561.2	8.2
	eCO_2	-	447.6	6.4

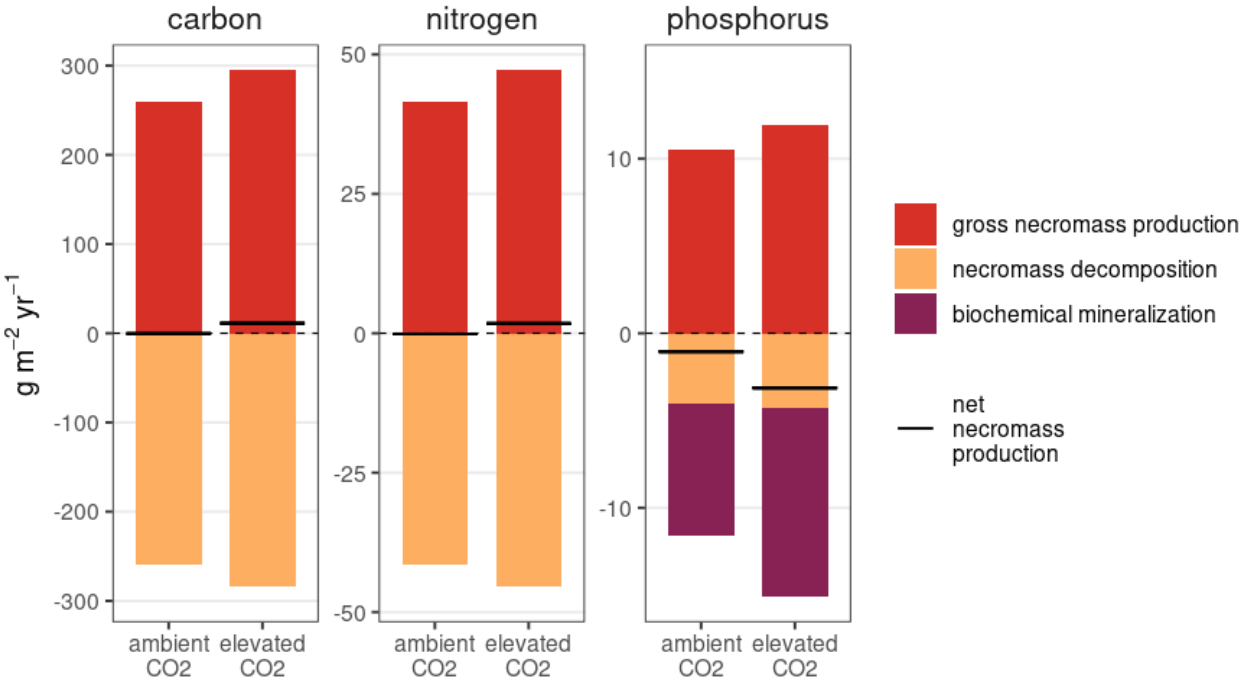

Figure 8: Simulated balance of C, N and P for microbial necromass (combined pool of microbial necromass and mineral associated microbial necromass) in topsoil (50 cm) under ambient and elevated CO_2. Gross production (red, above the dashed line) are compared with decomposition (yellow, below the dashed line) and, for P, biochemical mineralization (purple, below the dashed line). Black lines represent the net necromass production.

4. Discussion

~~Discussion~~

We developed and tested a model implementation for dynamic root exudation in a microbial–explicit terrestrial biosphere model and analyzed the consequences for increased root exudation under eCO_2 in a mature Eucalyptus forest. We found that – in our model – increased root exudation ~~represents a possible explanation for not measured GPP allocation fluxes under eCO_2. We analyzed how much of additional C input under eCO_2 was matched by increased~~ links enhanced GPP and heterotrophic respiration under eCO_2 and improved simulated allocation of additional GPP (Fig. 4, Fig. B8, Fig. ~~and how microbial nutrient acquisition contributed to further heterotrophic respiration and SOM cycling. Our simulations show that~~B9). Increased root exudation caused only minor increases in topsoil C, as more than 60 % of additional C input into soils was matched with increased heterotrophic respiration ~~for of two main reasons. First,~~and eCO_2. This was primarily caused by soil microbes ~~respired~~respiring a substantial amount of the new C input, ~~primarily root exudation. Second, enhanced necromass decomposition for nutrient acquisition offset increased necromass input, both driven by microbial growth. As a result, our model simulated only minor increases in topsoil C under eCO_2. The implementation of root exudation, provided a reasonable explanation for the partitioning of additional GPP and is in better agreement with observations. We discuss our results by focusing on the effect of eCO_2 on plant carbon allocation, heterotrophic respiration, microbial growth and microbial necromass cycling in the context of plant microbe interactions. Where possible we evaluate our results against previous studies and discuss model assumptions in relation to discrepancies.~~with an additional contribution through enhanced necromass decomposition for microbial N acquisition. Microbial P demands were primarily met by biochemical mineralization. Simulated results are constrained by model uncertainties and assumptions.

4. 1 Plant carbon allocation and root exudation

~~Observations in allocation of plant surplus GPP suggest a major C allocation belowground, suggested by increased soil respiration under eCO_2. Our model agrees with the increased belowground allocation under eCO_2 as a 22% increase in GPP, led to a 30 % increase in root exudation. Implementation of root exudation into the model also improved allocation of surplus GPP. However, even with root exudation, the model continued to overestimate the response in autotrophic respiration and BP, compared to observations. It is likely that our model does not yet replicate the full complexity of P limitation under eCO_2 on the system (Crous et al., 2015), therefore still allocating more C towards biomass production and less to soils than measured. Plant P availability under eCO_2 may be caused by the overestimation of organic soil pools, caused by strong accumulation in organic mineral associated pools. These pools do not directly determine C and N availability but are a P source through biochemical mineralization. Additionally, our model may underestimate the strong competition for PO_4 by microbes and sorption to soil, suggested by the P budget of the site (Jiang et al., 2024b).~~

~~It is unlikely that we underestimated the ambient root exudation flux, since the simulated ratio of root exudation to GPP under ambient conditions of 21 % is already very high compared to global estimations: For example, Chari et al. (2024) suggest that across 6 different biomes globally 5.6 % of GPP is allocated to root exudates, but with strong variations between biomes and measurements. On the other hand, plant growth in EucFACE is P-limited which could explain higher exudation rates. Nevertheless, it is possible that the simulated effect of eCO_2 on root exudation is too small. In the model, eCO_2 enhanced yearly root exudation rate per area and per fine root mass of up to 30 % during 7 years of CO_2 increase. Even though, the compiled carbon budget suggests an increased C allocation belowground (Jiang et al., 2020), a direct evaluation of the eCO_2 effect is impossible because there are no direct measurements of root exudation and large uncertainties are associated with the other components of the ecosystem carbon budget. In the Duke FACE experiment, eCO_2 was estimated to cause a 40 % increase in allocation to exudates and fungi (Drake et al., 2011) and in BIFoR FACE root exudation was estimated to increase by 42-63 % (Norby et al., 2024), but these effects were statistically not significant. In our simulation the increase in root exudation emerges from plant nutrient, C surplus status and fine root growth. A stronger P limitation of plant growth under eCO_2 may increase the CO_2 effect on root exudation and reduce allocation to BP in the model.~~

Our simulations indicate that increased root exudation is a major pathway for belowground C allocation under eCO_2, but the magnitude is difficult to validate due to the absence of direct measurements at EucFACE. Our model estimated a root exudation-to-GPP ratio of 21 % under ambient conditions, which is substantially higher than global estimates (Chari et al. 2024). Chari et al. (2024) suggests a global mean of 5.6 % based on upscaling measurements of free root exudation, primarily taken with the cuvette method (Phillips et al., 2008). Due to the lack of such measurements at EucFACE, we estimate root exudation from the ambient C budget. Our estimate therefore also includes other belowground allocations, e.g., mycorrhiza and losses through mucilage, and root exudation in deeper soil layers, which likely explains the differences between our results and global estimations (Brunn et al., 2025; Johansson et al., 2009; Jones et al., 2004).

Simulated C allocation to root exudation increased by 30 % under a 22 % increase in GPP under eCO_2, consistent with the observation-based hypothesis of increased belowground C allocation at EucFACE. Elevated CO_2 also enhanced mean annual root exudation rate per unit fine root mass by 18 % (Fig. B2). Our estimates are lower than increases reported at other FACE experiments. In Duke FACE allocation to exudates and fungi, increased by 40 % in upscaled annual flux per unit land area (Drake et al., 2011). At BIFoR FACE, specific C exudation (ug/g fine root /day) increased by 41-135% (P=0.037) (Reay et al., 2025), and upscaled annual flux per unit land area by 43-63% ($P = 0.042$) (Norby et al., 2024).

Uncertainties in exudation rates at EucFACE remain considerable. We parameterized our model using ambient GPP and plant pool observations and calculated root exudation flux base on fine root N concentration. The deviation from simulated BP and fine root C: N to observations leads to parameter uncertainty. The compiled C budget suggests increased C allocation belowground under eCO_2 (Jiang et al., 2020), but a direct evaluation of the root exudation is not possible, also due to large uncertainties associated with other components of the C budget. Additionally, our model only simulates the response in overstorey vegetation, whereas the understorey vegetation at EucFACE showed a strong NPP increase that likely affected soil

processes (Jiang et al., 2020; Piñeiro et al., 2023). Overall, more empirical data on belowground C allocation would aid the development and evaluation of TBMs.

The model also simulated a 33 % increase in overstorey BP under eCO_2, which was not observed in EucFACE. In the simulation, C accumulated primarily in woody biomass and labile plant pool (Fig. B10), but this had only a minor influence on soil processes because plant litter contributed little to microbial growth in C, N and P in the treatment period (Fig. 7). Instead, root exudation dominated the additional C input and the supply to microbial growth under eCO_2. Observational studies suggest that plant P limitation suppressed plant growth under eCO_2 (Jiang et al., 2020), suggesting that the model likely underestimates P constraints or overestimates plant adaptability to P limitation.

Despite these limitations, our model closes the gap between increased GPP and observed increased heterotrophic respiration under eCO_2, underlining the importance of root exudation as a key pathway for plant C allocation that deserves greater empirical and model attention.

4.2 Heterotrophic respiration and microbial growth

Our model identified root exudation as the dominant driver of higher heterotrophic respiration under eCO2, mainly as rapid microbial respiration of newly supplied labile C. Simulations showed that more than half of the additional root exudation-derived C was directly respired as overflow respiration. Although there is no partitioning in heterotrophic respiration by substrate origin in EucFACE, this result is consistent with other studies showing that under eCO_2, most soil respiration originates from recently fixed C (van Groenigen et al., 2017; Taneva et al., 2006). Microbial CUE was a key modulator of soil C sequestration and respiration (Spohn et al., 2016; Tao et al., 2023, 2025). Simulated annual microbial CUE ranged between 40 % and 50 % and did not change under eCO_2 (Fig. B11). ~~Additional allocation of C to soil is potentially offset by additional heterotrophic respiration caused by two mechanisms: direct respiration of fresh material and respiration of old material, i.e., priming. Our model suggests that both mechanisms contribute to increased heterotrophic respiration under eCO_2, with direct respiration having a stronger impact. Root exudation was the major additional soil C input under eCO_2, but microbes directly respired more than half of the additional root exudation. Therefore, eCO_2 only increased microbial growth by 14 %. The increased growth caused priming effects, i.e., decomposition of microbial necromass, and resulted in a further increase in heterotrophic respiration.~~

~~There is no analysis on the origin of increased heterotrophic respiration in EucFACE, but our results are consistent with other studies showing that under eCO_2 the majority soil respired C originates from new soil C input (van Groenigen et al., 2017; Taneva et al., 2006). The fraction of C that is respired from microbial DOM uptake is determined by microbial carbon use efficiency. Our model showed a yearly average microbial CUE between 40 % and 50 %, which did not change under eCO_2 (Fig. B12). A reduced microbial CUE under additional carbon input would lead to less microbial growth and an even larger proportion of root exudation as the source for heterotrophic respiration. Taking into account the important role of microbial growth and necromass for SOM formation (Miltner et al., 2012), the rapid respiration of fresh material and the additional decomposition of old material questions the capability of soils to sequester large amounts of C under eCO_2 in this system.~~

4.3 Microbial growth and nutrient feedback

Our model suggests a coupling of processes such that larger root exudation flux increased microbial growth, which increased depolymerisation for N acquisition and biochemical mineralization for P acquisition. Enhanced biochemical mineralization increased PO_4 availability. In the model, root exudation disproportionally drove microbial growth in C under eCO_2, suggesting that microbes might change their diet under eCO_2 to more easily available and more easily degradable substrates to gain carbon (Ai et al., 2023; Dijkstra et al., 2013; Zhou et al., 2021). Simulated root exudation showed a C to N ratio of 176 and contained no P, whereas microbial C to N ratio was 4.3 (N: P = 4.1). Consequently, increased root exudation enhanced microbial demand for nutrients. For N, this demand was partially satisfied by available inorganic N. As a result, microbial nutrient uptake from organic sources increased, but without a substantial shift in the contribution. Here our model partially disagreed with field observations: Measurements of soil enzymes found no increase in N degrading enzymes or microbial nutrient limitations under eCO_2 (Pihlblad et al., 2023). However, it is questionable if this effect would be statistically detectable in a FACE experiment, with inherently low sample size and difficulties in detecting changes in the soil (Filion et al., 2000).

In our model, increased biochemical mineralization satisfied additional microbial P demand. Therefore, organic sources substantially supported microbial growth in P. Microbes took up more than 95 % of the additional mineralized PO_4. Even though this underlines the microbial competitiveness for PO_4 at this site, the positive effect of additional gross mineralization to plant PO_4 availability may still be overestimated (Jiang et al., 2024b). Consequently, elevated CO_2 led to an increase in available PO_4 of 20 %. This is partially consistent with observations which report increased PO_4 concentrations under eCO_2 in the rhizosphere or deeper soil layers (Hasegawa et al., 2016; Ochoa-Hueso et al., 2017; Pihlblad et al., 2023). To our knowledge it is not yet resolved which processes caused the increased PO_4 concentration in EucFACE. Observations from other ecosystems report increased phosphatase activity under P limitation (Marklein and Houlton, 2012) and in ecosystems with high soil organic P content (Margalef et al., 2017). In EucFACE, eCO_2 caused no significant increase in phosphatase at the start of the experiment (Hasegawa et al., 2016), after 1 1/2 year (Ochoa-Hueso et al., 2017) or after 4 1/2 years (Pihlblad et al., 2023).

An alternative pathway may be increased exudation of carboxylates, which could have increased PO_4 concentrations via ligand exchange with Fe-Al oxides at soil surfaces (Hinsinger, 2001; Wang and Lambers, 2020). Increased carboxylate exudation has been reported for common EucFACE understorey species (Hasegawa et al., 2023). As we do not consider these processes in our model, the model resolves enhanced P requirements with increased biochemical mineralization, triggered by increased microbial growth but also by increased enzyme allocation. For N and P old SOM, e.g., necromass, therefore remained an important part for microbial nutrient supply under eCO_2.

4.4 Necromass cycling

Our model supports the theory that eCO_2 can lead to increased cycling of SOM without substantial increases in pool size (Drake et al., 2011; van Groenigen et al., 2014; Kuzyakov et al., 2019). While observations found no increase in topsoil C, our

~~simulation led only to a minimal increase in soil organic C in topsoil layers. Our results suggests that for microbial necromass, an essential part in C storage, increased input through microbial growth and increased decomposition for microbial nutrient acquisition counteract each other. There are no continuous measurements from EucFACE analyzing changes in age composition of soil organic matter. However, using a combination of litter bag and isotopic signature measuring, Castañeda-Gómez et al. (2020) showed that eCO_2 led to stronger losses of old SOC and increased input of new SOC at EucFACE in summer months.~~

~~Along with C, eCO_2 also increased N and P turnover in our simulations. For P, also pool sizes have changes such that P is mostly transferred from slow cycling microbial necromass to fast cycling microbial biomass. This disagrees with a recent study analyzing the P budget for EucFACE, concluding that eCO_2 treatment led to no significant changes of soil organic P pools (Jiang et al., 2024b). However, the simulated changes were small (e.g. < 2 % in necromass) and therefore it is questionable if they could have been detected in field observations.~~

~~Uncertainties in effects on necromass cycling arise from other processes we did not consider in our model, such as flexible recycling of N under eCO_2, or higher N content of root exudates, that might prevent priming effects. Additionally, in our model, eCO_2 caused a desorption in mineral-associated necromass. This led to more microbial available N-rich material and may have enhanced the CO_2 effect on SOM decomposition.~~

A decline in microbial CUE under greater C supply or nutrient limitation, would reduce microbial growth and increase the fraction of root exudates respired (Schimel and Weintraub, 2003). Our results are conservative in that respect but still support the hypothesis, that the majority of additional heterotrophic respiration originates from new plant-derived C.

In the model, root exudation disproportionally stimulated microbial C growth, and consequently gross necromass production, under eCO_2. This suggests that microbes might change their diet under eCO_2 to more easily available and more degradable substrates for C gain (Ai et al., 2023; Dijkstra et al., 2013; Zhou et al., 2021). However, higher gross microbial growth in C, also increased microbial nutrient requirements, influencing decomposition and nutrient acquisition processes.

4.3 Microbial nutrient acquisition

Our simulations suggest that, to meet increased nutrient demands under eCO_2, microbes enhanced necromass decomposition and biochemical mineralization; however, observations of enzyme activity only partially support this pattern. For N, demand was met by increased uptake of available inorganic N and decomposition of necromass. Priming of microbial necromass increased, but without a substantial shift in its relative contribution to growth. Here our model partially disagreed with field observations based on soil enzymes: (Pihlblad et al., 2023) found no increase in N-degrading enzymes or microbial nutrient limitations under eCO_2. However, it is questionable if this effect would be statistically detectable in a FACE experiment, with inherently low sample size and difficulties in detecting changes in the soil (Filion et al., 2000).

For P, our model suggests that additional microbial P demand was primarily satisfied by increased biochemical mineralization of organic sources, including necromass. As a consequence, eCO_2 increased available PO_4 by 20 % (Fig. B12). This is partially consistent with observations which report increased PO_4 concentrations under eCO_2 in rhizosphere or deeper soil layers

(Hasegawa et al., 2016; Ochoa-Hueso et al., 2017; Pihlblad et al., 2023). To our knowledge it is not yet resolved which processes caused the increased PO_4 concentration in EucFACE. In accordance with the model, observations from other ecosystems report increased phosphatase activity under P limitation (Marklein and Houlton, 2012) or under high soil organic P content (Margalef et al., 2017). In EucFACE, eCO_2 caused no significant increase in phosphatase at the start of the experiment (Hasegawa et al., 2016), after 1 1/2 year (Ochoa-Hueso et al., 2017) or after 4 1/2 years (Pihlblad et al., 2023).

Model uncertainties derive from assumptions on nutrient acquisition strategies and root exudation stoichiometry. NH_4 availability and recycling of microbial nutrients on microbial turnover strongly contributed to microbial N acquisition under eCO_2, but remain poorly constrained and require further field observations.

Additionally, we do not account for P acquisition by increased carboxylate exudation, which could have increased PO_4 concentrations via ligand exchange with Fe-Al-oxides at soil surfaces (Hinsinger, 2001; Wang and Lambers, 2020) and has been reported for common EucFACE understorey species (Hasegawa et al., 2023). We currently lack field observations to implement such mechanisms in the model, therefore the model resolves enhanced microbial P demand with increased biochemical mineralization.

Finally, simulated microbial nutrient demand is substantially controlled by root exudation stoichiometry. In our model root exudation C to N ratio was 176 (no P exudation), whereas microbial C to N ratio was 4.3 (N: P = 4.1). Simulated C:N ratio is higher than root exudation measurements (Li et al., 2021; Su et al., 2022; Zhang et al., 2016) but ensures that modelled root exudation does not cause an extensive N loss in plants. As a consequence, increased root exudation enhanced microbial nutrient demand, and plant-microbial competition for N and P (Thurner et al., 2023). Under a root exudation stoichiometry closer to microbial stoichiometry, increased root exudation may further promote microbial growth. Microbial N supply may be less dependent on decomposition of microbial necromass, resulting in stronger decomposition of litter for C acquisition. Instead, a substantial amount of N would be stored in SOM, unavailable for plants. Root exudation C:N ratio remains a key variable in plant- microbe nutrient dynamics, but further research regarding the fate of exudate N is needed to improve model assumptions in plant C-for-N trade mechanisms (Drake et al., 2013; Rumeau et al., 2025).

4.4 Soil C sequestration

Our model shows that under increased root exudation, microbial growth can simultaneously increase gross necromass gross production and necromass decomposition, resulting in no substantial net effect in soil C storage (Drake et al., 2011; van Groenigen et al., 2014; Kuzyakov et al., 2019). In our model, priming offset gross necromass production and contributed to increased heterotrophic respiration under eCO_2. There are no continuous measurements from EucFACE analyzing changes in soil organic matter age composition. However, using a combination of litter bag and isotopic signature measuring (Castañeda-Gómez et al., 2020) showed that eCO_2 increased losses of old SOC and input of new SOC at EucFACE in summer months, agreeing with our simulations.

Uncertainties in C storage arise from model representation of C cycling in deep soil layers and mineral sorption of necromass. The model predicts increased soil C in deep soil layers under eCO_2, caused by increased root exudation in these soil layers. As

the model assumes root exudation following root biomass distribution, eCO_2, enhances root exudation in deeper soil layers with low microbial activity (Fig. 4). As a consequence, additional labile C is adsorbed to the mineral surface and thereby sequestered. While specific exudation rate may differ with depth and function of roots, we are currently missing data to further calibrate this.

Additionally, necromass is partially protected from decomposition by association with soil mineral surfaces. Our model accounts for this process but we are lacking measurements for site-specific sorption capacity and affinity. Less mineral protection would translate in stronger microbial necromass cycling, as the simulated depolymerization flux depends on availability of decomposable material. Further, the model simulates increased desorption of mineral-associated necromass under eCO_2. This is partly caused by additional root exudation competing with necromass for sorption sites, but also by model assumptions about the amount of available mineral soil sorption sites with increasing organic matter and litter. This model assumption increased microbial-available N-rich material and may have enhanced the CO_2 effect on necromass decomposition in the model.

We further simulated small shifts in P pools from slow cycling microbial necromass to fast cycling microbial biomass (< 2 % change in necromass)., A recent analysis of the P budget for EucFACE that eCO_2 treatment led to no significant changes of soil organic P pools (Jiang et al., 2024b), but changes of this magnitude are likely below the detection limit of field observations.

4.5 Comparison to other models

~~Implementing root exudation in QUINCY-JSM did improve the predicted CO_2 response of C allocation, but results still indicate that further development is necessary. A recent model inter-comparison study demonstrated that most C-N-P cycle models, including QUINCY-JSM, overestimate the C sequestration of the EucFACE ecosystem under eCO_2 (Jiang et al., 2024a). In contrast to observations, the majority of models simulated a positive effect on net ecosystem productivity (NEP) under eCO_2. Additionally, all, except one model in (Jiang et al., 2024a), allocated most additional C fixed under eCO_2 to either autotrophic respiration, storage or structural biomass, and underestimated the increase in soil heterotrophic respiration. The exception was GDAYP, which implemented root exudation but no microbial dynamics and therefore simulated higher soil P immobilization under eCO_2.~~

Implementing root exudation in QUINCY-JSM improved the predicted CO_2 response of C allocation, but results still indicate that further development is necessary. A recent model inter-comparison study demonstrated that most C-N-P cycle models, including QUINCY-JSM, overestimate the ecosystem C sequestration of the EucFACE ecosystem under eCO_2 (Jiang et al., 2024a). In contrast to observations, most models simulated a positive effect on net ecosystem productivity (NEP) under eCO_2. Additionally, all, except one model, allocated most additional C fixed under eCO_2 to either autotrophic respiration, storage or structural biomass, and underestimated the increase in soil heterotrophic respiration. The exception was GDAYP, which implemented root exudation but no microbial dynamics

Implementing root exudation improved the allocation of additional GPP: Compared to other models in ~~Jiang et al. (2024a)~~Jiang et al. (2024a) and QUINCY-JSM without root exudation, and consistent with observations, ~~in~~ QUINCY-JSM with root exudation reproduces the increase in C respired via heterotrophic respiration and the decrease in C lost through autotrophic respiration. Additionally, less C remains in the system in ~~form of increased vegetation pools (Fig. B4). Consequently, the implementation of root exudation does improve the simulated CO_2 effect on heterotrophic respiration. However, adding root exudation flux to QUINCY-JSM did not improve the NEP response to eCO_2. The response is still stronger than observed, caused by accumulation of C in vegetation biomass and deep soil layers. While the first one is caused by an overestimation of BP, the latter is caused by the allocation of root exudation in deeper soil layers, as – in our model – root exudation followed root distribution, causing increased C input in layers with low microbial activity. Regardless of root exudation, QUNICY-JSM is consistent with observations in simulating~~the form of increased vegetation pools (Fig. B8). With consideration of root exudation, the model explains weak ~~response of~~responses in topsoil C to eCO_2 ~~(Fig. B11). However, in the version without~~ by respiration of root exudation ~~this is caused by low C soil input in form of litter~~and priming, rather than by ~~fast respiration of root exudates and priming effects. The current version of~~ low litter C input (Fig. B9).

Implementing root exudation improved the simulated CO_2 response in heterotrophic respiration, but not in NEP, due to the effect on BP and deep soil C accumulation. Regardless of root exudation, QUINCY-JSM simulates ~~an increase in~~increased net P mineralization under eCO_2~~, regardless of the implementation of root exudation~~. Therefore, it remains difficult to evaluate the actual effect of the implementation on PO_4 mineralization. Further model adjustment is needed to fully understand the feedback of plant-microbe interactions on plant nutrient uptake under eCO_2.

4.6 Suggestions for further advancements in modelling and experimental work

~~In the following we discuss modelling advancements and experimental work that could help to optimize representation of plant-soil interactions. We assess factors influencing plant nutrient availability and plant carbon allocation. We further~~ In the following we provide methodological directions for upcoming FACE experiments ~~that would advance~~and terrestrial biosphere models, to improve understanding of root exudation and microbial representation ~~and their implementation in models~~ under eCO_2.

4.6.1 Soil Phosphorus ~~availability~~limitation

~~FACE experiments suggest a strong interaction between nutrient limitation and CO_2 fertilization effect, but it remains uncertain how effectively current models represent nutrient limitation (Jiang et al., 2024b; Zaehle et al., 2014). The simulated, but not observed, response of BP, suggest that we underestimate the P limitation on plant growth under eCO_2 in our model. Overestimation in P pools may be solved with alternative model initialization approaches. However, PO_4-plant availability also depends on chemical and biochemical mechanisms like sorption, biochemical mineralization, and plant microbe-competition.~~

~~For validation with field conditions, Hedley fractions can be used to determine of extractability of P in soils, which can be translated in pools used in models (Hedley et al., 1982; Helfenstein et al., 2024). We further suggest future model development should consider the improved representation of sorption dynamics (Yu et al., 2023) and the influence of site-specific soil properties namely pH or Fe-Al-oxides on them (Wang et al., 2022). Aspects like C or N cost for biochemical mineralization, accessibility of mineral associated material for phosphatase or plant competitiveness against microbes need further investigation but currently lack data for parameterization.~~

~~4.6.2 Priming effects and soil organic matter decomposition~~

~~Our model emphasizes the role of old organic matter as nutrient source, but the discrepancies need to be further explored in models and field experiments. In comparison to most other models, which directly prescribed priming (Jiang et al., 2019; Thurner et al., 2024), our study provides an advancement by representing priming effects as an emergent process mediated by microbes. We found the priming effect was small because nitrogen acquisition via other sources was possible. Nonetheless priming effects may play a more prominent role in N-limited systems as increased degradation of necromass has the potential to reduce long-term carbon sequestration. However, the majority of ecosystem models currently lack representation of this process (Jiang et al., 2024a; Walker et al., 2015).~~

~~Key aspects for further research include the influence of different soil properties, such as pH and soil nutrient status, on priming (Bastida et al., 2019; Spohn et al., 2013; Sun et al., 2019) and feedback of SOM decomposition on plant nutrient availability. It is also uncertain to what extend eCO_2 causes desorption of necromass, which may contribute to priming by increasing the material available for decomposition. In field experiments, artificial root exudates can be used to simulate the effect of additional input of labile C into soils and produce evaluation output for models (Lopez-Sangil et al., 2017).~~

FACE experiments suggest a strong interaction between nutrient limitation and CO_2 fertilization effect, but it remains uncertain how effectively current models represent nutrient limitation (Fleischer et al., 2019; Jiang et al., 2024a; Zaehle et al., 2014). The simulated, but not observed, response of BP, suggests that our model underestimates P limitation on plant growth under eCO_2. Overestimation in P pools may be solved with alternative model initialization approaches, assisted by Hedley fractions to determine P extractability in soils (Hedley et al., 1982; Helfenstein et al., 2024).

We suggest future model development should consider improved representation of sorption dynamics (Yu et al., 2023) and site-specific soil properties namely pH or Fe-Al-oxides on them (Wang et al., 2022). Aspects like C or N cost for biochemical mineralization, accessibility of mineral-associated material for phosphatase or plant competitiveness against microbes need further investigation but currently lack data for parameterization.

4.6.2 Modelling dynamic root exudation

~~Global mean rates of root exudation can be benchmarked against with broad meta-analysis such as Chari et al. (2024). However, additional research is needed to understand the variation of root exudation with plant species and ecosystem properties to improve model representation (Brunn et al., 2022; Chari et al., 2024; Hasegawa et al., 2023). For example,~~

~~research is needed to identify patterns of root exudation in the context of atmospheric CO_2 increase on ecosystem level: Direct measurements used for example in BiforFACE or DukeFace (Drake et al., 2011; Norby et al., 2024) provide reliable data for model evaluation. Such measurements should consider scaling into ecosystem level e.g. (units of mass/surface area/time), implying a scaling by other observables such as root mass or soil volume (Norby et al., 2024), and seasonal changes of root exudation (Leuschner et al., 2022; Phillips et al., 2008; Zhang et al., 2022). Additionally, nutrient fertilization experiments (Ataka et al., 2020) or measurements along nutrient gradients (Jiang et al., 2022; Meier et al., 2020) help to unravel the relationship of plant nutrient, C surplus status and root exudation, and therefore to constrain model parameters.~~

~~A key limitation of our model is the lack of consideration of the chemical composition of root exudates: Next to being a source for C and nutrients for microbes, the composition of exudates can actively shape the microbial community, affect soil pH, suppress sorption of inorganic P from mineral surfaces (Jones et al., 2004). Our analysis suggests that the pure implementation of root exudation as substrate for microbial growth does not capture all of the observed P dynamics.~~

Global mean rates of root exudation can be benchmarked against broad meta-analysis such as Chari et al. (2024) but further data is needed to constrain root exudation variability (Brunn et al., 2022; Hasegawa et al., 2023). In the context of atmospheric CO_2 increase on ecosystem level, direct measurements used for example in BiforFACE or DukeFace (Drake et al., 2011; Reay et al., 2025) provide reliable data for model evaluation. Such measurements should consider upscaling into ecosystem level e.g. annual flux per unit land area, implying a scaling by other observables such as root mass or soil volume (Norby et al., 2024), and seasonal changes of root exudation (Brunn et al., 2025; Leuschner et al., 2022; Phillips et al., 2008; Zhang et al., 2022).

Additionally, nutrient fertilization experiments (Ataka et al., 2020) or measurements along nutrient gradients (Jiang et al., 2022; Meier et al., 2020) help unravel the relationship between plant nutrient and C surplus status, and root exudation, to constrain model parameters.

4.6.3 Representation of soil microbial organisms

~~Uncertainty also arises from parameterization and representation of microbial pools. Currently only a few ecosystem models implement microbes explicitly (QUINCY-JSM (Yu et al., 2020); OCHDX (Zhang et al., 2020); CLM5-MIMICS-CN (Wieder et al., 2015)). In these models, carbon use efficiency is a key parameter as it determines how much C initially enters the microbial cycle. In QUINCY-JSM, carbon use efficiency is dynamically determined by the microbial nutrient imbalance, to represent microbial community changes. Other modelling approaches make use of explicitly representing distinct decomposer pools with different stoichiometric requirements, to account for changes in turnover or stoichiometry (Zhang et al., 2020). Increased inputs of root exudation with high C-to-nutrient ratio under eCO_2 will increase mining of nutrients by bacterial communities (Chertov et al., 2022) or benefit fungal communities (Sistla et al., 2014). Further field studies are required to evaluate whether this affects soil C storage and respiration by measuring changes in microbial biomass, stoichiometry and community composition.~~

Uncertainty arises from parameterization and representation of microbial pools. Currently only a few ecosystem models implement microbes explicitly (QUINCY-JSM (Yu et al., 2020); OCHDX (Zhang et al., 2020); CLM5-MIMICS-CN (Wieder et al., 2015)). In these models, CUE is a key parameter as it determines how much C initially enters the microbial cycle. In QUINCY-JSM, CUE is dynamically determined by the microbial nutrient imbalance, to represent microbial community changes. Other modelling approaches explicitly represent distinct decomposer pools, to account for changes in turnover or stoichiometry (Zhang et al., 2020). Increased root exudation under eCO_2 may increase bacterial priming or benefit fungal communities (Chertov et al., 2022; Sistla et al., 2014). But further field studies are required to evaluate how community changes control soil C storage and respiration.

Additional uncertainty comes from the role of mycorrhizal associations under eCO_2 (Terrer et al., 2016). We assume that mycorrhizal activity and C allocation to mycorrhizal community are covered by a general microbial pool and root exudation flux. We thereby neglect variations in plant nutrient acquisition strategies (Reay et al., 2025; Talbot et al., 2008; Wen et al., 2022) but reduce the amount of additional parameters. Field experiments need to further quantify C allocation to mycorrhiza, to estimate total plant belowground C allocation. However, implementation of mycorrhiza in TBMs remains a subject of ongoing debate regarding necessary mechanisms and model simplifications (Thurner et al., 2023).

4.6.4 Priming effects and soil organic matter decomposition

Our model emphasizes the role of necromass decomposition and mineralization for nutrient acquisition, but identifying control mechanisms requires further model and field experiments. Priming effects depend on N availability and demand controlled by input stoichiometry. While priming effects were small in our simulations, they may play a more prominent role in N-limited systems, potentially reducing long-term soil C sequestration.

In comparison to most other models, which directly prescribed priming (Jiang et al., 2019; Thurner et al., 2023), representing priming effects as emergent, microbial-mediated processes allow the analysis of underlying processes. However, most ecosystem models currently lack representation of this process (Jiang et al., 2024a; Walker et al., 2015).

In field experiments, artificial root exudates can be used to simulate the effect of additional input of labile C into soils and produce evaluation output for models (Lopez-Sangil et al., 2017). Future research should focus on the influence of different soil properties, such as pH and nutrient status (Bastida et al., 2019; Spohn et al., 2013; Sun et al., 2019) and feedback on plant nutrient availability.

5. Conclusion

In this study we ~~tested~~implemented a ~~novel mechanism of~~ dynamic root exudation mechanism in a nutrient enabled terrestrial biosphere model, and demonstrated that this process substantially improved the ~~representation of the CO_2 effect on~~ plant C allocation ~~as observed~~ responses to eCO_2 in a mature forest FACE experiment~~. Our model exemplifies, how~~. A key insight from our analysis is that root exudation, as ~~the~~a largely hidden pathway~~ of plant soil carbon cycle, can contribute to offset~~

~~increases in GPP under eCO_2 due to~~, provides a mechanistic link between increased GPP and heterotrophic respiration ~~caused by direct respiration of exudates and increased decomposition of microbial necromass. We suspect that increased~~observed under eCO_2, thereby explaining why soil C storage in EucFACE remained largely unchanged despite greater C inputs. Our results further demonstrate that explicit coupling between root exudation ~~under eCO_2 may lead to increased~~ , microbial activity, and nutrient acquisition is essential for capturing plant–soil ~~respiration~~feedbacks in ~~many~~ nutrient–limited ~~ecosystems worldwide, altering the soil carbon cycle through priming of microbial necromass and increased cycling of soil organic matter~~forests. We therefore recommend further development in explicit representation of root exudation, microbial dynamics and plant-microbe-interactions to account for these effects in global models. Strengthening empirical data on ecosystem-scale exudation and microbial responses in FACE experiments will be essential to reduce uncertainty.

1175

~~5 Appendix A: Changes in parameters and processes compared to standard QUINCY-JSM~~

Appendix

To improve simulations under ambient conditions, we calibrated several parameters in QUINCY-JSM for simulations of EucFACE (Table A1). Additionally, we changed processes in microbial decay to allow for priming effects in QUINCY-JSM and altered inorganic soil P initialization for deeper soil layers to account for highly weathered soils in EucFACE. To account for low P levels in subsoils of deeply layered soils, we ~~decline~~ simulate an exponential decline in initial inorganic P pools (assoc_slow, occluded, primary, solute and assoc_fast) below 70cm depth.

A1 Calibrated Parameters

Table A ~~1:~~1: Parameters changed in QUINCY-JSM for EucFACE simulation

parameter	description	unit	QUINCY-JSM standard	This study	reference/reason for change
soil					
microbial_cue_max	Maximal microbial carbon use efficiency	[unitless]	0.6	0.5	Adjust to meet microbial biomass in EucFACE
k_slow_som_np	N:P ratio for microbial ~~residue~~necromass pool initialization	g g^{-1}	14	21	Reduce P in system
Microbial_cn	Microbial N:C ratio	g g^{-1}	7.6	4.3	Pihlblad et al., 2019
Microbial_np	Microbial N:P ratio	g g^{-1}	5.6	4.1	Pihlblad et al., 2019; Jiang et al., 2020; Jiang et al., 2024

Qmx_org_fp	maximum sorption capacity of OM to fine soil particle	molC (kg fine particle)$^{-1}$	6.5537	5.57	Reduce organic matter sorption to account for soils at EucFACE
km_mic_biochem_po4	Half-saturation microbial biomass for PO_4 biochemical mineralization	molC m^{-3}	0.42	12.49	Account for P-limited soils
vegetation					
Jmax2vcmax_C3	ratio of Jmax25/Vcmax25 for prescribed leaf N	[unitless]	1.92	1.64	Jiang et al., 2024
Root2leaf_cn	relative C: N of fine roots compared to leaves	[unitless]	0.85	0.62	Jiang et al., 2024
lambda_sinklim_PS	Weibull parameter for sink limitation	[unitless]	0.1	0.05	Reduced sink limitation to allow for root exudation
Wood2leaf_cn	relative C: N of sapwood biomass compared to leaves	[unitless]	0.145	0.32	Jiang et al., 2024
Root2leaf_np	relative N:P of fine roots compared to leaves	[unitless]	0.8	1.0	Jiang et al., 2024

Wood2leaf_np	relative N:P of sapwood biomass compared to leaves	[unitless]	0.64	1.0	Jiang et al., 2024
SLA	specific leaf area	mm (mg DW)$^{-1}$	8.99	6.01	Jiang et al., 2024
K_crtos	coarse root to sapwood mass ratio	[unitless]	0.4	0.1	Jiang et al., 2024
K_rtos	trade-off parameter for hydraulic investment into sapwood or fine roots	[unitless]	5.615	4.925	Adjusted to follow allocation in Jiang et al., 2020
K_latosa	leaf area to sapwood area ratio	[unitless]	4000	3000	Adjusted follow allocation in Jiang et al., 2020
Tau_fine_root	fine root turnover	yr	0.75	1.5	Jiang et al., 2024

A2 Enabling priming via microbial grazing

When microbes decay, in the model part of biomass is directly recycled as DOM, part enters ~~residue~~the necromass pool. We altered microbial decay, such that for nitrogen an additional part enters solute NH_4 to account for microbial grazing. Original JSM describes element transfer upon microbial turnover as:

~~$$\eta^{X}_{mic \rightarrow dom} = \sigma^{X}_{recycle} * \frac{X_{mic}}{\tau_{mic}} \quad (A1)$$~~

~~$$\eta^{X}_{mic \rightarrow res} = 1 - \eta^{X}_{mic \rightarrow dom} \quad (A2)$$~~

$$\eta^{X}_{mic \rightarrow dom} = \sigma^{X}_{recycle} * \frac{X_{mic}}{\tau_{mic}} \quad (A1)$$

$$\eta^{X}_{mic\rightarrow res} = 1 - \eta^{X}_{mic\rightarrow dom} \quad (A2)$$

Where $\eta^{X}_{mic\rightarrow dom}$ [molX m³ s^{-1}] and $\eta^{X}_{mic\rightarrow res}$ [molX m³ s^{-1}] are the fluxes from microbial pool to DOM and ~~residue~~necromass pool, respectively, X_{mic} [molX m³] is the microbial pool and τ_{mic} [s] is the microbial turnover time for C, N and P. $\sigma^{X}_{recycle}$ [unitless] is a constant recycling fraction for C and P, but flexible for N. Under N limitation microbes recycle up to 66 % of N, depending on microbial nutrient status. Therefore, microbes in need for N under additional growth would increase recycling but not change enzyme allocation. To bypass this, we fixed the recycling factor and simulate the effect of microbial grazing as:

~~$$\eta^{N}_{mic\rightarrow dom} = \sigma^{N}_{recycle} * \frac{N_{mic}}{\tau_{mic}} \quad (A3)$$~~

~~$$\eta^{N}_{mic\rightarrow NH4_{sol}} = \sigma^{N}_{grazing} * \frac{N_{mic}}{\tau_{mic}} \quad (A5)$$~~

~~$$\eta^{N}_{mic\rightarrow res} = 1 - \eta^{N}_{mic\rightarrow dom} - \eta^{N}_{mic\rightarrow NH4_{sol}} \quad (A6)$$~~

$$\eta^{N}_{mic\rightarrow dom} = \sigma^{N}_{recycle} * \frac{N_{mic}}{\tau_{mic}} \quad (A3)$$

$$\eta^{N}_{mic\rightarrow NH4_{sol}} = \sigma^{N}_{grazing} * \frac{N_{mic}}{\tau_{mic}} \quad (A5)$$

$$\eta^{N}_{mic\rightarrow res} = 1 - \eta^{N}_{mic\rightarrow dom} - \eta^{N}_{mic\rightarrow NH4_{sol}} \quad (A6)$$

Where $\eta^{N}_{mic\rightarrow NH4_{sol}}$ [molX m³ s^{-1}] is the grazing flux from microbial pool to soluble NH_4 pool and $\sigma^{N}_{grazing}$ [unitless] is the related fraction.

Table A ~~2:~~2: New parameters for microbial decay and recycling

	Unit	Standard Quincy-JSM	This study
$\sigma^{C}_{recycle}$	unitless	0.172	0.3
$\sigma^{N}_{recycle}$	unitless	(0.172-0.66), At least 0.6 if microbes under N limitation	0.4
$\sigma^{P}_{recycle}$	unitless	0.172	0.5
$\sigma^{X}_{grazing}$	unitless	-	0.2

6 Appendix B: Additional Tables and Figures

Table B ~~1.~~1: Comparison of mean annual of simulated pools (gC m^2) and fluxes (gC m^{-2} yr^{-1}) for EucFACE under ambient conditions with observed means and +- one standard deviation across 3 rings (2013-2016). NEP refers to 3 different alternative methods of estimation (Jiang et al., 2020; Jiang et al., 2024a)

Carbon pool (gC m^{-2})	**observed**	**simulated**
Leaf	151 (+-14)	145
Wood	4558 (+-321)	4218
Fine root	227 (+-5)	182
Coarse root	606 (+-60)	622
Soil carbon	2.183 (+-280) (top 10 cm)	2456(top 13 cm)
Microbial carbon	61 (+-3.6)	81
Carbon flux (gC m^{-2} yr^{-1})	**observed**	**simulated**
Overstorey GPP	1563 (+-200)	1702
NEP	-73 - 28	1
Biomass production	484 (+-63)	365
Soil respiration	1097 (+-86)	1207

Table B ~~2.~~2: Comparison of mean annual of simulated pool stoichiometry for EucFACE under ambient conditions with observations (2013-2016) (Jiang et al., 2024a)

Variable	**Observed CN**	**Simulated CN**	**Observed NP**	**Simulated NP**
leaf	35.5 ± 2.7	29.6	22.9 ± 0.1	24.4
sapwood	101.6 ± 14.7	110.9	35.6 ± 2.1	35.8
wood	110.2 ± 30.3	138.7	33.7 ± 2.7	35.8
fineroot	56.9 ± 4.6	47.7	28.7 ± 3.3	30.5
soil	13.8 ± 1.0	11.9	16.4 ± 3.4	16.2

Table B ~~3.~~3: Observed (2013-2016) and simulated (2013-2019 CO_2 effect on ecosystem fluxes at EucFACE. Our model did not include understorey. Observed values refer to overstorey gross primary productivity (~~GPPo~~GPP), biomass production on abovegound overstorey and whole vegetation root biomass production (BP), autotrophic respiration on abovegound overstorey and whole vegetation root respiration (~~AutResp~~Autotrophic respiration), heterotrophic respiration ~~(HetResp)~~ and soil respiration ~~(Rsoil).~~. Observed values from Jiang et al 2020.

Carbon Flux	Observed increase	Simulated increase
~~GPPo~~Overstorey GPP	12 %	22 %
~~BP~~Biomass production (BP)	3 %	33 %
~~AutResp~~Autotrophic respiration	5 %	13 %
~~HetResp~~Heterotrophic respiration	17 %	14 %
~~Rsoil~~soil respiration	12 %	13 %

Table B 4: Modelled turnover times under ambient and elevated CO_2 for the ecosystem (C), soil (C, N, P) and microbial necromass (C, N, P). Calculated for 2015-2019.

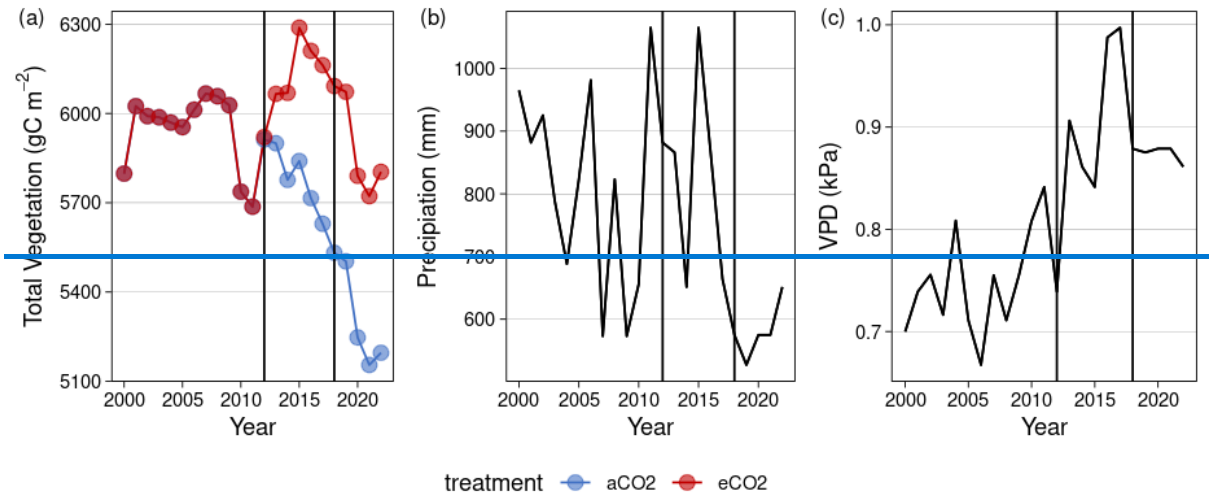

1235

		$\tau_{soil}(yr)$	$\tau_{necromass}(yr)$
carbon	aCO_2	17.1	30.4
	eCO_2	15.1	27.7
nitrogen	aCO_2	242.1	30.5
	eCO_2	193.2	27.7
phosphorus	aCO_2	561.2	8.2
	eCO_2	447.6	6.4

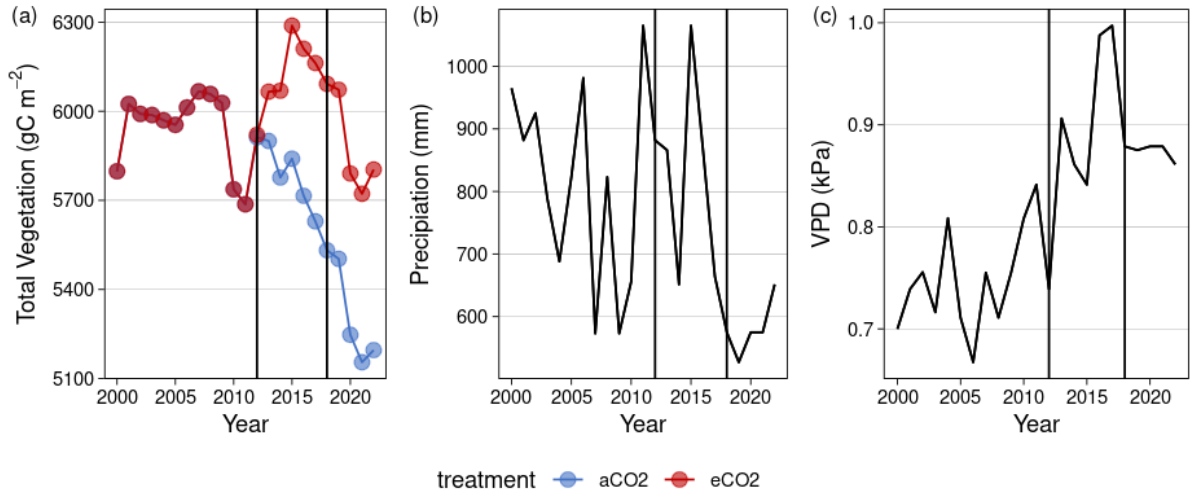

Figure B 1:1: Simulated total vegetation C, precipitation and vapor pressure deficit (VPD) from 2012 to 2022 for EucFACE under ambient conditions. Vegetation follows a downward trend from 2010-2022 due to climate extremes. Forcing from 2012-2018 (black bars) follows meteorological data observations, while forcing before and after this period follows repeated and randomized observations.

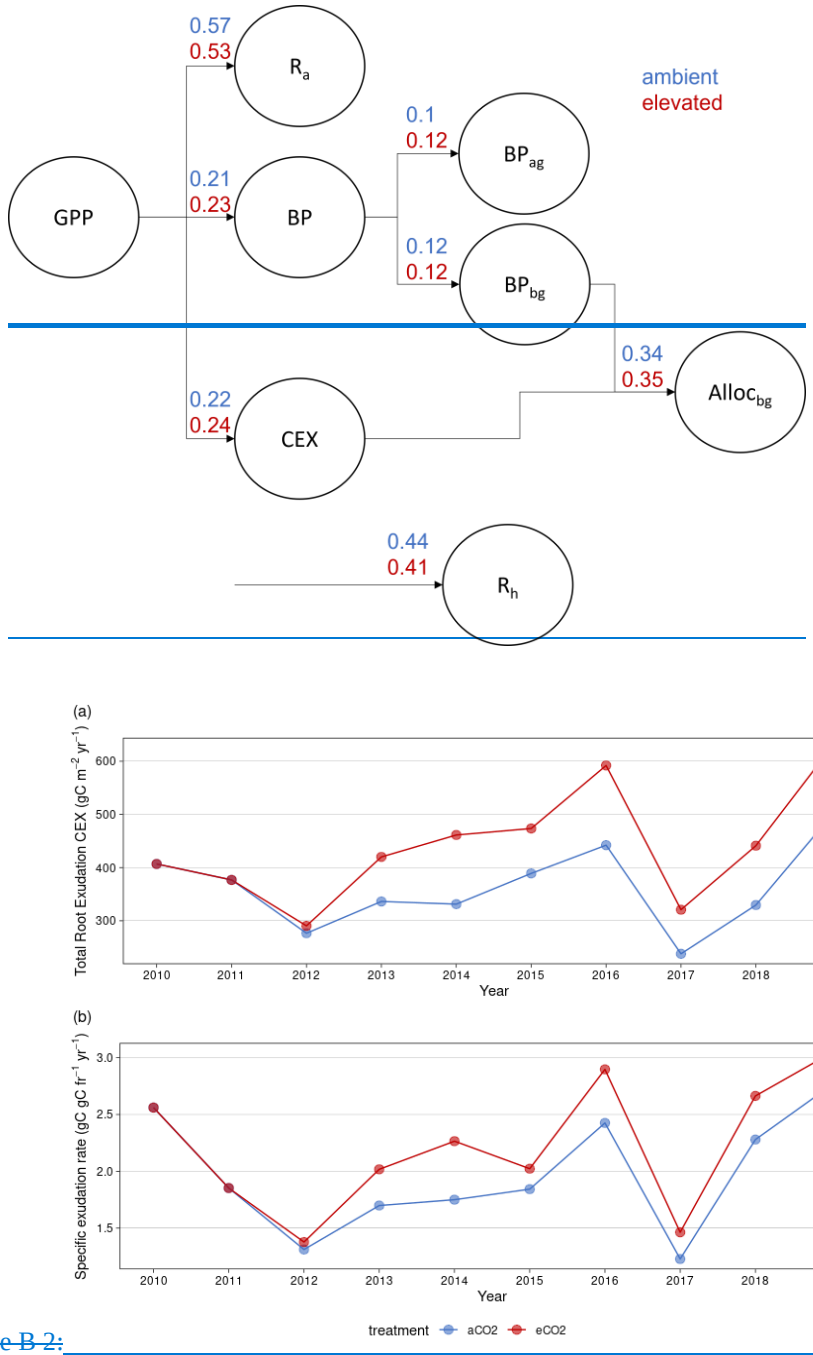

~~Figure B 2:~~

Figure B 2: Simulated total root exudation for 2010 to 2019 for EucFACE for ambient and elevated treatment as (a) Total root exudation flux and (b) Specific root exudation rate. CO_2 fumigation started with ramp up end of 2012.

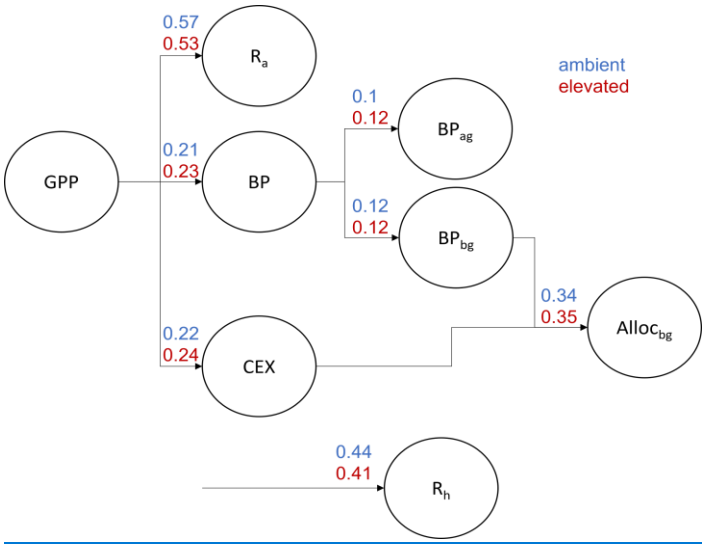

Figure B 3: Simulated allocation of GPP under ambient and elevated CO_2 treatment for EucFACE based on simulated annual mean of fluxes from 2012-2019. Numbers on arrows refer to fraction of GPP. GPP is allocated to autotrophic respiration (R_a), biomass production (BP), including aboveground (BP_{ag}) and belowground (BP_{bg}) biomass production and carbon root exudation (CEX). CEX and BP_{bg} add up to total belowground allocation. Additionally, the fraction of GPP that is respired via heterotrophic respiration (R_h) is shown.

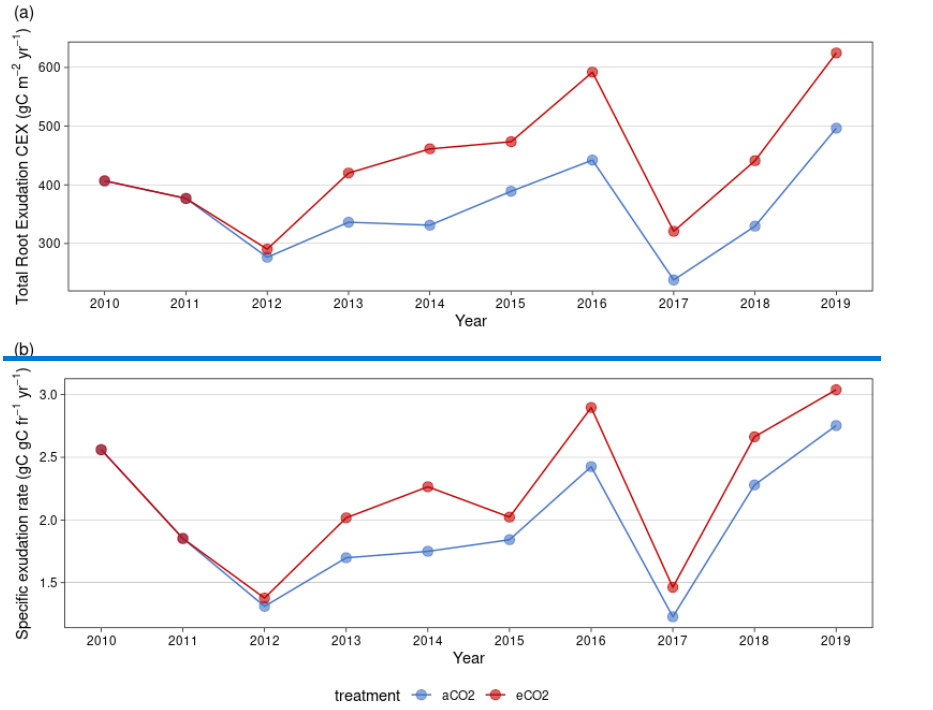

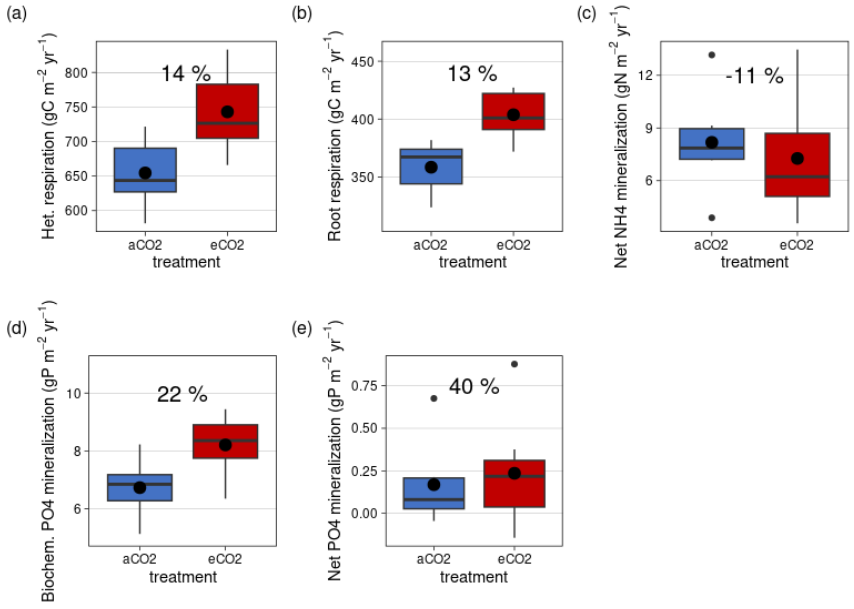

~~Figure B 3:~~

Figure B 4: Simulated major mineralization fluxes for C, N and P under ambient and elevated CO_2 (2013-2019) for topsoil layers. (a) Heterotrophic respiration, (b) Root respiration, (c) Net NH_4 mineralization, (d) biochemical mineralization, (e) Net PO_4

mineralization as sum of biological and biochemical mineralization. Boxplots show annual variation of fluxes, dots represent mean values. Percentage difference based on Annual mean for 2013-2019 is given for each flux.

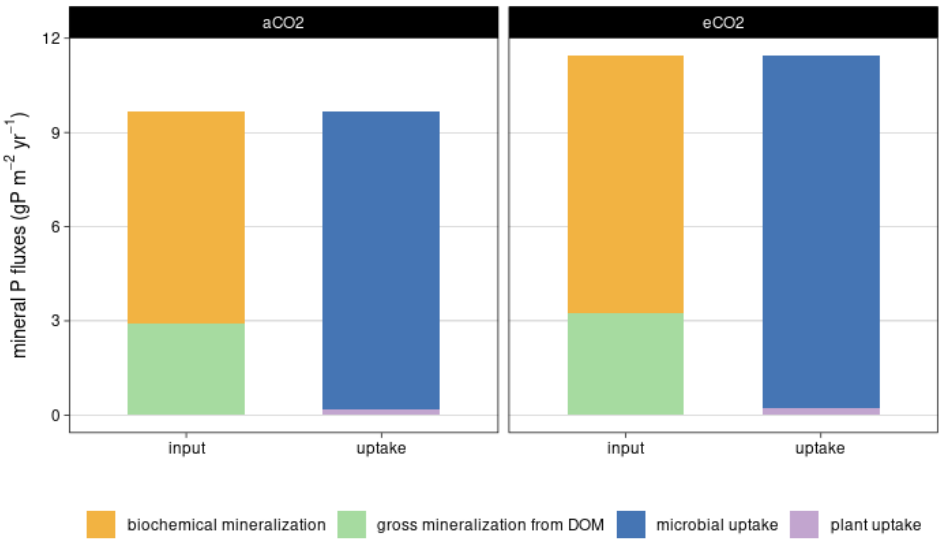

1260

Figure B 5 simulated mineral P fluxes in topsoil layers (50cm) for ambient (aCO2) and elevated (eCO2) treatment. Annual average from 2013-2019 fluxes which provide (input) plant and microbes available mineral P are gross biological mineralization from DOM and biochemical mineralization. Available P is immobilized via uptake by microbes or plants.

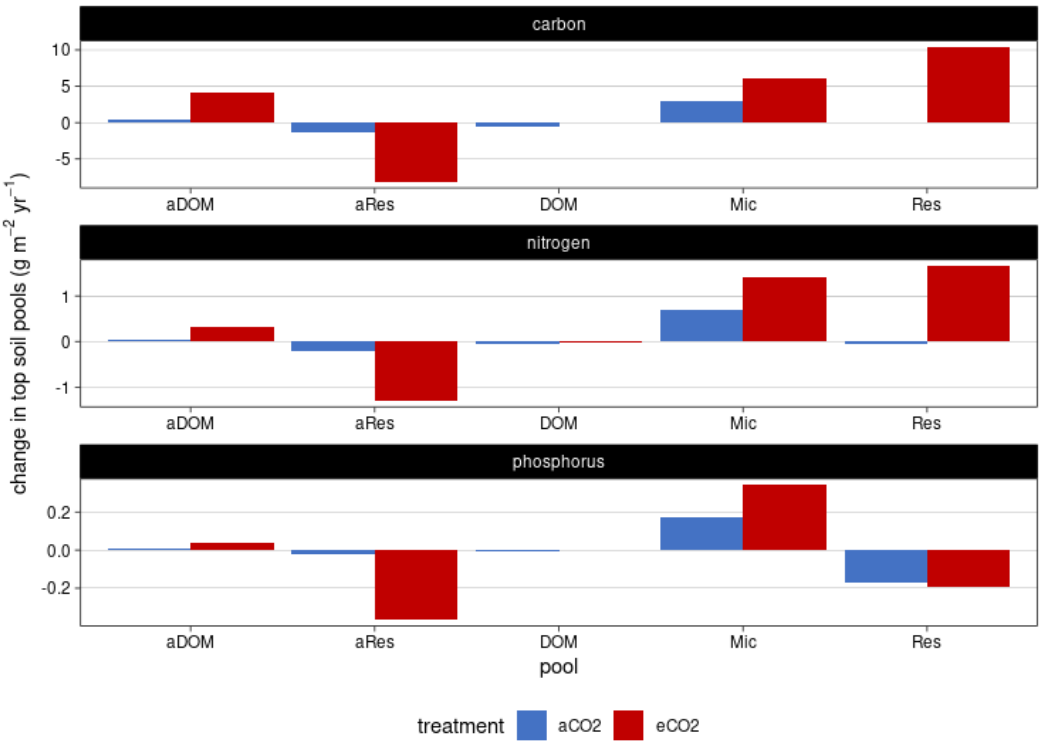

Figure B 6: Simulated changes in topsoil pools for EucFACE under ambient and elevated CO_2 treatment 2013-2019: mineral associated DOM (aDOM), mineral associated microbial necromass (aRes), dissolved organic matter (DOM), microbes (Mic) and microbial necromass (Res).

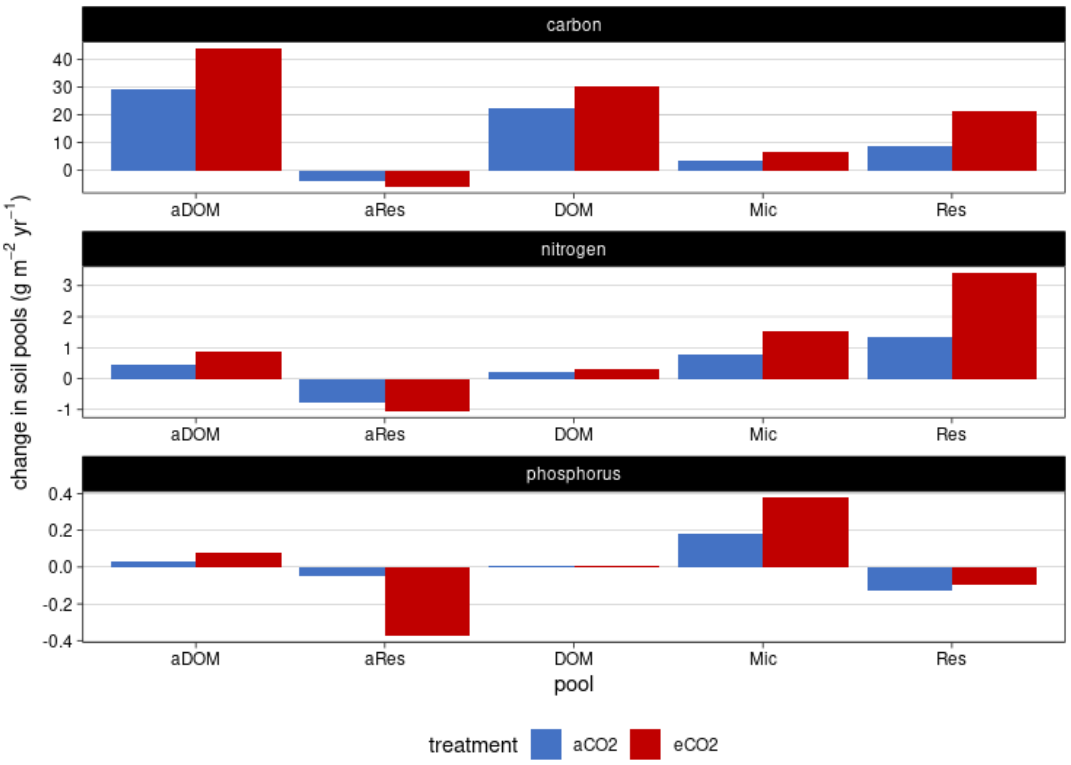

Figure B 7: Simulated changes in soil pools for whole soil column for EucFACE under ambient and elevated CO_2 treatment 2013-2019: mineral associated DOM (aDOM), mineral associated microbial necromass (aRes), dissolved organic matter (DOM), microbes (Mic) and microbial necromass (Res)

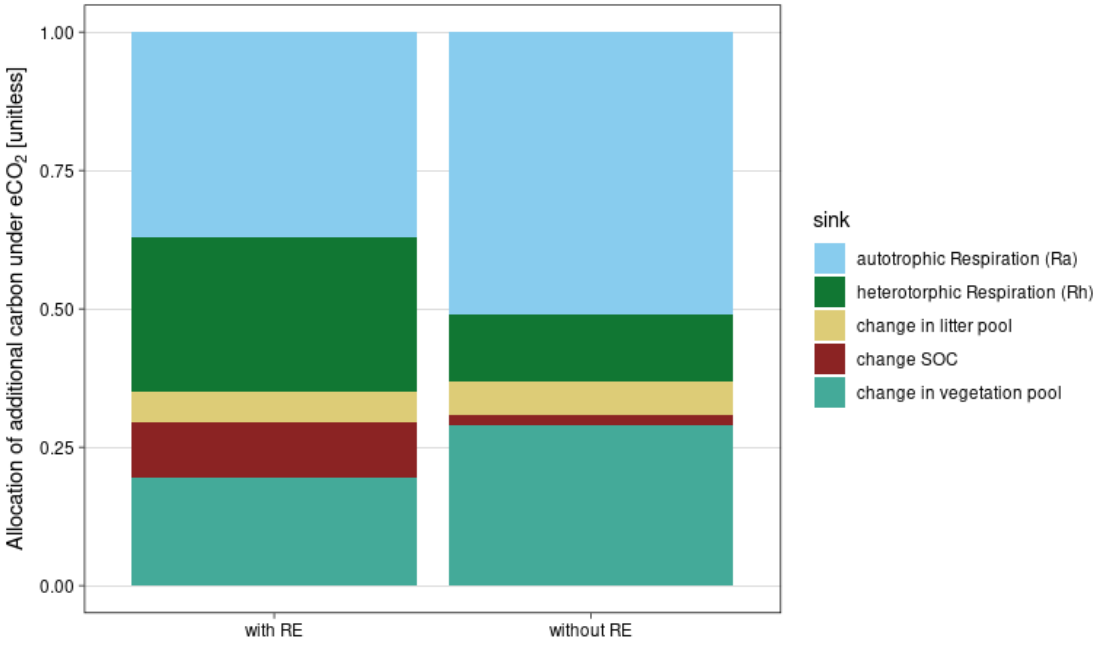

~~Figure B 8: Simulated total root exudation for 2010 to 2019 for EucFACE for ambient and elevated treatment as (a) Total root exudation flux and (b) Specific root exudation rate. CO_2 fumigation started with ramp up end of 2012.~~

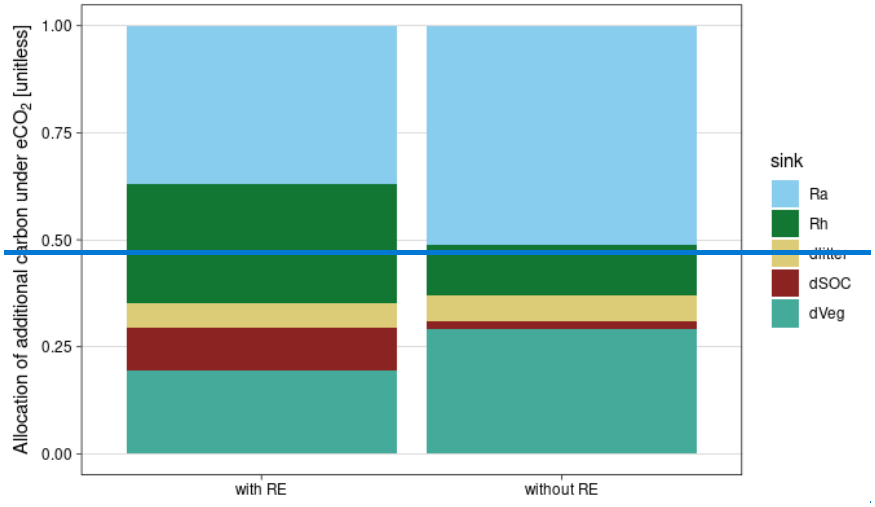

~~Figure B 4:~~ **Simulated allocation of additional GPP under eCO_2 with root exudation module (with RE) and without root exudation module (without RE) for 2013-2029. Additional GPP can be allocated into autotroph respiration (Ra), heterotrophic respiration (Rh), litter (dlitter), soil organic carbon (dSOC) or vegetation carbon (dVeg)**

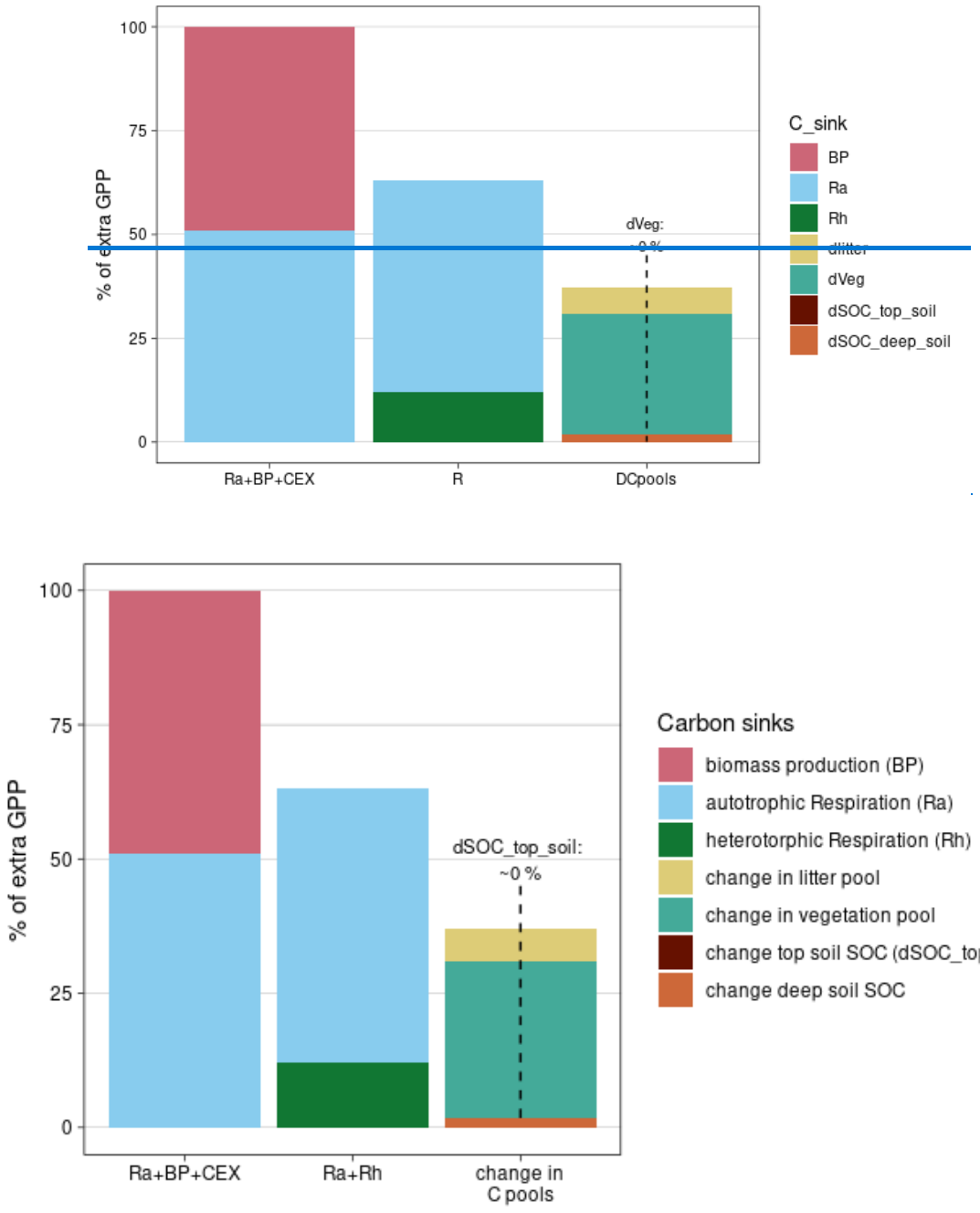

Figure B ~~5:~~9: Simulated fate of additional sequestered C under eCO_2 as percentage of increased overstorey gross primary productivity (GPP) for simulations without root exudation (2013-2019). For simulations additional GPP is transferred into autotrophic respiration (Ra), biomass production (BP). Ecosystem respiration (R) is composed of heterotrophic respiration (Rh) and autotrophic respiration (Ra). Change in ecosystem carbon Change in ecosystem carbon pools is composed of change in topsoil

organic C (dSOC_top_soil top 10 cm for observation, top 50 cm for simulation), change in deep soil SOC (dSOC_deep_soil, no observations) change in litter (dlitter) and change in vegetation (dVeg).

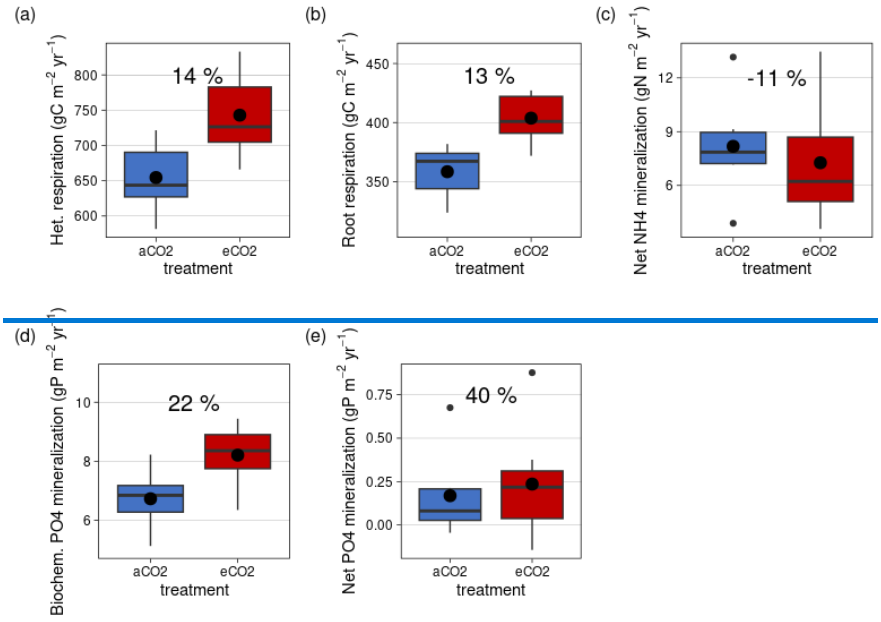

Figure B 6: ~~Simulated major mineralization fluxes for C, N and P under ambient and elevated CO_2 (2013-2019) for topsoil layers. (a) Heterotrophic respiration, (b) Root respiration, (c) Net NH_4 mineralization, (d) biochemical mineralization, (e) Net PO_4 mineralization as sum of biological and biochemical mineralization. Boxplots show annual variation of fluxes, dots represent mean values. Percentage difference based on Annual mean for 2013-2019 is given for each flux.~~

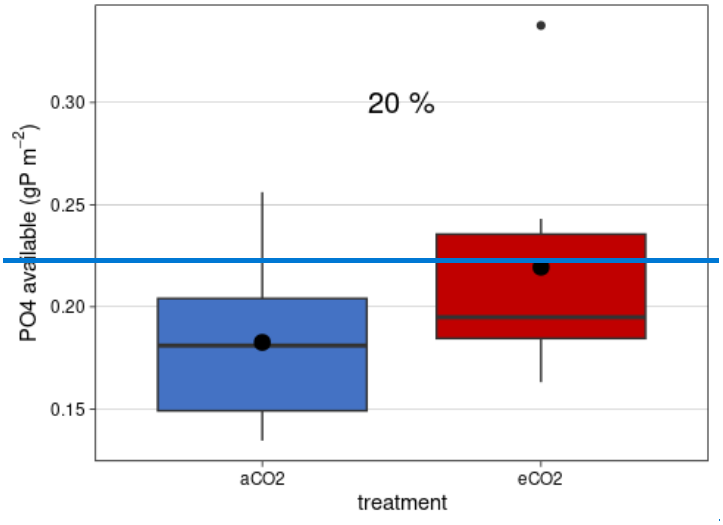

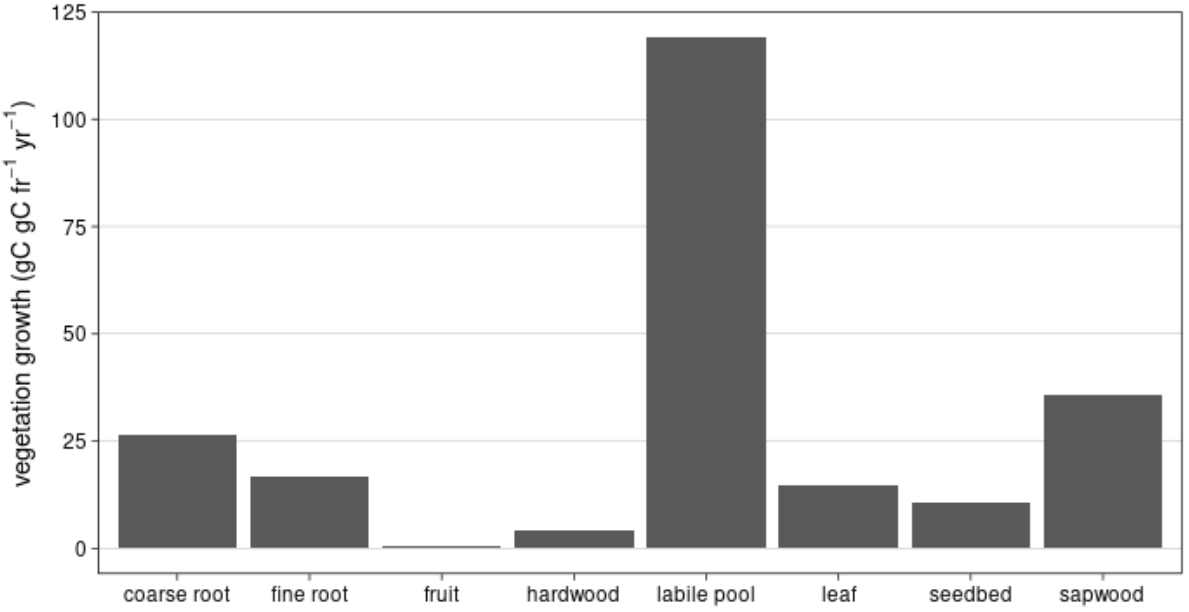

Figure B 10: Simulated mean annual vegetation growth response to eCO_2 from 2013-2019.

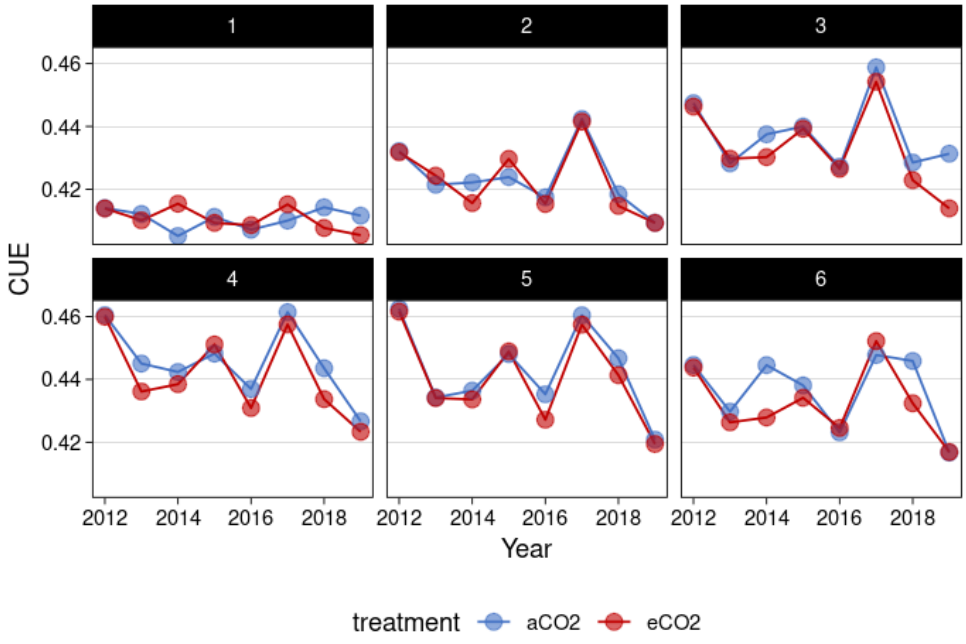

Figure B 11: Simulated microbial carbon use efficiency for top 6 soil layers (topsoil) in QUINCY-JSM JSM for EucFACE under ambient and elevated conditions (2013-2019).

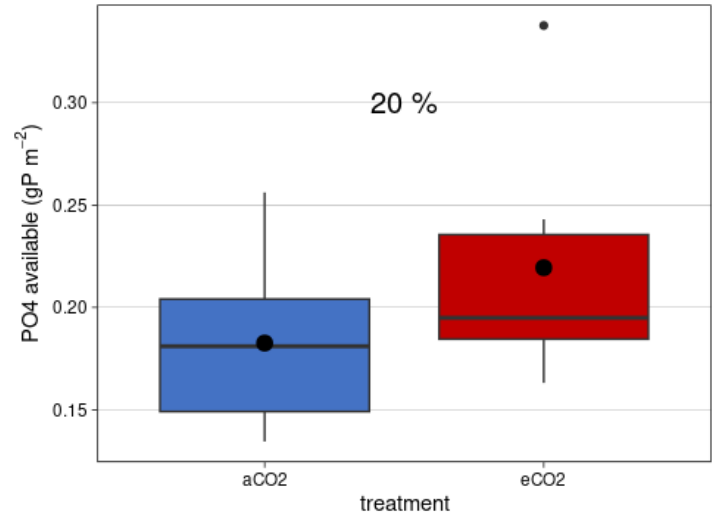

Figure B ~~7:~~12: Mean annual available PO_4 for plant and microbial uptake under ambient and elevated conditions in topsoil for 7 years of simulation (2013-2019). Boxplots show annual variation of fluxes, dots represent mean values. Percentage difference based on annual mean for 2013-2019 is shown above boxplots.

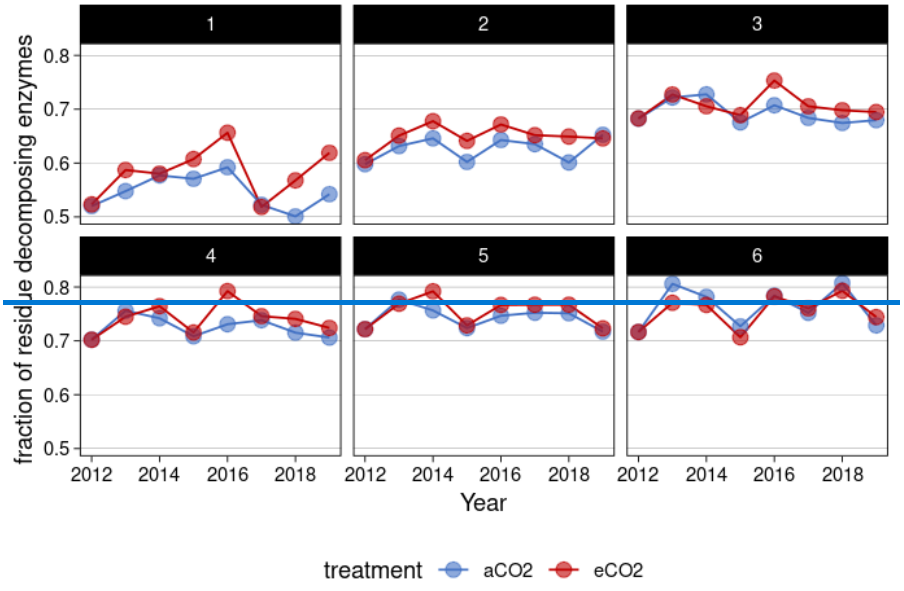

~~**Figure B 8: Simulated fraction of residue decomposing enzymes for top 6 soil layers (topsoil) in QUINCY-JSM for EucFACE under ambient and elevated conditions (2013-2019).**~~

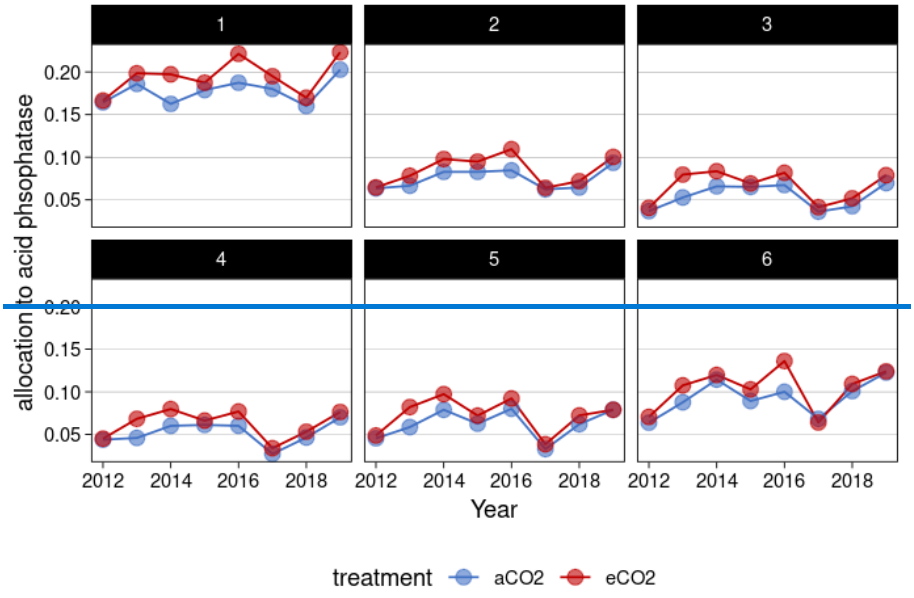

~~Figure B 9: Simulated acid phosphatase allocation in microbes for top 6 soil layers (topsoil) in QUINCY-JSM JSM for EucFACE under ambient and elevated conditions (2013-2019).~~

1315

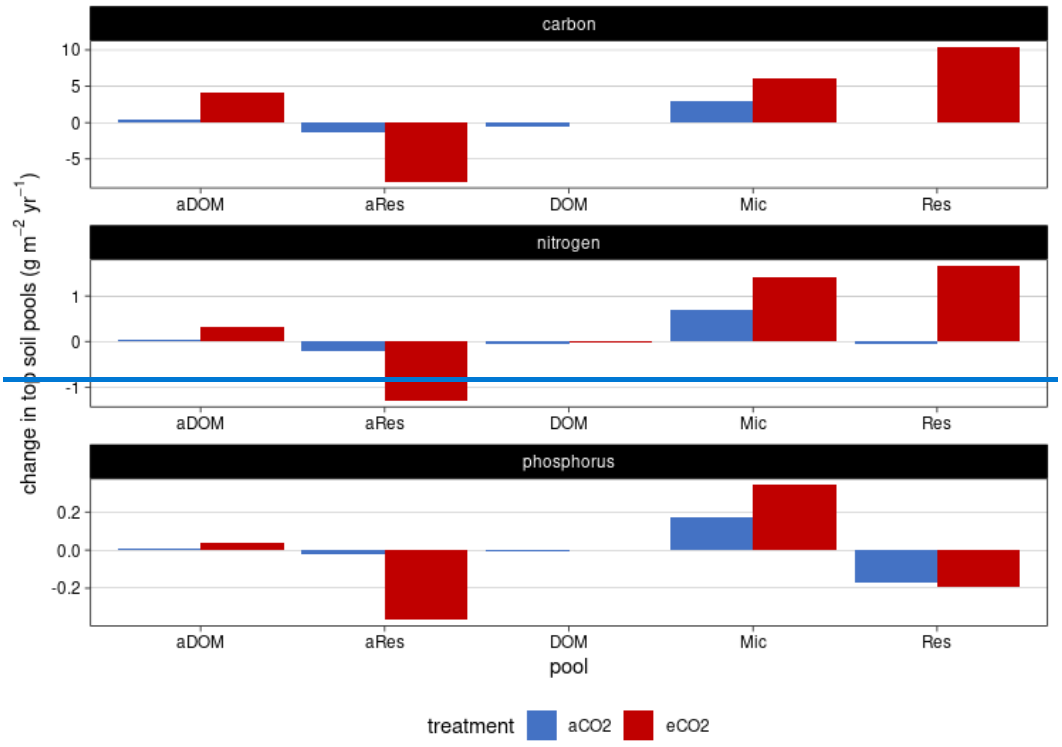

Figure B 10: Simulated changes in topsoil pools for EucFACE under ambient and elevated CO_2 treatment 2013-2019: ineral associated DOM (aDOM), mineral associated microbial residue (aRes), dissolved organic matter (DOM), microbes (Mic) and microbial residue (Res).

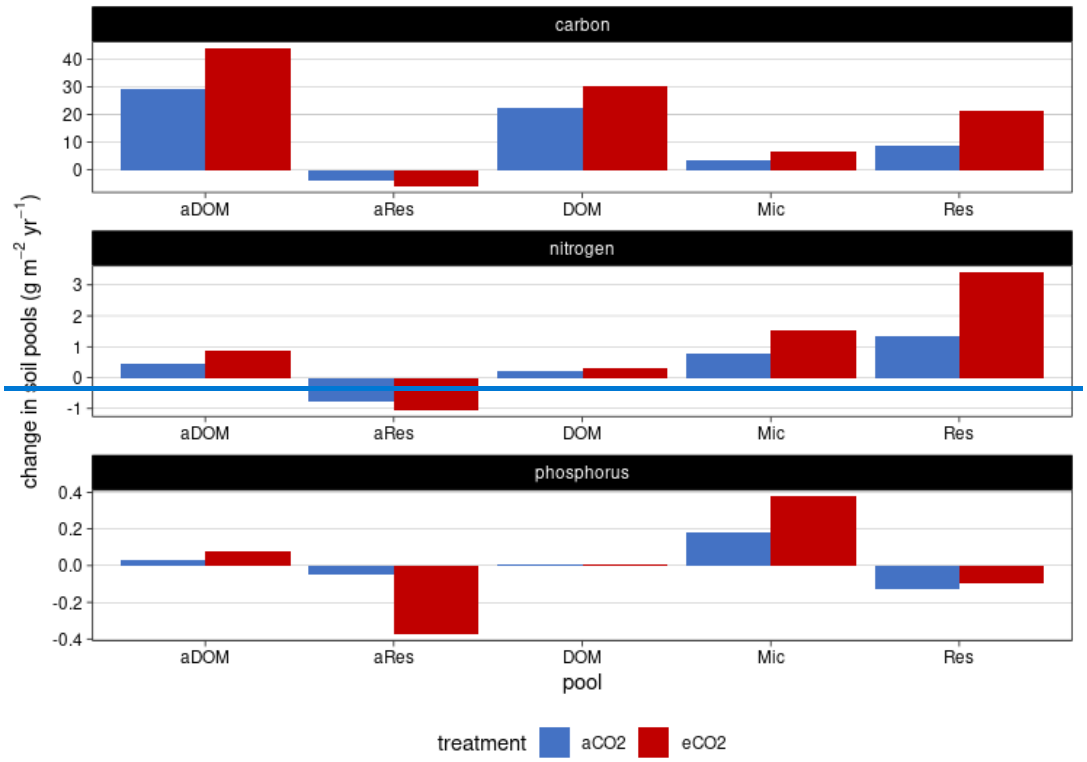

~~Figure B 11: Simulated changes in soil pools for whole soil column for EucFACE under ambient and elevated CO_2 treatment 2013-2019: mineral associated DOM (aDOM), mineral associated microbial residue (aRes), dissolved organic matter (DOM), microbes (Mic) and microbial residue (Res)~~

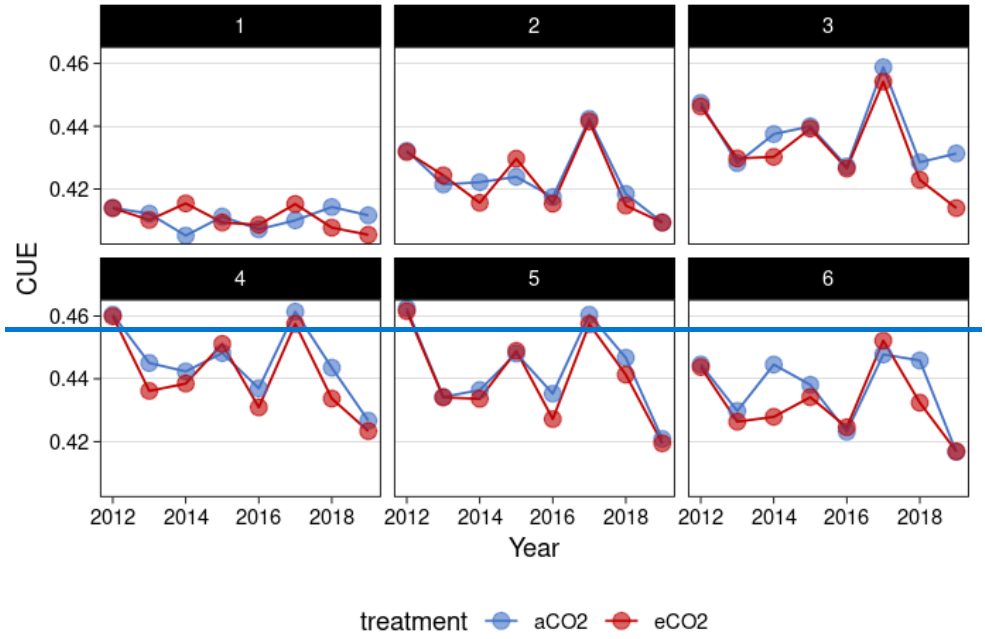

1325

Figure B 12: Simulated microbial carbon use efficiency for top 6 soil layers (topsoil) in QUINCY-JSM-JSM for EucFACE under ambient and elevated conditions (2013-2019).

Code availability. The model is open source under the GNU GPL vs3 and MPI-M ICON software license agreement (depending on module). The code is available under https://doi.org/10.17871/quincy-model-2019. A copy of the scientific code can be found in this temporary (01.12.2025) private link for review purposes: https://nextcloud.bgc-jena.mpg.de/s/w2EiXdBDZmGX4F9.
Forcing data to run the model for testbed simulations can be made available on request.

Competing interests. At least one of the (co-)authors is a member of the editorial board of Biogeosciences

Acknowledgement: KS acknowledges financial support from the IMPRS for Global Biogeochemical Cycles.

Contribution of authors. KS, KF and SZ designed the study. KS, KF and SZ interpreted the results. KS wrote model implementation and first draft of the manuscript. KF, AR, LY, MJ, BEM, SZ contributed to manuscript revision.

Additional Licences. ~~Two~~Three figures were made with Biorender.com. The licenses can be found with the following links:

https://biorender.com/4hh7q5c

https://biorender.com/7hjbj3d

https://biorender.com/b5hxuaa

References

Ai, J., Banfield, C. C., Shao, G., Zamanian, K., Stürzebecher, T., Shi, L., Fan, L., Liu, X., Spielvogel, S., and Dippold, M. A.: What controls the availability of organic and inorganic P sources in top- and subsoils? A 33P isotopic labeling study with root exudate addition, Soil Biology and Biochemistry, 185, 109129, https://doi.org/10.1016/j.soilbio.2023.109129, 2023.

Akatsuki, M. and Makita, N.: Influence of fine root traits on in situ exudation rates in four conifers from different mycorrhizal associations, Tree Physiology, 40, 1071–1079, https://doi.org/10.1093/treephys/tpaa051, 2020.

Ataka, M., Sun, L., Nakaji, T., Katayama, A., and Hiura, T.: Five-year nitrogen addition affects fine root exudation and its correlation with root respiration in a dominant species, Quercus crispula, of a cool temperate forest, Japan, Tree Physiology, 40, 367–376, https://doi.org/10.1093/treephys/tpz143, 2020.

Atkin, O. K., Meir, P., and Turnbull, M. H.: Improving representation of leaf respiration in large-scale predictive climate–vegetation models, New Phytologist, 202, 743–748, https://doi.org/10.1111/nph.12686, 2014.

Bastida, F., García, C., Fierer, N., Eldridge, D. J., Bowker, M. A., Abades, S., Alfaro, F. D., Asefaw Berhe, A., Cutler, N. A., Gallardo, A., García-Velázquez, L., Hart, S. C., Hayes, P. E., Hernández, T., Hseu, Z.-Y., Jehmlich, N., Kirchmair, M., Lambers, H., Neuhauser, S., Peña-Ramírez, V. M., Pérez, C. A., Reed, S. C., Santos, F., Siebe, C., Sullivan, B. W., Trivedi, P., Vera, A., Williams, M. A., Luis Moreno, J., and Delgado-Baquerizo, M.: Global ecological predictors of the soil priming effect, Nat Commun, 10, 3481, https://doi.org/10.1038/s41467-019-11472-7, 2019.

Brunn, M., Hafner, B. D., Zwetsloot, M. J., Weikl, F., Pritsch, K., Hikino, K., Ruehr, N. K., Sayer, E. J., and Bauerle, T. L.: Carbon allocation to root exudates is maintained in mature temperate tree species under drought, New Phytologist, 235, 965–977, https://doi.org/10.1111/nph.18157, 2022.

Brunn, M., Mueller, C. W., Chari, N. R., Meier, I. C., Obersteiner, S., Phillips, R. P., Taylor, B., Tumber-Dávila, S. J., Ullah, S., and Klein, T.: Tree carbon allocation to root exudates: implications for carbon budgets, soil sequestration and drought response, Tree Physiology, 45, tpaf026, https://doi.org/10.1093/treephys/tpaf026, 2025.

Castañeda-Gómez, L., Walker, J. K. M., Powell, J. R., Ellsworth, D. S., Pendall, E., and Carrillo, Y.: Impacts of elevated carbon dioxide on carbon gains and losses from soil and associated microbes in a *Eucalyptus* woodland, Soil Biology and Biochemistry, 143, 107734, https://doi.org/10.1016/j.soilbio.2020.107734, 2020.

~~Chari, N. R., Tumber-Dávila, S. J., Phillips, R. P., Bauerle, T. L., Brunn, M., Hafner, B. D., Klein, T., Obersteiner, S., Reay, M. K., Ullah, S., and Taylor, B. N.: Estimating the global root exudate carbon flux, Biogeochemistry, 167, 895–908, https://doi.org/10.1007/s10533-024-01161-z, 2024.~~

Chertov, O., Kuzyakov, Y., Priputina, I., Frolov, P., Shanin, V., and Grabarnik, P.: Modelling the Rhizosphere Priming Effect in Combination with Soil Food Webs to Quantify Interaction between Living Plant, Soil Biota and Soil Organic Matter, Plants, 11, 2605, https://doi.org/10.3390/plants11192605, 2022.

Cotrufo, M. F., Wallenstein, M. D., Boot, C. M., Denef, K., and Paul, E.: The Microbial Efficiency-Matrix Stabilization (MEMS) framework integrates plant litter decomposition with soil organic matter stabilization: do labile plant inputs form stable soil organic matter?, Global Change Biology, 19, 988–995, https://doi.org/10.1111/gcb.12113, 2013.

Crous, K. Y., Ósvaldsson, A., and Ellsworth, D. S.: Is phosphorus limiting in a mature Eucalyptus woodland? Phosphorus fertilisation stimulates stem growth, Plant Soil, 391, 293–305, https://doi.org/10.1007/s11104-015-2426-4, 2015.

De Andrade, S. A. L., Borghi, A. A., De Oliveira, V. H., Gouveia, L. de M., Martins, A. P. I., and Mazzafera, P.: Phosphorus Shortage Induces an Increase in Root Exudation in Fifteen Eucalypts Species, Agronomy, 12, 2041, https://doi.org/10.3390/agronomy12092041, 2022.

De Kauwe, M. G., Medlyn, B. E., Zaehle, S., Walker, A. P., Dietze, M. C., Wang, Y.-P., Luo, Y., Jain, A. K., El-Masri, B., Hickler, T., Wårlind, D., Weng, E., Parton, W. J., Thornton, P. E., Wang, S., Prentice, I. C., Asao, S., Smith, B., McCarthy, H. R., Iversen, C. M., Hanson, P. J., Warren, J. M., Oren, R., and Norby, R. J.: Where does the carbon go? A model–data intercomparison of vegetation carbon allocation and turnover processes at two temperate forest free-air CO2 enrichment sites, New Phytologist, 203, 883–899, https://doi.org/10.1111/nph.12847, 2014.

Dijkstra, F., Carrillo, Y., Pendall, E., and Morgan, J.: Rhizosphere priming: a nutrient perspective, Frontiers in Microbiology, 4, 2013.

Drake, J. E., Gallet-Budynek, A., Hofmockel, K. S., Bernhardt, E. S., Billings, S. A., Jackson, R. B., Johnsen, K. S., Lichter, J., McCarthy, H. R., McCormack, M. L., Moore, D. J. P., Oren, R., Palmroth, S., Phillips, R. P., Pippen, J. S., Pritchard, S. G., Treseder, K. K., Schlesinger, W. H., DeLucia, E. H., and Finzi, A. C.: Increases in the flux of carbon belowground stimulate nitrogen uptake and sustain the long-term enhancement of forest productivity under elevated CO2, Ecology Letters, 14, 349–357, https://doi.org/10.1111/j.1461-0248.2011.01593.x, 2011.

Drake, J. E., Darby, B. A., Giasson, M.-A., Kramer, M. A., Phillips, R. P., and Finzi, A. C.: Stoichiometry constrains microbial response to root exudation- insights from a model and a field experiment in a temperate forest, Biogeosciences, 10, 821–838, https://doi.org/10.5194/bg-10-821-2013, 2013.

Drake, J. E., Macdonald, C. A., Tjoelker, M. G., Crous, K. Y., Gimeno, T. E., Singh, B. K., Reich, P. B., Anderson, I. C., and Ellsworth, D. S.: Short-term carbon cycling responses of a mature eucalypt woodland to gradual stepwise enrichment of atmospheric CO2 concentration, Global Change Biology, 22, 380–390, https://doi.org/10.1111/gcb.13109, 2016.

Drake, J. E., Macdonald, C. A., Tjoelker, M. G., Reich, P. B., Singh, B. K., Anderson, I. C., and Ellsworth, D. S.: Three years of soil respiration in a mature eucalypt woodland exposed to atmospheric CO2 enrichment, Biogeochemistry, 139, 85–101, https://doi.org/10.1007/s10533-018-0457-7, 2018.

Du, E., Terrer, C., Pellegrini, A. F. A., Ahlström, A., van Lissa, C. J., Zhao, X., Xia, N., Wu, X., and Jackson, R. B.: Global patterns of terrestrial nitrogen and phosphorus limitation, Nat. Geosci., 13, 221–226, https://doi.org/10.1038/s41561-019-0530-4, 2020.

Ellsworth, D. S., Anderson, I. C., Crous, K. Y., Cooke, J., Drake, J. E., Gherlenda, A. N., Gimeno, T. E., Macdonald, C. A., Medlyn, B. E., Powell, J. R., Tjoelker, M. G., and Reich, P. B.: Elevated CO2 does not increase eucalypt forest productivity on a low-phosphorus soil, Nature Clim Change, 7, 279–282, https://doi.org/10.1038/nclimate3235, 2017.

Filion, M., Dutilleul, P., and Potvin, C.: Optimum experimental design for Free-Air Carbon dioxide Enrichment (FACE) studies, Global Change Biology, 6, 843–854, https://doi.org/10.1046/j.1365-2486.2000.00353.x, 2000.

~~Finzi, A. C., Norby, R. J., Calfapietra, C., Gallet-Budynek, A., Gielen, B., Holmes, W. E., Hoosbeek, M. R., Iversen, C. M., Jackson, R. B., Kubiske, M. E., Ledford, J., Liberloo, M., Oren, R., Polle, A., Pritchard, S., Zak, D. R., Schlesinger, W. H., and Ceulemans, R.: Increases in nitrogen uptake rather than nitrogen-use efficiency support higher rates of temperate forest productivity under elevated CO2, Proceedings of the National Academy of Sciences, 104, 14014–14019, https://doi.org/10.1073/pnas.0706518104, 2007.~~

Fleischer, K., Rammig, A., De Kauwe, M. G., Walker, A. P., Domingues, T. F., Fuchslueger, L., Garcia, S., Goll, D. S., Grandis, A., Jiang, M., Haverd, V., Hofhansl, F., Holm, J. A., Kruijt, B., Leung, F., Medlyn, B. E., Mercado, L. M., Norby, R. J., Pak, B., von Randow, C., Quesada, C. A., Schaap, K. J., Valverde-Barrantes, O. J., Wang, Y.-P., Yang, X., Zaehle, S., Zhu, Q., and Lapola, D. M.: Amazon forest response to CO2 fertilization dependent on plant phosphorus acquisition, Nat. Geosci., 12, 736–741, https://doi.org/10.1038/s41561-019-0404-9, 2019.

Friend, A. D. and Kiang, N. Y.: Land Surface Model Development for the GISS GCM: Effects of Improved Canopy Physiology on Simulated Climate, Journal of Climate, 18, 2883–2902, https://doi.org/10.1175/JCLI3425.1, 2005.

~~Grant, R. F.: Modelling changes in nitrogen cycling to sustain increases in forest productivity under elevated atmospheric CO_2 and contrasting site conditions, Biogeosciences, 10, 7703–7721, https://doi.org/10.5194/bg-10-7703-2013, 2013.~~

van Groenigen, K. J., Qi, X., Osenberg, C. W., Luo, Y., and Hungate, B. A.: Faster Decomposition Under Increased Atmospheric CO2 Limits Soil Carbon Storage, Science, 344, 508–509, https://doi.org/10.1126/science.1249534, 2014.

van Groenigen, K. J., Osenberg, C. W., Terrer, C., Carrillo, Y., Dijkstra, F. A., Heath, J., Nie, M., Pendall, E., Phillips, R. P., and Hungate, B. A.: Faster turnover of new soil carbon inputs under increased atmospheric CO2, Global Change Biology, 23, 4420–4429, https://doi.org/10.1111/gcb.13752, 2017.

Hasegawa, S., Macdonald, C. A., and Power, S. A.: Elevated carbon dioxide increases soil nitrogen and phosphorus availability in a phosphorus-limited Eucalyptus woodland, Global Change Biology, 22, 1628–1643, https://doi.org/10.1111/gcb.13147, 2016.

Hasegawa, S., Ryan, M. H., and Power, S. A.: CO2 concentration and water availability alter the organic acid composition of root exudates in native Australian species, Plant Soil, 485, 507–524, https://doi.org/10.1007/s11104-022-05845-z, 2023.

Hedley, M. J., Stewart, J. W. B., and Chauhan, B. S.: Changes in Inorganic and Organic Soil Phosphorus Fractions Induced by Cultivation Practices and by Laboratory Incubations, Soil Science Society of America Journal, 46, 970–976, https://doi.org/10.2136/sssaj1982.03615995004600050017x, 1982.

Helfenstein, J., Ringeval, B., Tamburini, F., Mulder, V. L., Goll, D. S., He, X., Alblas, E., Wang, Y., Mollier, A., and Frossard, E.: Understanding soil phosphorus cycling for sustainable development: A review, One Earth, 7, 1727–1740, https://doi.org/10.1016/j.oneear.2024.07.020, 2024.

Hinsinger, P.: Bioavailability of soil inorganic P in the rhizosphere as affected by root-induced chemical changes: a review, Plant and Soil, 237, 173–195, https://doi.org/10.1023/A:1013351617532, 2001.

Jiang, M., Zaehle, S., De Kauwe, M. G., Walker, A. P., Caldararu, S., Ellsworth, D. S., and Medlyn, B. E.: The quasi-equilibrium framework revisited: analyzing long-term CO_2 enrichment responses in plant–soil models, Geoscientific Model Development, 12, 2069–2089, https://doi.org/10.5194/gmd-12-2069-2019, 2019.

Jiang, M., Medlyn, B. E., Drake, J. E., Duursma, R. A., Anderson, I. C., Barton, C. V. M., Boer, M. M., Carrillo, Y., Castañeda-Gómez, L., Collins, L., Crous, K. Y., De Kauwe, M. G., dos Santos, B. M., Emmerson, K. M., Facey, S. L., Gherlenda, A. N., Gimeno, T. E., Hasegawa, S., Johnson, S. N., Kännaste, A., Macdonald, C. A., Mahmud, K., Moore, B. D., Nazaries, L., Neilson, E. H. J., Nielsen, U. N., Niinemets, Ü., Noh, N. J., Ochoa-Hueso, R., Pathare, V. S., Pendall, E., Pihlblad, J., Piñeiro, J., Powell, J. R., Power, S. A., Reich, P. B., Renchon, A. A., Riegler, M., Rinnan, R., Rymer, P. D., Salomón, R. L., Singh, B. K., Smith, B., Tjoelker, M. G., Walker, J. K. M., Wujeska-Klause, A., Yang, J., Zaehle, S., and Ellsworth, D. S.: The fate of carbon in a mature forest under carbon dioxide enrichment, Nature, 580, 227–231, https://doi.org/10.1038/s41586-020-2128-9, 2020.

Jiang, M., Medlyn, B. E., Wårlind, D., Knauer, J., Fleischer, K., Goll, D. S., Olin, S., Yang, X., Yu, L., Zaehle, S., Zhang, H., Lv, H., Crous, K. Y., Carrillo, Y., Macdonald, C., Anderson, I., Boer, M. M., Farrell, M., Gherlenda, A., Castañeda-Gómez, L., Hasegawa, S., Jarosch, K., Milham, P., Ochoa-Hueso, R., Pathare, V., Pihlblad, J., Nevado, J. P., Powell, J., Power, S. A., Reich, P., Riegler, M., Ellsworth, D. S., and Smith, B.: Carbon-phosphorus cycle models overestimate CO2 enrichment response in a mature Eucalyptus forest, Science Advances, 10, eadl5822, https://doi.org/10.1126/sciadv.adl5822, 2024a.

Jiang, M., Crous, K. Y., Carrillo, Y., Macdonald, C. A., Anderson, I. C., Boer, M. M., Farrell, M., Gherlenda, A. N., Castañeda-Gómez, L., Hasegawa, S., Jarosch, K., Milham, P. J., Ochoa-Hueso, R., Pathare, V., Pihlblad, J., Piñeiro, J., Powell, J. R., Power, S. A., Reich, P. B., Riegler, M., Zaehle, S., Smith, B., Medlyn, B. E., and Ellsworth, D. S.: Microbial competition for phosphorus limits the CO2 response of a mature forest, Nature, 1–6, https://doi.org/10.1038/s41586-024-07491-0, 2024b.

Jiang, Z., Thakur, M. P., Liu, R., Zhou, G., Zhou, L., Fu, Y., Zhang, P., He, Y., Shao, J., Gao, J., Li, N., Wang, X., Jia, S., Chen, Y., Zhang, C., and Zhou, X.: Soil P availability and mycorrhizal type determine root exudation in sub-tropical forests, Soil Biology and Biochemistry, 171, 108722, https://doi.org/10.1016/j.soilbio.2022.108722, 2022.

Johansson, E. M., Fransson, P. M. A., Finlay, R. D., and van Hees, P. A. W.: Quantitative analysis of soluble exudates produced by ectomycorrhizal roots as a response to ambient and elevated CO2, Soil Biology and Biochemistry, 41, 1111–1116, https://doi.org/10.1016/j.soilbio.2009.02.016, 2009.

Jones, D. L., Hodge, A., and Kuzyakov, Y.: Plant and mycorrhizal regulation of rhizodeposition, New Phytologist, 163, 459–480, https://doi.org/10.1111/j.1469-8137.2004.01130.x, 2004.

Kästner, M., Miltner, A., Thiele-Bruhn, S., and Liang, C.: Microbial Necromass in Soils—Linking Microbes to Soil Processes and Carbon Turnover, ~~Frontiers in Environmental Science, 9~~Front. Environ. Sci., 9, https://doi.org/10.3389/fenvs.2021.756378, 2021.

Kull, O. and Kruijt, B.: Leaf photosynthetic light response: a mechanistic model for scaling photosynthesis to leaves and canopies, Functional Ecology, 12, 767–777, https://doi.org/10.1046/j.1365-2435.1998.00257.x, 1998.

Kuzyakov, Y., Horwath, W. R., Dorodnikov, M., and Blagodatskaya, E.: Review and synthesis of the effects of elevated atmospheric CO2 on soil processes: No changes in pools, but increased fluxes and accelerated cycles, Soil Biol. Biochem., 128, 66–78, https://doi.org/10.1016/j.soilbio.2018.10.005, 2019.

Lambers, H.: Phosphorus Acquisition and Utilization in Plants, Annu. Rev. Plant Biol., 73, 17–42, https://doi.org/10.1146/annurev-arplant-102720-125738, 2022.

Leuschner, C., Tückmantel, T., and Meier, I. C.: Temperature effects on root exudation in mature beech (Fagus sylvatica L.) forests along an elevational gradient, Plant Soil, https://doi.org/10.1007/s11104-022-05629-5, 2022.

Li, Z., Liu, Z., Gao, G., Yang, X., and Gu, J.: Shift from Acquisitive to Conservative Root Resource Acquisition Strategy Associated with Increasing Tree Age: A Case Study of Fraxinus mandshurica, Forests, 12, 1797, https://doi.org/10.3390/f12121797, 2021.

Liang, C., Schimel, J. P., and Jastrow, J. D.: The importance of anabolism in microbial control over soil carbon storage, Nat Microbiol, 2, 1–6, https://doi.org/10.1038/nmicrobiol.2017.105, 2017.

Liang, C., Amelung, W., Lehmann, J., and Kästner, M.: Quantitative assessment of microbial necromass contribution to soil organic matter, Global Change Biology, 25, 3578–3590, https://doi.org/10.1111/gcb.14781, 2019.

Lloyd, J. and Taylor, J. A.: On the Temperature Dependence of Soil Respiration, Functional Ecology, 8, 315, https://doi.org/10.2307/2389824, 1994.

Lopez-Sangil, L., George, C., Medina-Barcenas, E., Birkett, A. J., Baxendale, C., Bréchet, L. M., Estradera-Gumbau, E., and Sayer, E. J.: The Automated Root Exudate System (ARES): a method to apply solutes at regular intervals to soils in the field, Methods in Ecology and Evolution, 8, 1042–1050, https://doi.org/10.1111/2041-210X.12764, 2017.

Manzoni, S., Taylor, P., Richter, A., Porporato, A., and Ågren, G. I.: Environmental and stoichiometric controls on microbial carbon-use efficiency in soils, New Phytologist, 196, 79–91, https://doi.org/10.1111/j.1469-8137.2012.04225.x, 2012.

Margalef, O., Sardans, J., Fernández-Martínez, M., Molowny-Horas, R., Janssens, I. A., Ciais, P., Goll, D., Richter, A., Obersteiner, M., Asensio, D., and Peñuelas, J.: Global patterns of phosphatase activity in natural soils, Sci Rep, 7, 1337, https://doi.org/10.1038/s41598-017-01418-8, 2017.

Marklein, A. R. and Houlton, B. Z.: Nitrogen inputs accelerate phosphorus cycling rates across a wide variety of terrestrial ecosystems, New Phytologist, 193, 696–704, https://doi.org/10.1111/j.1469-8137.2011.03967.x, 2012.

McGill, W. B. and Cole, C. V.: Comparative aspects of cycling of organic C, N, S and P through soil organic matter, Geoderma, 26, 267–286, https://doi.org/10.1016/0016-7061(81)90024-0, 1981.

~~McLeod, A. R. and Long, S. P.: Free-air Carbon Dioxide Enrichment (FACE) in Global Change Research: A Review, in: Advances in Ecological Research, vol. 28, edited by: Fitter, A. H. and Raffaelli, D., Academic Press, 1–56, https://doi.org/10.1016/S0065-2504(08)60028-8, 1999.~~

Medlyn, B. E., De Kauwe, M. G., Zaehle, S., Walker, A. P., Duursma, R. A., Luus, K., Mishurov, M., Pak, B., Smith, B., Wang, Y.-P., Yang, X., Crous, K. Y., Drake, J. E., Gimeno, T. E., Macdonald, C. A., Norby, R. J., Power, S. A., Tjoelker, M. G., and Ellsworth, D. S.: Using models to guide field experiments: a priori predictions for the CO2 response of a nutrient- and water-limited native Eucalypt woodland, Global Change Biology, 22, 2834–2851, https://doi.org/10.1111/gcb.13268, 2016.

Meier, I. C., Tückmantel, T., Heitkötter, J., Müller, K., Preusser, S., Wrobel, T. J., Kandeler, E., Marschner, B., and Leuschner, C.: Root exudation of mature beech forests across a nutrient availability gradient: the role of root morphology and fungal activity, New Phytologist, 226, 583–594, https://doi.org/10.1111/nph.16389, 2020.

~~Miltner, A., Bombach, P., Schmidt Brücken, B., and Kästner, M.: SOM genesis: microbial biomass as a significant source, Biogeochemistry, 111, 41–55, https://doi.org/10.1007/s10533-011-9658-z, 2012.~~

Nannipieri, P., Giagnoni, L., Landi, L., and Renella, G.: Role of Phosphatase Enzymes in Soil, in: Phosphorus in Action: Biological Processes in Soil Phosphorus Cycling, edited by: Bünemann, E., Oberson, A., and Frossard, E., Springer, Berlin, Heidelberg, 215–243, https://doi.org/10.1007/978-3-642-15271-9_9, 2011.

Norby, R. J~~., DeLucia, E. H., Gielen, B., Calfapietra, C., Giardina, C. P., King, J. S., Ledford, J., McCarthy, H. R., Moore, D. J. P., Ceulemans, R., De Angelis, P., Finzi, A. C., Karnosky, D. F., Kubiske, M. E., Lukac, M., Pregitzer, K. S., Scarascia-Mugnozza, G. E., Schlesinger, W. H., and Oren, R.: Forest response to elevated CO2 is conserved across a broad range of productivity, Proceedings of the National Academy of Sciences, 102, 18052–18056, https://doi.org/10.1073/pnas.0509478102, 2005~~.: Forest productivity response to elevated CO_2 in free-air CO_2 enrichment experiments: the 23 percent solution, revisited, New Phytologist, https://doi.org/10.1111/nph.70162, 2025.

Norby, R. J., Warren, J. M., Iversen, C. M., Medlyn, B. E., and McMurtrie, R. E.: CO2 enhancement of forest productivity constrained by limited nitrogen availability, Proceedings of the National Academy of Sciences, 107, 19368–19373, https://doi.org/10.1073/pnas.1006463107, 2010.

Norby, R. J., Loader, N. J., Mayoral, C., Ullah, S., Curioni, G., Smith, A. R., Reay, M. K., van Wijngaarden, K., Amjad, M. S., Brettle, D., Crockatt, M. E., Denny, G., Grzesik, R. T., Hamilton, R. L., Hart, K. M., Hartley, I. P., Jones, A. G., Kourmouli, A., Larsen, J. R., Shi, Z., Thomas, R. M., and MacKenzie, A. R.: Enhanced woody biomass production in a mature temperate forest under elevated CO2, Nat. Clim. Chang., 14, 983–988, https://doi.org/10.1038/s41558-024-02090-3, 2024.

Ochoa-Hueso, R., Hughes, J., Delgado-Baquerizo, M., Drake, J. E., Tjoelker, M. G., Piñeiro, J., and Power, S. A.: Rhizosphere-driven increase in nitrogen and phosphorus availability under elevated atmospheric CO2 in a mature Eucalyptus woodland, Plant Soil, 416, 283–295, https://doi.org/10.1007/s11104-017-3212-2, 2017.

~~Pantigoso, H. A., Manter, D. K., Fonte, S. J., and Vivanco, J. M.: Root exudate-derived compounds stimulate the phosphorus solubilizing ability of bacteria, Sci Rep, 13, 4050, https://doi.org/10.1038/s41598-023-30915-2, 2023.~~

Phillips, R. P., Erlitz, Y., Bier, R., and Bernhardt, E. S.: New approach for capturing soluble root exudates in forest soils, Functional Ecology, 22, 990–999, https://doi.org/10.1111/j.1365-2435.2008.01495.x, 2008.

Phillips, R. P., Finzi, A. C., and Bernhardt, E. S.: Enhanced root exudation induces microbial feedbacks to N cycling in a pine forest under long-term CO2 fumigation, Ecology Letters, 14, 187–194, https://doi.org/10.1111/j.1461-0248.2010.01570.x, 2011.

Pihlblad, J., Andresen, L. C., Macdonald, C. A., Ellsworth, D. S., and Carrillo, Y.: The influence of elevated CO_2 and soil depth on rhizosphere activity and nutrient availability in a mature *Eucalyptus* woodland, Biogeosciences, 20, 505–521, https://doi.org/10.5194/bg-20-505-2023, 2023.

Piñeiro, J., Ochoa-Hueso, R., Drake, J. E., Tjoelker, M. G., and Power, S. A.: Water availability drives fine root dynamics in a Eucalyptus woodland under elevated atmospheric CO2 concentration, Functional Ecology, 34, 2389–2402, https://doi.org/10.1111/1365-2435.13660, 2020.

Piñeiro, J., Ochoa-Hueso, R., Serrano-Grijalva, L., and Power, S. A.: Phosphorus and water supply independently control productivity and soil enzyme activity responses to elevated CO2 in an understorey community from a Eucalyptus woodland, Plant Soil, 483, 643–657, https://doi.org/10.1007/s11104-022-05763-0, 2023.

Prescott, C. E., Grayston, S. J., Helmisaari, H.-S., Kaštovská, E., Körner, C., Lambers, H., Meier, I. C., Millard, P., and Ostonen, I.: Surplus Carbon Drives Allocation and Plant–Soil Interactions, Trends in Ecology & Evolution, 35, 1110–1118, https://doi.org/10.1016/j.tree.2020.08.007, 2020.

Reay, M. K., Sayer, E. J., Smith, A., Pastor, V., Kourmouli, A., Marshall, M., Grzesik, R. T., Evans, I., Rumeau, M., Hart, K., Ma, J., Norby, R. J., MacKenzie, A. R., Hamilton, R. L., Hartley, I. P., and Ullah, S.: Elevated CO2 alters relative belowground carbon investment for nutrient acquisition in a mature temperate forest, Proceedings of the National Academy of Sciences, 122, e2503595122, https://doi.org/10.1073/pnas.2503595122, 2025.

Reichert, T., Rammig, A., Fuchslueger, L., Lugli, L. F., Quesada, C. A., and Fleischer, K.: Plant phosphorus-use and -acquisition strategies in Amazonia, New Phytologist, 234, 1126–1143, https://doi.org/10.1111/nph.17985, 2022.

Ross, G. M., Horn, S., Macdonald, C. A., Powell, J. R., Reynolds, J. K., Ryan, M. M., Cook, J. M., and Nielsen, U. N.: Metabarcoding mites: Three years of elevated CO2 has no effect on oribatid assemblages in a *Eucalyptus* woodland, Pedobiologia, 81–82, 150667, https://doi.org/10.1016/j.pedobi.2020.150667, 2020.

Rumeau, M., Pihlblad, J., Sgouridis, F., Fereday, G., Reay, M. K., Carrillo, Y., Hartley, I. P., Sayer, E., Hamilton, L., Mackenzie, A. R., and Ullah, S.: Root exudate stoichiometry is a key driver of soil N cycling: implications for forest responses to global change, Soil Biology and Biochemistry, 208, 109856, https://doi.org/10.1016/j.soilbio.2025.109856, 2025.

Schimel, J. P. and Weintraub, M. N.: The implications of exoenzyme activity on microbial carbon and nitrogen limitation in soil: a theoretical model, Soil Biology and Biochemistry, 35, 549–563, https://doi.org/10.1016/S0038-0717(03)00015-4, 2003.

Sistla, S. A., Rastetter, E. B., and Schimel, J. P.: Responses of a tundra system to warming using SCAMPS: a stoichiometrically coupled, acclimating microbe–plant–soil model, Ecological Monographs, 84, 151–170, https://doi.org/10.1890/12-2119.1, 2014.

Sokol, N. W., Kuebbing, Sara. E., Karlsen-Ayala, E., and Bradford, M. A.: Evidence for the primacy of living root inputs, not root or shoot litter, in forming soil organic carbon, New Phytologist, 221, 233–246, https://doi.org/10.1111/nph.15361, 2019.

Spohn, M.: Microbial respiration per unit microbial biomass depends on litter layer carbon-to-nitrogen ratio, Biogeosciences, 12, 817–823, https://doi.org/10.5194/bg-12-817-2015, 2015.

Spohn, M., Ermak, A., and Kuzyakov, Y.: Microbial gross organic phosphorus mineralization can be stimulated by root exudates – A 33P isotopic dilution study, Soil Biology and Biochemistry, 65, 254–263, https://doi.org/10.1016/j.soilbio.2013.05.028, 2013.

Spohn, M., Klaus, K., Wanek, W., and Richter, A.: Microbial carbon use efficiency and biomass turnover times depending on soil depth – Implications for carbon cycling, Soil Biology and Biochemistry, 96, 74–81, https://doi.org/10.1016/j.soilbio.2016.01.016, 2016.

Su, Y., Xu, G., Lu, X., Jiang, H., Peng, S., Zhao, H., Liu, M., and Duan, B.: Interactive effects of citric acid and mineral fertilization on soil microbial carbon use efficiency in the rhizosphere of two coniferous species, European Journal of Soil Biology, 112, 103428, https://doi.org/10.1016/j.ejsobi.2022.103428, 2022.

Sun, L., Kominami, Y., Yoshimura, K., and Kitayama, K.: Root-exudate flux variations among four co-existing canopy species in a temperate forest, Japan, Ecological Research, 32, 331–339, https://doi.org/10.1007/s11284-017-1440-9, 2017.

Sun, L., Ataka, M., Han, M., Han, Y., Gan, D., Xu, T., Guo, Y., and Zhu, B.: Root exudation as a major competitive fine-root functional trait of 18 coexisting species in a subtropical forest, New Phytologist, 229, 259–271, https://doi.org/10.1111/nph.16865, 2021.

Sun, Z., Liu, S., Zhang, T., Zhao, X., Chen, S., and Wang, Q.: Priming of soil organic carbon decomposition induced by exogenous organic carbon input: a meta-analysis, Plant Soil, 443, 463–471, https://doi.org/10.1007/s11104-019-04240-5, 2019.

Talbot, J. M., Allison, S. D., and Treseder, K. K.: Decomposers in disguise: mycorrhizal fungi as regulators of soil C dynamics in ecosystems under global change, Functional Ecology, 22, 955–963, https://doi.org/10.1111/j.1365-2435.2008.01402.x, 2008.

Taneva, L., Pippen, J. S., Schlesinger, W. H., and Gonzalez-Meler, M. A.: The turnover of carbon pools contributing to soil CO2 and soil respiration in a temperate forest exposed to elevated CO2 concentration, Global Change Biology, 12, 983–994, https://doi.org/10.1111/j.1365-2486.2006.01147.x, 2006.

Tang, J. Y. and Riley, W. J.: A total quasi-steady-state formulation of substrate uptake kinetics in complex networks and an example application to microbial litter decomposition, Biogeosciences, 10, 8329–8351, https://doi.org/10.5194/bg-10-8329-2013, 2013.

Tao, F., Huang, Y., Hungate, B. A., Manzoni, S., Frey, S. D., Schmidt, M. W. I., Reichstein, M., Carvalhais, N., Ciais, P., Jiang, L., Lehmann, J., Wang, Y.-P., Houlton, B. Z., Ahrens, B., Mishra, U., Hugelius, G., Hocking, T. D., Lu, X., Shi, Z., Viatkin, K., Vargas, R., Yigini, Y., Omuto, C., Malik, A. A., Peralta, G., Cuevas-Corona, R., Di Paolo, L. E., Luotto, I., Liao, C., Liang, Y.-S., Saynes, V. S., Huang, X., and Luo, Y.: Microbial carbon use efficiency promotes global soil carbon storage, Nature, 618, 981–985, https://doi.org/10.1038/s41586-023-06042-3, 2023.

Tao, J., Riley, W., Tang, J., Zhu, Q., Pegoraro, E., Castanha, C., Abramoff, R., Torn, M., Tao, J., Riley, W., Tang, J., Zhu, Q., Pegoraro, E., Castanha, C., Abramoff, R., and Torn, M.: Representing Soil Microbial Dynamics and Organo-Mineral Interactions in the E3SM Land Model (ELM-ReSOM), Journal of Advances in Modeling Earth Systems, 17, https://doi.org/10.1029/2024ms004874, 2025.

Terrer, C., Vicca, S., Hungate, B. A., Phillips, R. P., and Prentice, I. C.: Mycorrhizal association as a primary control of the CO2 fertilization effect, Science, 353, 72–74, https://doi.org/10.1126/science.aaf4610, 2016.

Terrer, C., Phillips, R. P., Hungate, B. A., Rosende, J., Pett-Ridge, J., Craig, M. E., van Groenigen, K. J., Keenan, T. F., Sulman, B. N., Stocker, B. D., Reich, P. B., Pellegrini, A. F. A., Pendall, E., Zhang, H., Evans, R. D., Carrillo, Y., Fisher, J. B., Van Sundert, K., Vicca, S., and Jackson, R. B.: A trade-off between plant and soil carbon storage under elevated CO2, Nature, 591, 599–603, https://doi.org/10.1038/s41586-021-03306-8, 2021.

Thum, T., Caldararu, S., Engel, J., Kern, M., Pallandt, M., Schnur, R., Yu, L., and Zaehle, S.: A new model of the coupled carbon, nitrogen, and phosphorus cycles in the terrestrial biosphere (QUINCY v1.0; revision 1996), Geoscientific Model Development, 12, 4781–4802, https://doi.org/10.5194/gmd-12-4781-2019, 2019.

Thurner, M. A., Caldararu, S., Engel, J., Rammig, A., and Zaehle, S.: Modelled forest ecosystem carbon–-nitrogen dynamics with integrated mycorrhizal processes under elevated CO_2, Biogeosciences~~, 21, 1391–1410~~ Discussions, 1–30, https://doi.org/10.5194/bg-~~21-1391-2024, 2024~~2023-109, 2023.

Turner, B. L., Wells, A., and Condron, L. M.: Soil organic phosphorus transformations along a coastal dune chronosequence under New Zealand temperate rain forest, Biogeochemistry, 121, 595–611, https://doi.org/10.1007/s10533-014-0025-8, 2014.

Vestergård, M., Reinsch, S., Bengtson, P., Ambus, P., and Christensen, S.: Enhanced priming of old, not new soil carbon at elevated atmospheric CO2, Soil Biology and Biochemistry, 100, 140–148, https://doi.org/10.1016/j.soilbio.2016.06.010, 2016.

Walker, A. P., Zaehle, S., Medlyn, B. E., De Kauwe, M. G., Asao, S., Hickler, T., Parton, W., Ricciuto, D. M., Wang, Y.-P., Wårlind, D., and Norby, R. J.: Predicting long-term carbon sequestration in response to CO2 enrichment: How and why do current ecosystem models differ?, Global Biogeochemical Cycles, 29, 476–495, https://doi.org/10.1002/2014GB004995, 2015.

Walker, A. P., De Kauwe, M. G., Medlyn, B. E., Zaehle, S., Iversen, C. M., Asao, S., Guenet, B., Harper, A., Hickler, T., Hungate, B. A., Jain, A. K., Luo, Y., Lu, X., Lu, M., Luus, K., Megonigal, J. P., Oren, R., Ryan, E., Shu, S., Talhelm, A., Wang, Y.-P., Warren, J. M., Werner, C., Xia, J., Yang, B., Zak, D. R., and Norby, R. J.: Decadal biomass increment in early secondary succession woody ecosystems is increased by CO2 enrichment, Nat Commun, 10, 454, https://doi.org/10.1038/s41467-019-08348-1, 2019.

Walker, A. P., De Kauwe, M. G., Bastos, A., Belmecheri, S., Georgiou, K., Keeling, R. F., McMahon, S. M., Medlyn, B. E., Moore, D. J. P., Norby, R. J., Zaehle, S., Anderson-Teixeira, K. J., Battipaglia, G., Brienen, R. J. W., Cabugao, K. G., Cailleret,

M., Campbell, E., Canadell, J. G., Ciais, P., Craig, M. E., Ellsworth, D. S., Farquhar, G. D., Fatichi, S., Fisher, J. B., Frank, D. C., Graven, H., Gu, L., Haverd, V., Heilman, K., Heimann, M., Hungate, B. A., Iversen, C. M., Joos, F., Jiang, M., Keenan, T. F., Knauer, J., Körner, C., Leshyk, V. O., Leuzinger, S., Liu, Y., MacBean, N., Malhi, Y., McVicar, T. R., Penuelas, J., Pongratz, J., Powell, A. S., Riutta, T., Sabot, M. E. B., Schleucher, J., Sitch, S., Smith, W. K., Sulman, B., Taylor, B., Terrer, C., Torn, M. S., Treseder, K. K., Trugman, A. T., Trumbore, S. E., van Mantgem, P. J., Voelker, S. L., Whelan, M. E., and Zuidema, P. A.: Integrating the evidence for a terrestrial carbon sink caused by increasing atmospheric CO2, New Phytologist, 229, 2413–2445, https://doi.org/10.1111/nph.16866, 2021.

Walker, T. W. and Syers, J. K.: The fate of phosphorus during pedogenesis, Geoderma, 15, 1–19, https://doi.org/10.1016/0016-7061(76)90066-5, 1976.

Wang, Y. and Lambers, H.: Root-released organic anions in response to low phosphorus availability: recent progress, challenges and future perspectives, Plant Soil, 447, 135–156, https://doi.org/10.1007/s11104-019-03972-8, 2020.

Wang, Y.-P., Huang, Y., Augusto, L., Goll, D. S., Helfenstein, J., and Hou, E.: Toward a Global Model for Soil Inorganic Phosphorus Dynamics: Dependence of Exchange Kinetics and Soil Bioavailability on Soil Physicochemical Properties, Global Biogeochemical Cycles, 36, e2021GB007061, https://doi.org/10.1029/2021GB007061, 2022.

Wen, Z., White, P. J., Shen, J., and Lambers, H.: Linking root exudation to belowground economic traits for resource acquisition, New Phytologist, 233, 1620–1635, https://doi.org/10.1111/nph.17854, 2022.

Wieder, W. R., Cleveland, C. C., Smith, W. K., and Todd-Brown, K.: Future productivity and carbon storage limited by terrestrial nutrient availability, Nature Geosci, 8, 441–444, https://doi.org/10.1038/ngeo2413, 2015.

Wutzler, T., Zaehle, S., Schrumpf, M., Ahrens, B., and Reichstein, M.: Adaptation of microbial resource allocation affects modelled long term soil organic matter and nutrient cycling, Soil Biology and Biochemistry, 115, 322–336, https://doi.org/10.1016/j.soilbio.2017.08.031, 2017.

Wutzler, T., Yu, L., Schrumpf, M., and Zaehle, S.: Simulating long-term responses of soil organic matter turnover to substrate stoichiometry by abstracting fast and small-scale microbial processes: the Soil Enzyme Steady Allocation Model (SESAM; v3.0), Geoscientific Model Development, 15, 8377–8393, https://doi.org/10.5194/gmd-15-8377-2022, 2022.

Yin, H., Li, Y., Xiao, J., Xu, Z., Cheng, X., and Liu, Q.: Enhanced root exudation stimulates soil nitrogen transformations in a subalpine coniferous forest under experimental warming, Global Change Biology, 19, 2158–2167, https://doi.org/10.1111/gcb.12161, 2013.

Yu, L., Ahrens, B., Wutzler, T., Schrumpf, M., and Zaehle, S.: Jena Soil Model (JSM v1.0; revision 1934): a microbial soil organic carbon model integrated with nitrogen and phosphorus processes, Geoscientific Model Development, 13, 783–803, https://doi.org/10.5194/gmd-13-783-2020, 2020.

Yu, L., Caldararu, S., Ahrens, B., Wutzler, T., Schrumpf, M., Helfenstein, J., Pistocchi, C., and Zaehle, S.: Improved representation of phosphorus exchange on soil mineral surfaces reduces estimates of phosphorus limitation in temperate forest ecosystems, Biogeosciences, 20, 57–73, https://doi.org/10.5194/bg-20-57-2023, 2023.

Zaehle, S., Medlyn, B. E., De Kauwe, M. G., Walker, A. P., Dietze, M. C., Hickler, T., Luo, Y., Wang, Y.-P., El-Masri, B., Thornton, P., Jain, A., Wang, S., Warlind, D., Weng, E., Parton, W., Iversen, C. M., Gallet-Budynek, A., McCarthy, H., Finzi, A., Hanson, P. J., Prentice, I. C., Oren, R., and Norby, R. J.: Evaluation of 11 terrestrial carbon–nitrogen cycle models against observations from two temperate Free-Air CO2 Enrichment studies, New Phytologist, 202, 803–822, https://doi.org/10.1111/nph.12697, 2014.

Zerihun, A., McKENZIE, B. A., and Morton, J. D.: Photosynthate costs associated with the utilization of different nitrogen–forms: influence on the carbon balance of plants and shoot–root biomass partitioning, New Phytologist, 138, 1–11, https://doi.org/10.1046/j.1469-8137.1998.00893.x, 1998.

Zhang, C., Cai, Y., Zhang, T., He, T., Li, J., Li, X., and Zhao, Q.: Litter removal increases the plant carbon input to soil in a Pinus massoniana plantation, Eur J Forest Res, 141, 833–843, https://doi.org/10.1007/s10342-022-01476-2, 2022.

Zhang, H., Goll, D. S., Wang, Y.-P., Ciais, P., Wieder, W. R., Abramoff, R., Huang, Y., Guenet, B., Prescher, A.-K., Viscarra Rossel, R. A., Barré, P., Chenu, C., Zhou, G., and Tang, X.: Microbial dynamics and soil physicochemical properties explain large-scale variations in soil organic carbon, Global Change Biology, 26, 2668–2685, https://doi.org/10.1111/gcb.14994, 2020.

Zhang, Z., Qiao, M., Li, D., Yin, H., and Liu, Q.: Do warming-induced changes in quantity and stoichiometry of root exudation promote soil N transformations via stimulation of soil nitrifiers, denitrifiers and ammonifiers?, European Journal of Soil Biology, 74, 60–68, https://doi.org/10.1016/j.ejsobi.2016.03.007, 2016.

Zhou, J., Wen, Y., Shi, L., Marshall, M. R., Kuzyakov, Y., Blagodatskaya, E., and Zang, H.: Strong priming of soil organic matter induced by frequent input of labile carbon, Soil Biology and Biochemistry, 152, 108069, https://doi.org/10.1016/j.soilbio.2020.108069, 2021.